

**The impact of nutritional interventions
on the progression of intestinal tumors in
*Drosophila melanogaster***

Dissertation

zur Erlangung des Doktorgrades
der Mathematisch-Naturwissenschaftlichen Fakultät
der Christian-Albrechts-Universität
zu Kiel

vorgelegt von

Roxana Pfefferkorn

Kiel, September 2018

Erstgutachter: Prof. Dr. Thomas Roeder

Zweitgutachter: Prof. Dr. Holger Heine

Tag der mündlichen Prüfung: 14. November 2018

Summary

Every year more than 700,000 people die from colorectal cancer (CRC) making it the 4th most often cancer-related cause of death. Albeit advanced diagnostics and increasingly sophisticated treatment options, the incidence of CRC increases steadily and overall prognosis remains poor. In recent years, nutrition has once again attracted attention as a supportive systemic cancer treatment since tumors are highly sensitive to their nutrient environment. The two major interventions that have been shown to be beneficial during tumor development are diets with the vast majority of calories being derived from fats, as well as different regimes of dietary restriction (DR) through protein limitation.

I investigated the effects of high fat (HF) dieting and strict DR on the development of stem cell-derived intestinal tumors in a *Drosophila melanogaster* model expressing a constitutively active human isoform of the EGFR pathway component *RAF*. Feeding a HF diet neither increased nor reduced tumor load but resulted in wasting of muscle and lean body mass in tumor bearing flies. This pathologic phenotype can also be observed in up to 80% of patients with advanced CRC. Cachexia-like wasting is likely due to tumor-induced insulin resistance which is potentiated by HF-induced insulin resistance. Subjection to DR, on the other hand, resulted in the reduction of tumor mass and reinstated gut functionality. Nevertheless, tumor bearing flies subjected to DR experienced severe wasting and died prematurely. I subsequently applied an alternating feeding regime of recurrent protein limitation to exploit the benefits of protein limitation on tumor growth while circumventing tissue wasting. Indeed, the recurrent diet was able to mimic lifelong protein restriction in terms of tumor development and gut functionality, while it restored the lifespan of tumor bearing flies to the level of healthy control flies. Transcriptomic alterations induced by DR remained modified throughout phases of refeeding thus allowing the recurrent diet to mimic lifelong DR. Furthermore, refeeding specifically induced a genetic subset which seems to confer additional health- and lifespan promoting benefits.

An alternating recurrent diet combining phases of strict DR with phases of refeeding effectively mimics lifelong DR and drastically reduces tumor growth in the fruit fly. In the future it will be vital to explore the ideal time span lengths of DR and refeeding, in order to establish an optimized recurrent feeding regime with high patient compliance that is applicable as supportive cancer treatment in humans.

Zusammenfassung

Mit mehr als 700,000 Todesfällen jährlich ist Darmkrebs die vierthäufigste Krebs-assoziierte Todesursache. Trotz sich stetig verbessernder Diagnose- und Behandlungsmöglichkeiten steigt die Anzahl der Betroffenen beständig an, während sich die Überlebensrate kaum erhöht. In den letzten Jahrzehnten ist Ernährung wieder verstärkt als ergänzende Krebstherapie in den Fokus der wissenschaftlichen Forschung gerückt, da Tumorwachstum stark von den verfügbaren Nährstoffen abhängt. Hierbei zeigen Diäten mit einem hohen Fettanteil (HF), sowie Diäten mit geringem Proteingehalt (DR) den stärksten Einfluss auf die Tumorentwicklung.

Ich habe die Effekte von HF und strikter DR auf die Tumorentwicklung, induziert durch die Expression von humanem, konstitutiv aktivem *RAF* in den intestinalen Stammzellen, in dem Modelorganismus *Drosophila melanogaster* untersucht. Eine HF Diät beeinflusste das Wachstum der Tumore nicht, induzierte jedoch einen Kachexie-ähnlichen Schwund von Fett- und Muskelgewebe. Dieser Gewebeabbau bedingt sich vermutlich durch eine Tumor-induzierte Insulinresistenz, die zusätzlich durch eine Fett-induzierte Insulinresistenz potenziert wird. DR hingegen reduzierte die Tumormasse drastisch und normalisierte zudem die Verdauungstätigkeit. Dennoch verstarben auch DR-gefütterte Fliegen vorzeitig, da sie Fett- und Muskelschwund erlitten. Ich etablierte daher eine Diät mit wiederkehrender DR, um das Tumorwachstum zu vermindern und dem Gewebeschwund entgegenzuwirken. Tatsächlich konnte ich zeigen, dass wiederkehrende DR die gleichen Effekte auf das Tumorwachstum zeigt wie kontinuierliche DR. Gleichzeitig zeigten Tumorfiegen durch wiederkehrende DR die gleiche Lebensspanne wie gesunde Kontrollfliegen. Analysen der Transkriptome der Därme zeigten, dass nicht nur DR-bedingte Änderungen über Zufütterungsphasen hinweg aufrechterhalten blieben, sondern auch, dass die erneute Zufütterung zusätzliche Gesundheits- und Lebensspannen-fördernde Änderungen induziert.

Eine Diät mit abwechselnden Phasen aus DR und Zufütterung kann wirksam die Effekte einer lebenslangen DR imitieren und vermindert das Tumorwachstum in der Fruchtfliege. In Zukunft wird es von vorrangiger Bedeutung sein, herauszufinden, wie die DR- und Zufütterungsphasen optimal zusammen wirken, um einen möglich starken Wachstum-limitierenden Effekt mit der größtmögliche Compliance zu vereinen, und so eine unterstützende Krebstherapie für den Menschen zu verwirklichen.

Table of Contents

1. Introduction	1
1.1. Colorectal cancer	1
1.1.1. Colorectal cancer development and progression	1
1.1.2. Treatment options in colorectal cancer	2
1.1.3. Initiation of colorectal cancer	4
1.1.4. Mechanisms of carcinogenesis	5
1.1.5. EGFR signaling in colorectal cancer	6
1.2. Nutrition-mediated growth in cancer	9
1.2.1. Cancer metabolism	9
1.2.2. Dietary interventions as cancer treatment	11
1.3. <i>Drosophila melanogaster</i> as a research model	13
1.3.1. <i>Drosophila</i> in disease-associated research	13
1.3.2. EGFR signaling in <i>Drosophila</i>	14
1.3.3. The intestine of <i>Drosophila</i>	16
1.3.4. Nutritional sensing in <i>Drosophila</i>	19
1.4. Aims of the study	22
2. Material & Methods	23
2.1. Fly husbandry	23
2.2. Fly food	23
2.3. Microscopy	24
2.4. Luciferase assay	24
2.5. Gut length	25
2.6. Vibratome sectioning	25
2.7. Fecal output measurements	25

2.8.	Transit time assay _____	26
2.9.	Gut integrity _____	26
2.10.	Bacterial DNA profiling _____	27
2.11.	Dechoriation and recolonization _____	27
2.12.	Survival _____	28
2.13.	Body composition _____	28
2.14.	Metabolic rate assay _____	29
2.15.	Activity monitoring _____	30
2.16.	Feeding behavior _____	30
2.17.	RNA isolation _____	30
2.18.	Transcriptomic profiling _____	31
2.19.	Bodipy staining _____	32
2.20.	Statistics _____	32
3.	Results _____	33
3.1.	Verification of the HF and DR model in healthy flies _____	33
3.2.	The effects of HF and DR on the development of intestinal tumors _____	36
3.2.1.	Gut morphology upon <i>RAF^{gof}</i> induction in ISCs and EB _____	36
3.2.2.	Effects of <i>RAF^{gof}</i> -induced tumors on digestion _____	42
3.2.3.	The impact of nutrition on the lifespan of tumor bearing flies _____	45
3.2.4.	Intestinal tumors alter body composition and energy demands _____	46
3.3.	The effects of a recurrent diet on the development of intestinal tumors _____	50
3.3.1.	A recurrent diet prolongs the lifespan of tumor bearing flies _____	50
3.3.2.	The effects of a recurrent diet on gut morphology and functionality _____	52
3.3.3.	Body composition and energy demands after subjection to a recurrent diet _____	58
3.3.4.	Transcriptome analysis of intestines of flies subjected to a recurrent diet _____	61
3.3.5.	Changes of the microbial composition after subjection to a recurrent diet _____	67

4. Discussion	72
4.1. Model validation	72
4.2. Expression of <i>RAF^{gof}</i> results in the formation of excessive <i>esg⁺</i> tissue	73
4.3. HF diet does not affect tumor load but promotes cachexia-like wasting	74
4.4. DR limits intestinal tumor growth but promotes cachexia-like wasting	77
4.5. A recurrent diet limits tumor growth and restores lifespan	81
4.6. DR induces long-lasting transcriptional alterations	84
4.7. Intestinal tumors result in a dysbiotic shift of the intestinal microbiota	87
5. Conclusion & Outlook	90
6. References	93
7. Acknowledgements	113
8. Declaration	114
9. Curriculum Vitae	115
10. Appendix	116

1. Introduction

1.1. Colorectal cancer

1.1.1. Colorectal cancer development and progression

Colorectal cancer (CRC) is the third most often diagnosed type of cancer in men and women worldwide with a total of 1.4 million new cases and 700.000 deaths in 2012 alone (1). The incidence of CRC steadily increases and has almost doubled within the last 22 years from 783,000 in 1990 to 1,361,000 in 2012 (2). The increase is expected to reach 2.2 million new cases and 1.1 million deaths annually by 2030 (1). The global distribution of CRC incidences largely varies with economically developed countries exhibiting a higher number of diagnosed cases but a lower relative mortality than developing countries (3). Educating the population in regard of preventive measures, as well as the increased effort to diagnose CRC at an early stage alongside with advanced treatment options clearly contributes to this trend. However, the incidence of CRC correlates with industrialization and the subsequent increase of the Human Development Index (HDI). This development is linked to adopting a Western lifestyle which entails the increased exposure to CRC risk factors such as obesity and diabetes, physical inactivity, as well as tobacco and alcohol abuse (4–7).

CRC is classified using two different stage identification systems. The most widely used system categorizes CRC development into five stages ranging from stage 0 to stage IV with multiple subclasses each (8) (Fig. 1.1). A stage 0 polyp is a benign cluster of abnormal cells that is located inside the colon wall and does not invade any other layers of the colon. If not resected these abnormal cells can further develop and invade the colon lumen as well as the submucosa and the intestinal muscle layer (stage I). An adenoma, an epithelial derived tumor, is considered stage II once it has invaded the serosa, the outer boundary of the colon, and stage III as soon as the tumorous mass has spread to lymph nodes adjacent to the intestinal tissue. In a stage IV carcinoma, cells have undergone epithelial-mesenchymal-transition (EMT), a mechanism by which adhesion molecules are downregulated in order to facilitate the disruption of tissue integrity and the migration of cancerous cells into distant tissues (9, 10). The relocation from the primary tumor side to distant organs is provided *via* lymph and blood vessels.

Introduction

On the other hand, the TNM-classification system identifies tumors in a similar manner but is more sophisticated and identifies more than 20 tumor subclasses (11). While T categorizes the primary tumor cell mass in regard of extend and tissue invasion, N gives an insight into regional lymph node involvement and M classifies metastatic spread of the tumor to distant organs (12).

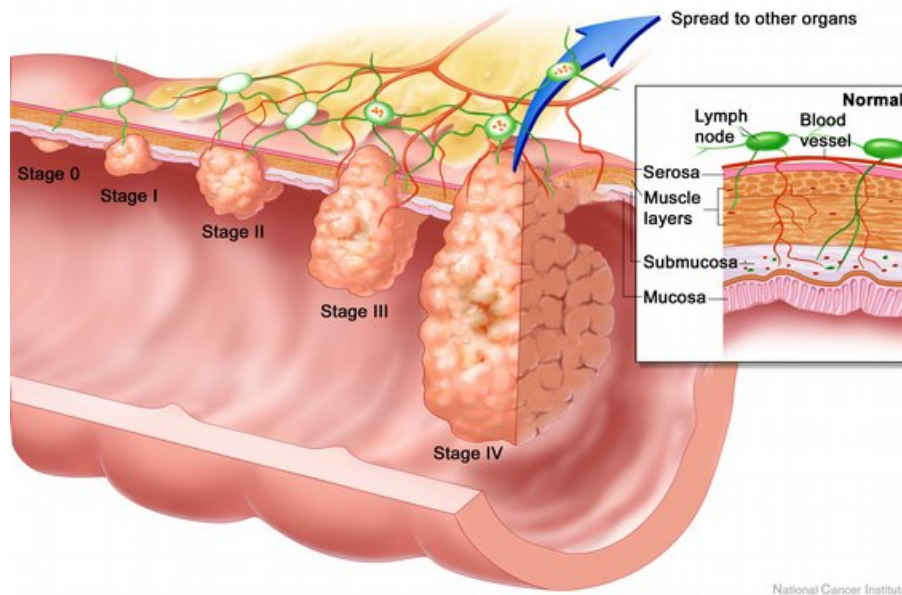


Fig. 1.1: Identification of colorectal cancer stages according to the National Institute of Health. While stage 0 displays a benign, spatially defined polyp, stages I to IV describe increasingly invasive tumors. In stage IV metastases form in distant body sites by intravasation of tumor cells into the blood and lymph vessels (13).

1.1.2. Treatment options in colorectal cancer

CRC is frequently detected in rather late stages (III or IV) since early stages often are perceived asymptomatic or presented symptoms are inconclusive or misinterpreted (14). The prognosis for CRC patients strongly depends on the stage a tumor has reached upon diagnosis and 5-year survival rates drastically decline in dependence of tumor stage (Tab. 1.1). Clearly the treatment success has multiple dependencies aside from the diagnosed tumor stage alone. Important factors are the individual patient's life history, overall health, nutritional status as well as the patient's individual genetic cancer signature and aggressiveness.

Introduction

Tab. 1.1: Relative 5-year survival rates for patients diagnosed at different stages of CRC (15).

<i>Stage at diagnosis</i>	<i>Number of cases</i>	<i>5-year relative survival (%)</i>
I	26,727	93.2
II	72,784	77
III	72,806	47.7
IV	28,377	6.6

This is a cohort study of 308,734 patients in England diagnosed with CRC in 1996-2002. Stage 0 is not represented due to a lack of detection.

While small polyps can be removed directly during colonoscopy, the most common treatment upon diagnosis of larger tumors is the surgical resection of the aberrant tissue including some surrounding healthy tissue and nearby lymph nodes. Radiation and chemotherapy are treatments that are additionally applied before, during or after resection and in cases where resection is not possible. Radiation therapy uses high-intensity X-rays to target malignant tissue in a spatially restricted setting (16). Chemotherapy on the other hand entails the intravenous or oral administration of drugs that specifically addresses cell growth and division. Tumor growth can be limited by the disruption of different cell proliferation associated processes like inhibiting DNA replication or protein biosynthesis (17). Since reagents inhibiting cell growth naturally also affect healthy proliferating cells like stem cells or progenitor cells, the side effects of chemotherapy are usually strong and highly diverse, ranging from hair loss to heavy vomiting and neuropathy (18). The sequencing of tumor tissue has facilitated the identification of the mutational signature of individual CRC tumors. Knowing the mutational landscape that enables tumor growth in a specific patient complements treatment options by facilitating the application of personalized medicine including targeted chemotherapy and immunotherapy. Targeted chemotherapy uses tyrosine kinase inhibitors to specifically block signaling from mutated signaling components that promote tumor development (19). Targeted immunotherapy eliminates cancer cells by using monoclonal antibodies to either block growth promoting signaling in cancer cells, to flag cancer cells in order for the immune system to recognize and eradicate them, or by delivering drugs specifically to cancer cells (20). Despite the fast paced advances in cancer therapy tumors recur in about 40-60% of patients after curative surgery (21) with 20-30% recurrence in patients with CRC stage II and 50-80% recurrence in patients with CRC stage III (22).

Introduction

1.1.3. Initiation of colorectal cancer

Different intestinal cell types have been proposed to serve as the cancer cells of origin in colorectal tumorigenesis (23–25) but intestinal stem cells (ISCs) remain the most common initiators of CRC (26, 27). The proliferative potential of ISCs fosters the progressive aggregation of mutations and therefore the degeneration of healthy cells to tumor stem cells. Proliferating tissue accumulates mutations in a stepwise manner with carcinogenesis proceeding with little regard to the order of the acquired mutations. A multitude of somatic mutations accumulates in proliferating tissues over time with about half of these mutations being already present before tumor initiation takes place (28). These passenger mutations provide no growth advantage and have no obvious impact on tumor development. Tumor initiation only takes place upon the introduction of driver mutations which provide growth advantages and induce neoplasia. Although approximately 100 mutations have been identified to serve as possible drivers in CRC, it has been hypothesized that a subset of six to seven combined driver mutations is necessary to induce solid intestinal tumors (29, 30). It is noteworthy, that recent *in silico* studies revised this estimation and suggest that as little as three driver mutations are sufficient to initiate tumorigenesis (31). However, tumors usually contain a plethora of mutations with or without growth promoting properties and are therefore vastly heterogeneous on the genetic level with complexity increasing throughout carcinogenesis.

In order for a tissue to overcome its physiological function and not only become overproliferative but to attain cancerous properties, a multiplicity of conditions has to be met. A key factor in tumorigenesis is the ability to acquire self-sufficiency in proliferative signaling. This autonomous cell growth can be achieved by either cells providing the growth signals themselves or by altering their responsiveness to autocrine signaling, *e.g.* by increasing the expression or efficiency of growth factor receptors, or by facilitating ligand-independent signaling (32–34). To maintain proliferative potential, cancer cells also need to enable replicative immortality by promoting telomerase activity (35). Telomeres are repetitive sequences protecting the DNA from end-to-end fusions which would eventually result in cellular clearance *via* apoptosis. In healthy cells, telomeres shorten with every division, thereby limiting a cells proliferative capability. Checkpoints in a cell and in the cellular niche environment keep track of a cells physiological functionality, thereby limiting growth and clearing cells with an altered physiological signature (36). So while tumor cells acquire

Introduction

potentially endless replication potential, they also must overcome sensitivity to growth inhibitors, acquire resistance to apoptosis, and evade the immune system. Once a solid tumor has formed, the excessive tissue induces angiogenesis to provide oxygen and nutrients directly to the primary tumor side (37).

1.1.4. Mechanisms of carcinogenesis

The initial step for a cell to lose its physiological function and enter into an uncontrolled proliferative state depends on the acquisition of growth promoting mutations. Three genetic modes of action have been identified to initiate tumor formation by inducing genome instability either alone or in combination (Fig. 1.2). The CpG island methylator phenotype (CIMP) is characterized by an overall hypomethylation of cytosine bases combined with locally defined hypermethylation of tumor suppressor promoters, most importantly *MLH1*, the human homolog of bacterial mismatch repair gene *mutL*, and is often associated with B-Rat fibrosarcoma (*BRAF*) mutations (38, 39).

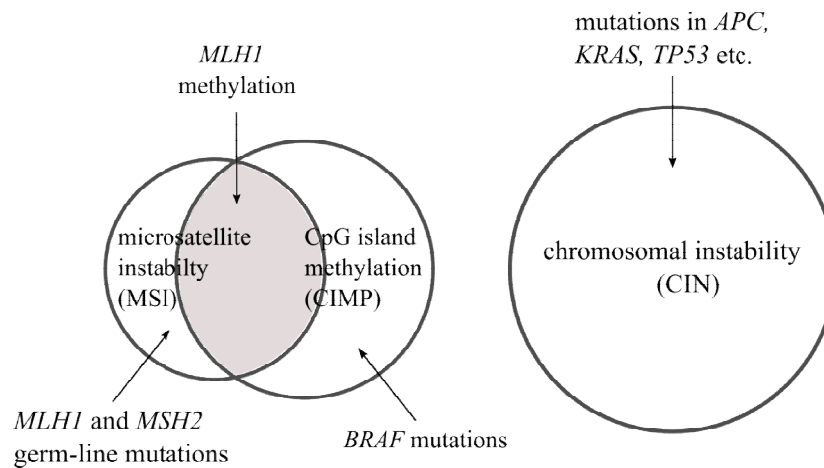


Fig. 1.2: Overview of mechanisms resulting in genomic instability in colorectal cancer. *APC*: adenomatous polyposis coli, *KRAS*: Kristen rat sarcoma viral oncogene homolog, *BRAF*: B-rat fibrosarcoma proto-oncogene, *TP53*: tumor protein 53, *MLH1*: *mutL* homolog1, *MSH2*: *mutS* homolog2. Modified from (40).

CIMP often co-occurs with microsatellite instability (MSI) which is another mechanism that initiates CRC and prevails in about 12-28% of sporadic CRCs (41). MSI is induced by mutations that inactivate the DNA mismatch repair mechanism, thus leading to multiple

Introduction

genetic alterations that foster CRC progression (42). MSI tumors usually display a low frequency of otherwise common CRC mutations in adenomatous poliposis coli (*APC*) and Kristen rat sarcoma (*KRAS*) but exhibit high frequencies of *BRAF* mutations (43). Chromosomal instability (CIN) is the third and most frequently occurring mechanism of CRC carcinogenesis and can be observed in about 85% of all sporadic colorectal tumors (43). CIN tumors are characterized by changes in chromosome number and structure, like aneuploidy and loss of heterozygosity, which can result from impaired chromosomal segregation or malfunctioning DNA repair mechanisms, respectively. Tumors that develop due to CIN usually exhibit an inhibitory mutation of the tumorsuppressor gene *APC* followed by an activating mutation in *KRAS* and subsequent mutations of either tumor suppressors like tumor protein 53 (*TP53*) or oncogenes like mothers against decapentaplegic homolog 2 (*SMAD2*) (29).

1.1.5. EGFR signaling in colorectal cancer

The epidermal growth factor receptor (EGFR) is a transmembrane receptor tyrosine kinase (RTK) and part of the protein family of ErbB cell membrane receptors. In mammals there are four receptors in this family which are HER 1 (EGFR) to HER 4. The receptor consists of an extracellular cysteine-rich ligand-binding motif, one alpha-helical membrane-spanning region and an intracellular tyrosine kinase domain (44, 45). Binding of a ligand to the extracellular binding domain leads to homo- or heterodimerization of the receptor and trans-autophosphorylation of the cytoplasmic tyrosine kinase domains (Fig. 1.3). The subsequent intracellular signal transduction addresses two main pathways which are the mitogen-activated protein kinase (MAPK) pathway and the phosphatidylinositol-3-kinase (PI3K)/protein kinase B (AKT) pathway (46). Both of which are associated with tissue proliferation, differentiation, migration, and angiogenesis (46, 47).

EGFR signaling plays a multitudinous role in tumorigenesis by providing cells with independence of growth signals. All levels of the EGFR signaling cascade can potentially contribute to tumor formation through different modes of action including increased copy number, protein overexpression and hyperactivating gene mutations. EGFR pathway components most frequently mutated in CRC are *EGFR*, *KRAS*, *BRAF*, *PI3KCA* (encoding

Introduction

PI3K) and *PTEN* (Tab. 1.2) (45, 48). Activating mutations usually occur early during carcinogenesis in the *KRAS* gene and are found in 30-40% of all CRCs (45).

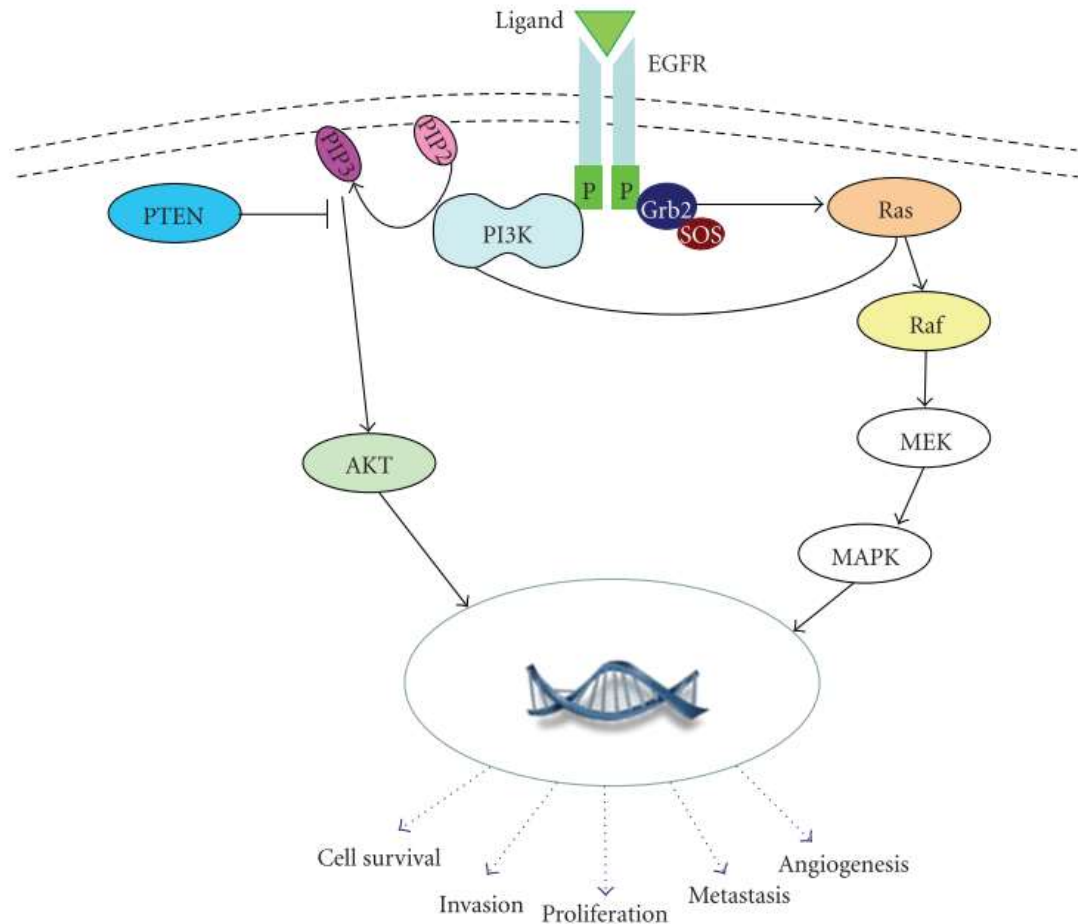


Fig. 1.3: Signaling via the EGFR pathway. Binding of a ligand to the EGF receptor results in transphosphorylation of the intracellular tyrosine kinase domains and subsequent intracellular signal transduction. Phosphorylation of Rat sarcoma (Ras) occurs via growth factor receptor-bound protein 2 (Grb2) and son of sevenless (SOS). The phosphorylation proceeds from Ras to mitogen-activated protein kinase (MAPK)/extracellular signal-regulated kinase (ERK) kinase (MEK) to MAPK. In parallel, ligand binding to EGFR induces the translocation of phosphatidylinositol 3-kinase (PI3K) to the cell membrane where it produces phosphatidylinositol-3,4,5-triphosphate (PIP3). PIP3 phosphorylates protein kinase B (AKT) but can itself be reverted to phosphatidylinositol-4,5-biphosphate (PIP2) through a negative feedback loop via phosphatase with tensin homology (PTEN). Both pathways initiate pathways associated with proliferation, metastasis and cell survival (45).

Tumors containing these mutations do respond poorly to EGFR targeted therapy since the signaling path is misregulated downstream of the receptor. Mutations of *BRAF* arise in 5-22% of CRCs and are most often a valine-to-glutamic acid amino acid substitution called V600E

Introduction

(49). Mutations in *KRAS* and *BRAF* are mutually exclusive and seem to be similar in their tumorigenic properties (50).

Tab. 1.2: Alterations of EGFR pathway components in CRC (45).

Component (gene/protein)	Protein function	Defect in CRC	Frequency
<i>EGFR/EGFR</i>	Transmembrane tyrosine kinase receptor	Protein expression Mutation Increased copy number	25–90% Rare 0–50%*
<i>KRAS/KRAS</i>	GDP-/GTP-binding protein; facilitates ligand-dependent signaling	Activating mutation (codons 12, 13, 61, 146); leads to activation of MAPK pathway	30–40%
<i>BRAF/B-Raf</i>	Serine-threonine protein kinase downstream of KRas	Activating mutation (V600E)	5–12%
<i>PIK3CA/PI3K</i>	A key signal transducer in the PI3K-AKT pathway	Activating mutation (exons 9 and 20)	14–18%
<i>PTEN/PTEN</i>	A protein tyrosine phosphatase enzyme; inactivates PI3K pathway	Loss of protein expression; mutation; LOH	13–19%

CRC: colorectal cancer; LOH: loss of heterozygosity; * low % for high amplification (> 10), high % for low amplification (3-5)

Given its manifold involvement in tumorigenesis, several approaches have been made to interfere with EGFR signaling targeting both the extracellular ligand-binding domain as well as the cytoplasmic tyrosine kinase domain. Currently, Cetuximab (51) and Panitumumab (52) are the only two US Food and Drug Administration (FDA) approved antibody therapeutic drugs and frequently used as cancer treatment in CRCs with wildtype *KRAS*. Both are monoclonal antibodies (mABs) targeted against EGFR that competitively inhibit ligand binding to the receptor, thus restraining downstream signal transduction. Furthermore, the mABs induce receptor internalization and lead to a long-lasting downregulation of EGFR (53). Beside mAB therapy, tyrosine kinase inhibitors (TKI) are used to specifically target cells with activated EGFR signaling. TKIs bind either reversibly or irreversibly to the intracellular tyrosine kinase domain of EGFR and prohibit downstream signaling (54, 55). However,

Introduction

EGFR mABs are largely ineffective if downstream targets, like *KRAS*, *BRAF* or *PI3KCA* are also mutated (56, 57).

1.2. Nutrition-mediated growth in cancer

1.2.1. Cancer metabolism

As early as 1931 Otto Warburg proposed an altered mode of carbohydrate metabolism for cancer cells (58). Since then, intensive research has elucidated a number of metabolic traits specific to hyperproliferative and cancer cells that cover all levels of metabolic interactions. These traits include the increased acquisition and altered usage of available resources, allocation of intermediate metabolites to specific pathways as well as tissue transformation due to altered cell fate determination (59). The altered cellular metabolism is deemed indispensable for cancer cells and therefore is considered a hallmark of cancer (35, 59).

Proliferating cells display a high demand of macromolecules in order to synthesize cellular components and give rise to daughter cells. Glucose serves as a principal macronutrient required for these biosyntheses. Healthy cells metabolize glucose to pyruvate which is then transported into the mitochondria where it is subjected to oxidative phosphorylation in order to yield ATP as an energy resource (Fig. 1.4). Under anaerobic conditions cells ferment pyruvate and subsequently secrete lactate. This anaerobic glycolysis is far less efficient and yields about 18 times less ATP than mitochondrial oxidative phosphorylation (35). Cancer cells mainly process glucose into lactate even under aerobic conditions and feed only about 5% of available pyruvate into mitochondria for ATP generation *via* oxidative phosphorylation (60). To compensate for the lower ATP levels generated through this aerobic glycolysis cancer cells increase glucose uptake by up to 30 times (61) while upregulating glucose transporters and glycolysis pathway components (62). It has been proposed that the switch to aerobic glycolysis is beneficial to cancer cells in a bipartite manner. Firstly, it has been shown, that glucose consumption levels are highly diverse throughout tumor tissues (63). Subpopulations of cancer cells consume glucose and secrete lactate whereas other subpopulations mainly metabolize lactate by feeding it into the citrate cycle (64). Secondly, it has been suggested that the altered glucose mechanism observed in cancer cells allows the

Introduction

cells to feed glycolytic intermediates into other anabolic pathways, thereby sustaining biosynthesis of macromolecules that are required for cell proliferation (65).

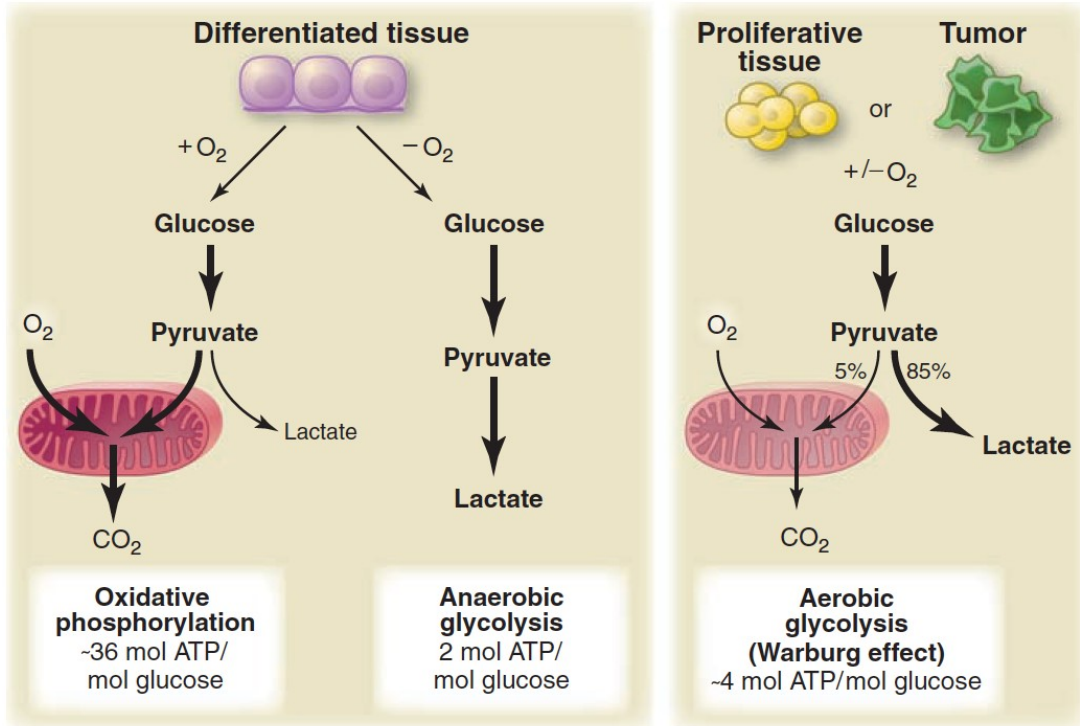


Fig. 1.4: Glycolysis in differentiated tissue or proliferative tissue and tumors. In the presence of oxygen differentiated cells metabolize glucose to pyruvate which is then taken up by mitochondria and undergoes oxidative phosphorylation in order to generate ATP. Under oxygen restricted conditions, differentiated cells ferment pyruvate and generate ATP by anaerobic glycolysis. Anaerobic glycolysis is about 18 times less efficient than oxidative phosphorylation. Proliferative tissues and tumor cells act independently of the oxygen status by feeding only about 5% of available pyruvate into oxidative phosphorylation while mainly generating ATP *via* fermentation. This aerobic glycolysis yields about 9 times less ATP than oxidative phosphorylation. ATP: adenosine triphosphate (66).

Fast proliferating tumors soon experience heterogeneous nutrient scarcity and need to reallocate available nutrients to support further tissue growth. A well-studied phenomenon on resource acquisition is angiogenesis, which describes the tumor-induced *de novo* formation of new blood vessels that deliver oxygen and nutrients directly to the primary tumor site. Tumors that do not induce vascularization are restricted in their expansion and remain in a static phase until angiogenesis is induced (37, 67). Aside from inducing vascularization, cancer cells acquire mutations that facilitate the uptake of macromolecules directly from the extracellular space. While growth factors are needed in healthy cells to internalize nutrients *via* transporters, cancer cells are able to internalize extracellular macromolecules *via*

Introduction

macropinocytosis (68). Furthermore, cells bearing *KRAS* mutations have been observed to engulf wildtype adjacent cells through entosis, thereby accessing formerly unobtainable macromolecules (69).

In contrast to local nutrient shortage, prolonged systemic nutrient scarcity cannot be completely compensated. Cells are able to survive nutrient depletion for extended periods of time through autophagy, a mechanism of degrading intracellular macromolecules. While healthy cells mainly use autophagy to eliminate dysfunctional mitochondria, there seems to be a more vital role of autophagy in tumor cells which greatly contributes to tumor survival (70) at the expense of healthy tissue.

1.2.2. Dietary interventions as cancer treatment

Recurrence is high in CRC and greatly depends on the tumor stage at the time of diagnosis (22). Especially the activation of the EGFR pathway has proven to be associated with poor prognosis and elevated recurrence risk (71, 72). At the same time, treatment resistances arise in up to 90% of CRC patients (73). While resistance to general chemotherapeutics can be acquired by increasing the efflux of drugs or limiting the drug uptake and metabolism (74), resistance to targeted therapies is mediated by genomic alterations including changes in copy number, activating mutations of downstream targets and mutations allowing bypassing of a specific pathway (73, 75).

In recent years, nutrition has attracted attention as a sustentative, non-targeted cancer treatment since CRC is highly sensitive to nutritional cues (76–79). Nutrition influences cancer outcome in a bipartite way; on the one hand, nutrition directly influences cell viability and tumor growth. On the other hand, harsh nutritional interventions threaten organismal health and might foster cancer-induced tissue wasting. Until today, the exact modes of action conferred by nutritional interventions and how to take advantage of the potential benefits remains poorly understood. Nevertheless, researchers have tried to exploit the altered carbohydrate metabolism of cancer cells (58) to reduce growth of cancer cells while sustaining organismal health. Indeed, cancer cell growth was shown to be limited by applying a normocaloric diet that very strictly limits carbohydrate supply while providing 80-90% of calories *via* fats (80–83). In contrast, high fat (HF) intake is also clearly associated with diabetes and obesity, which in turn are linked to promoting CRC (84–86). Interestingly, recent

Introduction

studies not only emphasize the growth-promoting effect of HF dieting *via* the activation of the insulin signaling pathway, but also state that HF promotes tumor growth by increasing the stemness of cancer stem cells (CSC) (25, 87).

Limiting dietary regimes are the treatment most consistently associated with prolonged lifespan, improved overall health and reduced tumor growth (88–91). Caloric restriction (CR) is the reduction of the overall caloric intake by diluting food or limiting access to the food source. While CR has proven to prolong health- and lifespan, it depends on a variety of factors including hydration, nutrient supply, sex and genetic background (92, 93). Furthermore, it is uncertain whether the beneficial effects of caloric restriction are mediated by the overall reduction of caloric intake or by the reduction of one particular macronutrient. Dietary restriction (DR), on the other hand, is described by the sole reduction in available protein while not altering other macronutrients. It has been discussed that DR is accountable for the health benefits observed in CR. However, it is not clear to what extent. Studies identified DR to play a superordinate role in lifespan extension in model organisms like *Drosophila melanogaster* and mice (94–97). Furthermore, DR reduces growth in multiple tumor models including cell culture and human xenografts (98–101). Insulin and target of rapamycin (TOR) signaling are the main integrators of nutritional cues (102–104). Under DR conditions, low insulin signaling is conferring a state of growth arrest and stress resistance *via* the transcription factor FOXO. At the same time FOXO increases sensitivity to insulin signaling by increasing the expression of the insulin receptor itself (105). Furthermore, upon amino acid scarcity TOR dephosphorylates and activates 4E-BP, a translational repressor, thus inhibiting growth. Additionally, TOR is regulated by PI3K/AKT signaling, which acts downstream of the insulin signaling pathway and systemically confers altered nutritional input (106, 107). Despite its benefits on tumor growth and overall health, DR presents a pitfall during CRC progression by restricting energy resources and thereby potentially fostering tissue wasting. Tumor growth is a vastly energy consuming process and in patients often results in massive weight loss that is further exacerbated by loss of appetite and anorexia. This organismal wasting, termed cachexia, occurs in up to 80% of cancer patients (108) and is characterized by extensive loss of adipose and muscle tissue (109). Interestingly, studies show that cachexia is not only characterized by the lack of meeting energy demands but is mediated independently of the nutritional intake by impaired insulin signaling (110, 111). Therefore, DR might on the one hand foster cachexia by limiting macromolecule supply while on the other hand, DR might counteract cachexia by reinstating insulin sensitivity (112–114).

1.3. *Drosophila melanogaster* as a research model

1.3.1. *Drosophila* in disease-associated research

Drosophila melanogaster has been used as a research model for more than 100 years. The short life cycle (Fig. 1.5 A) and the large amount of offspring fostered the early research of elucidating basic cellular mechanisms, developmental processes, and general genetics. Multiple genetic tools have been established over the past 30 years which are quickly advancing in complexity and ingenuity since the *Drosophila* whole genome sequencing in 2000 (115). One of these tools is the Gal4-UAS system which is derived from the yeast transcription factor Gal4 and its optimized binding site, the upstream activation sequence (UAS) (116). The bipartite system requires one parental *Drosophila* driver line carrying a tissue or cell type specific promoter or enhancer fused to the Gal4 sequence. The other parental line contains the gene of interest fused to the UAS. The filial generation will then contain both constructs ubiquitously. Upon promoter/enhancer activity, Gal4 is expressed in a spatially confined manner and binds to the UAS in these specific cells, thereby activating transcription of the target genes (Fig. 1.5 B). Another level of specificity is achieved by temporal control through the temporal and regional gene expression targeting (TARGET) system (117). The ubiquitously expressed Gal80^{ts}, which is co-expressed by the driver line, binds to Gal4 at low temperatures (19 °C), thus preventing Gal4 from binding to UAS and activating target gene transcription. Switching to a higher temperature (29 °C) releases Gal4 from Gal80^{ts} (117). The Gal4-UAS TARGET system thereby provides a method to express a gene of interest in a strictly controlled spatiotemporal manner.

Within the past decades *Drosophila* has become of special interest in clinically relevant, human disease-associated research. Genetic models are less time intensive to produce in the fly (as opposed to mammalian models) while still providing a whole animal system (as opposed to cell culture). About 62% of human disease-associated genes have homologs in the fruit fly, many of which are highly conserved genes involved in metabolism, development and tumorigenesis (118). Natural tumors occasionally arise during aging of the fruit fly (119, 120). However, cancer phenotypes can easily be induced in *Drosophila* by manipulating highly conserved pathways that regulate cell proliferation and tissue maintenance. It has been proposed that the hallmarks of cancer (35, 121) can each be addressed in *Drosophila* (122). Indeed, *Drosophila* has been established as a model for various types of cancer including

Introduction

brain, lung and colorectal malignancies (123–125). Furthermore, multiple studies successfully used *Drosophila* as a high throughput model organism to identify the potential of chemotherapeutic drugs and investigate new treatment options (124, 126).

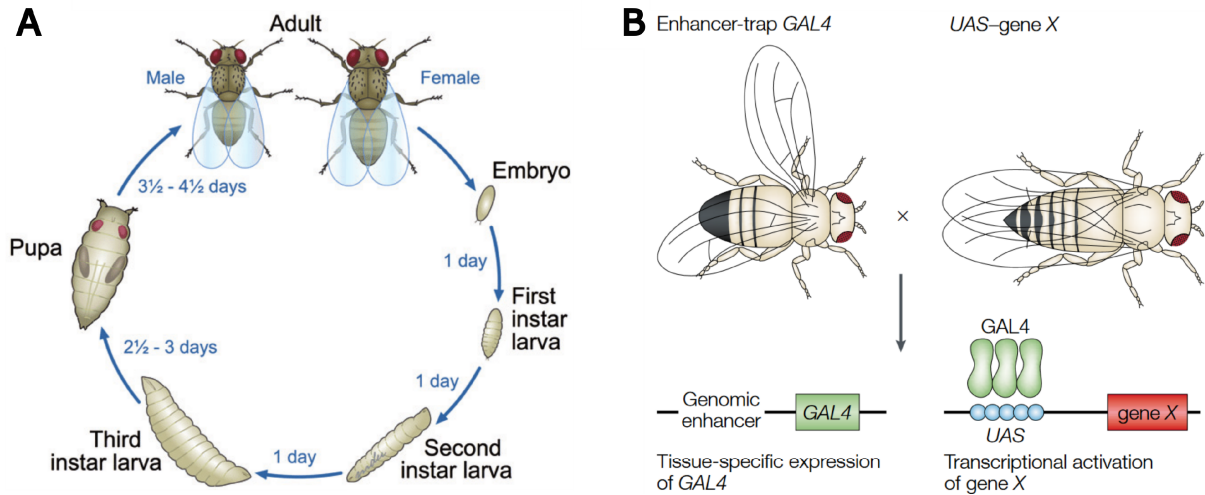


Fig. 1.5: Life cycle of *Drosophila melanogaster* at 25 °C and schematic Gal4-UAS system. (A) The *Drosophila* life cycle is temperature-dependent and takes approximately 10-12 days at 25 °C. The eggs are placed in the medium where the 1st instar larvae hatch after one day. The larvae undergo two more moltings and reach 3rd instar stage three days after egg deposition. The 3rd instar larvae pupate upon reaching a critical weight. Adult flies eclose from the pupae after 3.5 to 4.5 days (127). (B) The two-component Gal4-UAS system comprises a Gal4 driver line with Gal4 fused to a tissue specific enhancer or promoter and a UAS responder line carrying the UAS fused to the gene of interest. The F1 generation expresses both constructs, thereby expressing the gene of interest in a tissue-specific manner (128).

1.3.2. EGFR signaling in *Drosophila*

The *Drosophila* Egfr is involved in a plethora of developmental processes including oogenesis (129), imaginal disc and eye development (130, 131), as well as tissue homeostasis (132). It is the sole member of the ErbB family of cell membrane receptors in the fruit fly and shares great functional and structural similarities with its mammalian counterpart HER1 (133). The receptor can be activated by the four extracellular ligands Gurken, Spitz, Vein and Keren with largely redundant and overlapping activities (133–135) (Fig. 1.6). The TGF- α homologs Spitz, Keren and Gurken are produced as inactive, transmembrane precursors that undergo cleavage by intermembrane proteases of the Rhomboid family before being released and binding to Egfr (136).

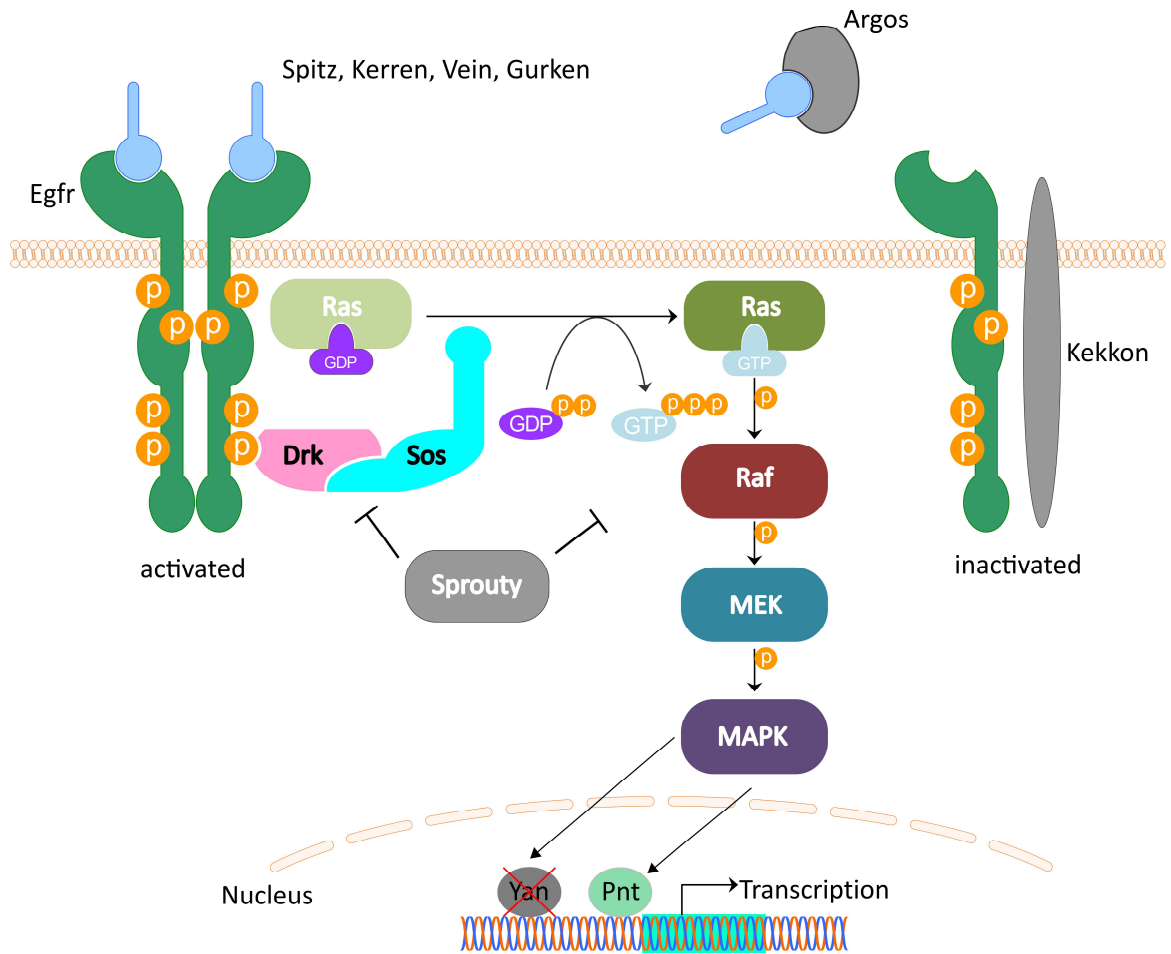


Fig. 1.6: Egfr signaling pathway in *Drosophila melanogaster*. The Egfr dimerizes upon binding of an activating ligand (Spitz, Kerren, Vein or Gurken) and trans-autophosphorylates. The phosphorylated tyrosine kinase domain recruits Drk which in turn interacts with Sos to activate Ras. The signaling cascade successively phosphorylates Raf, MEK and MAPK. The transcription factor Pointed (Pnt) activates transcription whereas Yan inhibits transcription and is released upon MAPK activity. Kekkron inhibits signaling by binding to the receptor monomer, Argos inhibits signaling by scavenging receptor ligands and Sprouty inhibits signaling on multiple levels downstream of the receptor. Egfr: epidermal growth factor receptor; Ras: rat sarcoma; Drk: downstream of receptor kinase; Sos: son of sevenless; Raf: rat fibrosarcoma; MEK: mitogen-activated protein kinase/extracellular signal-regulated kinase kinase; MAPK: mitogen-activated protein kinase; Pnt: pointed; GDP: guanosine diphosphate; DTP: guanosine triphosphate; p: phosphate.

Vein is the only activating ligand that is directly secreted. Spitz is considered the primary systemic activator with the highest signal strength (alongside with Kerren) (137) while Gurken and Vein exhibit tissue specific involvement (134). The inhibiting ligand Argos is also directly secreted upon high levels of Egfr signaling (138) and initiates a negative feedback loop by blocking receptor dimerization and prohibiting activating ligands from binding to Egfr (139, 140). The transmembrane protein Kekkron suppresses downstream signaling by binding to Egfr and inhibiting its dimerization (141). Additionally, the signaling pathway can

Introduction

be inhibited downstream of the receptor by the receptor tyrosine kinase inhibitor Sprouty, which is proposed to have multiple intersections with the Egfr signaling pathway (142). Upon binding of an activating ligand, Egfr dimerizes and trans-autophosphorylates its intracellular tyrosine kinase domain. The phosphorylation recruits Drk which interacts with Sos to promote guanosine triphosphate (GTP) binding and phosphorylation of Ras. The phosphorylation proceeds *via* Raf and MEK to MAPK and finally regulates target gene transcription *via* Pointed (Pnt) and Yan. Dephosphorylated Yan blocks Pnt target gene binding sites and suppresses target gene expression. Yan is released upon Egfr signaling (138) exposing Pnt binding sites and facilitating Pnt-mediated target gene expression.

1.3.3. The intestine of *Drosophila*

The *Drosophila* intestine shares great structural and functional similarities with the mammalian intestine (Fig. 1.7). The digestive tract can be divided into three regions based on the origin of the tissue. The foregut and hindgut are of ectodermal origin, whereas the midgut is of endodermal origin. The midgut is an epithelial monolayer surrounded by visceral muscle and lined with an inner protective mucus layer in mammals or a chitinous peritrophic matrix in *Drosophila* (143), and serves as the first line of defense against microorganisms.

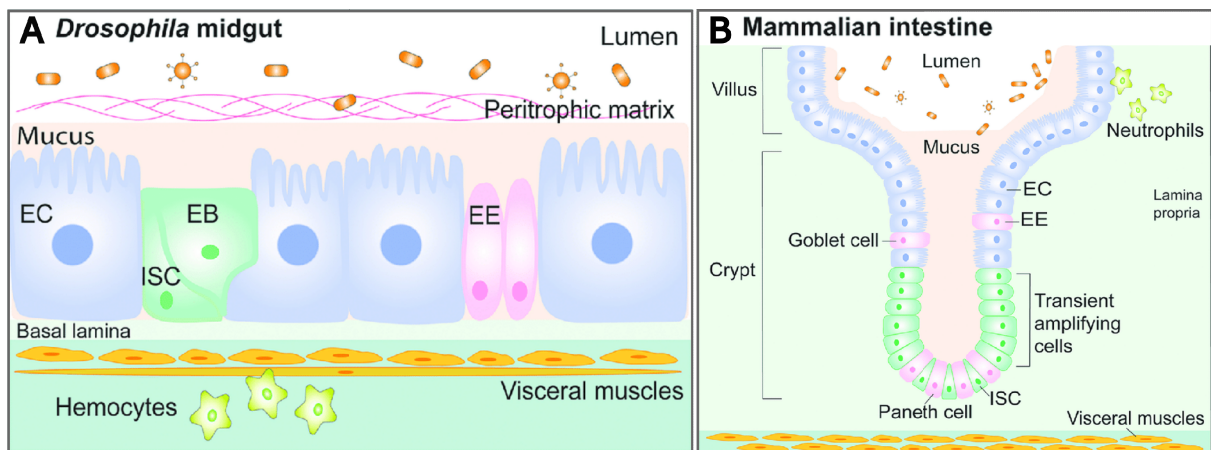


Fig. 1.7: Comparison of *Drosophila* and mammalian intestinal tract. (A) The *Drosophila* intestine is composed of intestinal stem cells (ISC), pluripotent enteroblasts (EB), absorptive enterocytes (EC) and secretor enteroendocrine cells (EE). The monolayer is protected by a chitinous peritrophic matrix towards the lumen and surrounded by visceral muscle towards the body cavity. (B) Mammalian crypts contain ISCs and niche factor providing Paneth cells. ISCs divide into pluripotent transit amplifying cells which then give rise to all other cell types including secretory Goblet and EE cells as well as absorptive EC (144).

Introduction

Intestinal stem cells (ISCs) are engaged in continuous epithelial renewal in mammals and fruit flies. *Drosophila* ISCs usually divide asymmetrically, giving rise to one ISC and one pluripotent enteroblast (EB) which further differentiates into either an enterocyte (EC), the main absorptive cell type, or an enteroendocrine cell (EE), the only hormone-secreting cell type in the intestine of *Drosophila* (145, 146) (Fig. 1.7 A). The mammalian digestive epithelium is made up of crypts that harbor ISCs (Fig. 1.7 B). Similarly to *Drosophila*, the ISCs self-renew and generate progenitor cells called transient amplifying cells, which further divide and differentiate into ECs and secretory cells as they proceed towards the upper crypt and villus region.

The *Drosophila* midgut can be divided into five major regions, R1 to R5 (Fig. 1.8 A) which can be further subcategorized by multiple features allowing for varying levels of complexity in subclassification (Fig. 1.8 B) (147, 148). Ingested food is temporarily stored in the crop before it passes the sphincter-like proventriculus and enters the anterior midgut. The anterior midgut (R1 and R2) is mildly alkaline and initiates digestion by secreting digestive enzymes. The middle midgut (R3) functionally resembles the stomach with an acidic milieu (149), providing an optimal pH for proteolysis while enabling lipid and metal uptake as well as eliminating microorganisms (148). The posterior midgut (R4 and R5) is again mildly alkaline and facilitates nutrient uptake until it reaches the hindgut where water resorption and finally excretion of nutritional waste take place (147).

Tissue maintenance is a tightly regulated process that facilitates cellular turnover and tissue regeneration in a controlled manner. The intestinal turnover is highly depending on multiple extrinsic factors like overall health status and nutritional intake. For *Drosophila* complete homeostatic intestinal turnover is estimated to take between four days and three weeks (151–153). While the majority of ISCs divide asymmetrically during homeostasis, giving rise to one self-renewed ISC and one EB daughter cell, stochastic events frequently result in symmetric division with one ISC giving rise to either two ISCs or two EBs. However, the overall number of ISCs remains unchanged leaving the ISC pool in a state of neutral drift (154, 155). The ISC environment contains numerous factors that contribute to niche formation with signals being provided by healthy differentiated cells, dying ECs, visceral muscles and tracheae. Egfr signaling (Fig. 1.6) is a major player in homeostatic tissue renewal (132) in *Drosophila*.

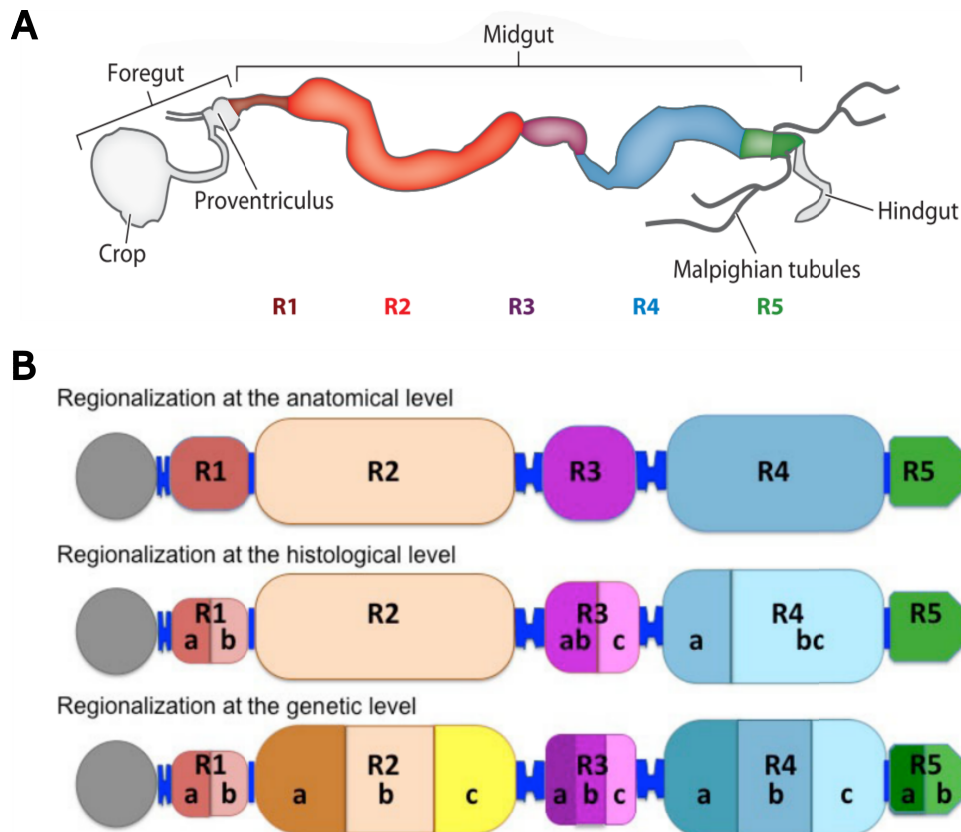


Fig. 1.8: Representation of the intestinal tract of *Drosophila melanogaster* and multiple compartmentalization schemes. (A) The foregut (including the crop and proventriculus) and hindgut are of ectodermal origin, the midgut originates from the endoderm. Malpighian tubules are renal-like organs that are derived ectodermally (148, 150). (B) The *Drosophila* midgut can be divided into multiple regions by anatomical, histological or genetic level (147).

The weak ligand Vein is secreted by cells of the visceral muscle during homeostasis whereas the strong ligands Spitz and Keren are expressed by progenitor cells and ECs, respectively (152). Cytokines stimulating the Janus kinase/Signal transducer and activator of transcription proteins (Jak/Stat) signaling pathway are produced in a similar, cell-type specific manner with the cytokines *unpaired* (*Upd*) being expressed in progenitor cells, *Upd2* in progenitor cells and ECs, and *Upd3* in ECs (156). While the natural microbiota is largely beneficial, for example by providing nutrients (157–159) or preventing fungal infections (160), dysbiotic shifts of the microbial consortium or the invasion of pathogenic bacteria give rise to potentially lethal infections, trigger regeneration in response to tissue destruction and can induce excessive intestinal proliferation (161–163). Upon disruption of tissue integrity due to invasion of pathogenic bacteria, toxins or mechanic destruction not only the homeostasis mediating Wingless, Egfr and Jak/Stat signaling pathways are activated but pathways

Introduction

involved in stress response, development or apoptosis, like the Jun N-terminal kinase (JNK) pathway, the Bone morphogenic protein (BMP) pathway and the Hippo pathway, directly or indirectly facilitate regeneration in *Drosophila* (156).

1.3.4. Nutritional sensing in *Drosophila*

The fat body of the fruit fly is the main storage organ for carbohydrates, proteins and lipids, and consists of loosely connected cells that are in direct contact with the hemolymph. Its large surface area provides maximal exchange between the adipocytes and the hemolymph. Upon ingestion, macronutrients are digested in the *Drosophila* midgut and nutrients are released into the hemolymph wherefrom they are taken up by the fat body. The fat body stores lipids and carbohydrates in the form of calorically dense triglycerides (164), which are proteolytically degraded upon nutrient scarcity and released back into the hemolymph to sustain homeostasis of distant organs. When nutrients are abundant, the fat body releases humoral factors that promote growth by activating insulin signaling. Amino acids have been shown to initiate this tissue crosstalk in a Tor signaling dependent manner (165), whereas the leptin-like peptide Upd2 (166) and the *Drosophila* insulin-like peptide 6 (Dilp6) (167) are released from the fat body in response to high levels of circulating carbohydrates and lipids (Fig. 1.9). At least eight *Drosophila* insulin-like peptides (Dilps) can be found in the fruit fly. The diversity of spatio-temporal expression patterns suggests different physiological functions including growth, development and adult tissue homeostasis (164, 168, 169). Dilps 2, 3, and 5 are produced by a cluster of 12-16 insulin producing cells (IPCs) located in the pars intercerebralis (170, 171) and are released upon Upd2 and Dilp6 signaling from the fat body (Fig. 1.9). Interestingly, Dilps not only mediate systemic growth responses but are also produced to integrate local nutritional cues. The intestine of *Drosophila* is a very plastic organ that grows and shortens upon nutritional abundance. *Dilp3* has been shown to be expressed in the visceral muscle of the *Drosophila* midgut (172) where it interacts with ISCs to promote asymmetric as well as symmetric division in order to restore gut length upon refeeding (173).

Introduction

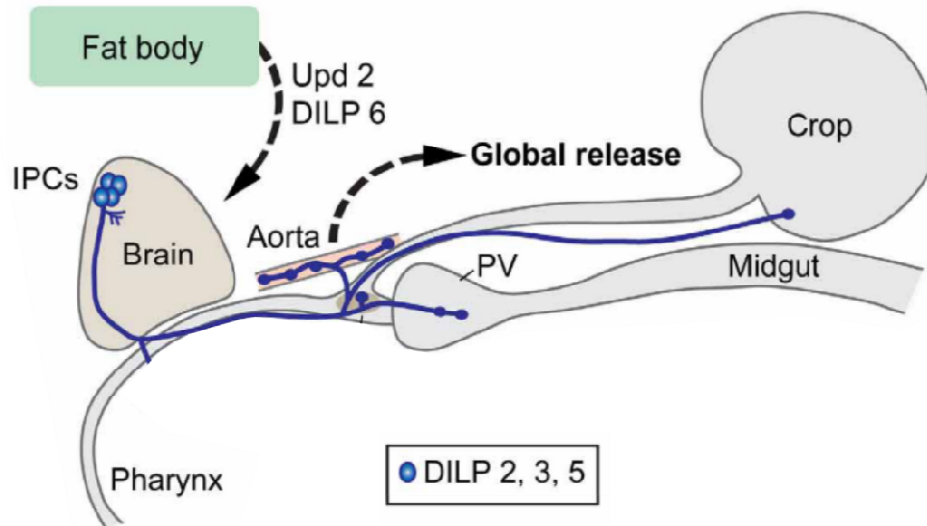


Fig. 1.9: Tissue cross-talk between brain and fat body. The fat body releases the leptin-like peptide Unpaired 2 (Upd2) and *Drosophila* insulin-like peptide 6 (Dilp6) when nutrients are abundant. The proteins in turn trigger the release of Dilp2, 3, and 5 from the insulin producing cells (IPCs) into surrounding tissues and the hemolymph. PV = proventriculus. Modified from (171).

The *Drosophila* insulin receptor (IR), like its mammalian counterpart, is a receptor tyrosine kinase composed of two extracellular α -subunits and two transmembrane β -subunits (174). Upon binding of Dilp2, 3, or 5 to the α -subunits of the receptor, the β -subunits autophosphorylate and subsequently phosphorylate the insulin receptor substrate (IRS) Chico (Fig. 1.10). On the one hand, activated Chico recruits Downstream of receptor kinase (Drk) which in turn interacts with Son of sevenless (Sos) to phosphorylate Rat sarcoma (Ras). This activation of the MAPK signaling pathway influences cellular processes like cell proliferation and differentiation (175).

On the other hand, activated Chico recruits Phosphatidylinositol-3-kinase (Pi3K) which phosphorylates phosphatidylinositol-4,5-bisphosphate (Pip2) to phosphatidylinositol-3,4,5-trisphosphate (Pip3), a process that can be reversed by Phosphatase and tensin homolog (Pten) (176). Phosphoinositid-dependent protein kinase (Pdk) subsequently phosphorylates Akt (also known as Protein kinase B (Pkb)) in a Pip3-dependent manner (177). Akt regulates cellular responses in a twofold manner. Firstly, Akt phosphorylates Foxo, thereby preventing the transcription factor from translocating into the nucleus (178). Foxo acts as a regulator of a multitude of cellular responses including DNA repair, stress resistance, cell cycle arrest and apoptosis (179) and modulates transcription by activating the transcriptional inhibitor 4E-binding protein (4E-BP) (180). Furthermore, upon nutrient scarcity Foxo induces 4E-BP as a

Introduction

translational brake and upregulates the IR to increase Dilp sensitivity (105, 181, 182). Secondly, Akt phosphorylates Tuberous sclerosis 1-2 (Tsc1-2), thereby releasing its inhibition of Tor (183). The Tor signaling pathway is a key regulator of protein biosynthesis and cell proliferation. Tor regulates transcription by repressing the translational inhibitor 4E-BP and by facilitating ribosome biogenesis *via* S6 kinase (S6K). Besides its indirect activation through the insulin signaling pathway, Tor can be directly activated by amino acids which are imported by the Slimfast transporter (184).

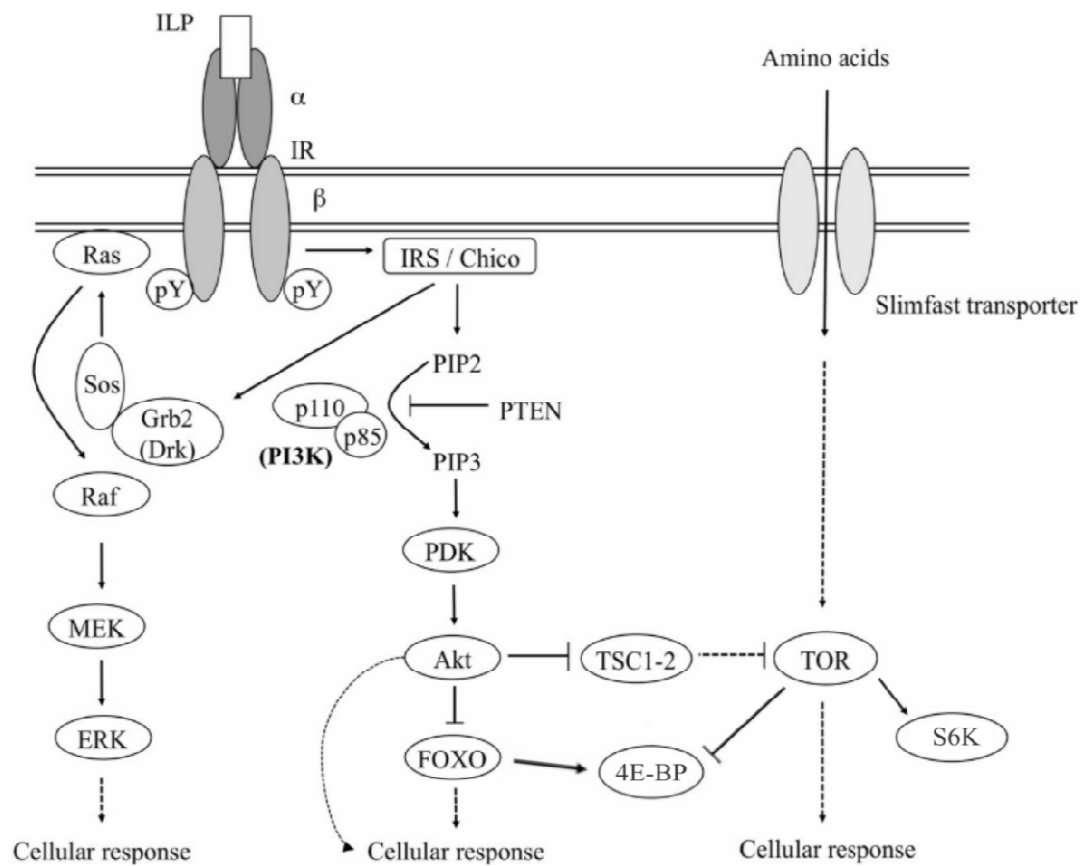


Fig. 1.10: Nutritional sensing and growth regulation in *Drosophila melanogaster*. When nutrients are abundant, insulin-like peptides (ILPs) bind to the insulin receptor (IR) and activate the mitogen-activated protein kinase (MAPK) signaling pathway *via* Rat sarcoma (Ras) as well as the PI3K signaling pathway to induce cellular responses. Target of rapamycin (TOR) dependent cell proliferation can be activated by either PI3K signaling or directly by amino acids imported through Slimfast. Dashed lines indicate interactions with non depicted intermediates. For detailed pathway descriptions see text. ILP: insulin-like peptide; IR: insulin receptor; Ras: rat sarcoma; Sos: son of sevenless; Drk: downstream of receptor kinase (Grb2: growth factor receptor bound protein 2, mammalian homolog); Raf: rat fibrosarcoma; MEK: mitogen-activated ERK-activating kinase; ERK: extracellular signal regulated kinase; IRS: insulin receptor substrate; PIP2: phosphatidylinositol-4,5-bisphosphate; PIP3: phosphatidylinositol-3,4,5-trisphosphate; PTEN: phosphatase and tensin homolog; PI3K: posphatidylinositol-3-kinase; PDK: phosphoinositide-dependent protein kinase; FOXO: forkhead box O; TSC1-2: tuberous sclerosis 1-2; TOR: target of rapamycin; S6K: S6 kinase. Modified from (164).

1.4. Aims of the study

Colorectal cancer remains a great burden in modern medicine with patients suffering from late stage detection, limited treatment options and high rates of cancer recurrence. In recent years nutrition has come into focus as a potential sustentative treatment prospect. It has been demonstrated that both high fat dieting and protein limited dietary restriction can provide benefits to individuals suffering from intestinal cancers. However, the results of these studies are largely inconsistent and partially contradictory. I induced epithelial overproliferation in the intestine by driving the expression of constitutively active human *RAF* (*RAF gain-of-function*, further on called *RAF^{gof}*) in ISCs in a temporally controlled manner. Upon induction, intestinal overproliferation was initiated, resulting in a tumor phenotype. I used the tumor bearing flies to address the following research questions:

1) To what extend are nutritional interventions capable of influencing the development of *RAF*-driven stem cell-derived intestinal tumors in *Drosophila melanogaster*?

- i) How does a high fat diet influence tumor development?
- ii) How does dietary restriction influence tumor development?
- iii) Does dietary restriction foster wasting?

In 2017 Romey-Glüsing et al. (185) found that the application of a recurrent feeding regime, consisting of alternating phases of subjection to dietary restriction and feeding on fully nutritious medium, was able to mimic the effects of lifelong dietary restriction and resulted in a similar extension of lifespan of *Drosophila melanogaster*. I subjected fruit flies with the *RAF*-driven stem cell-derived intestinal tumor phenotype to a recurrent dietary restriction regime to answer these questions:

2) Is it possible to mimic the effects of lifelong dietary restriction on tumor progression by applying a recurrent protein restrictive regime?

- i) How does recurrent dietary restriction influence intestinal tumor development?
- ii) Which metabolic mechanisms enable the recurrent dietary restriction to mimic lifelong dietary restriction?

2. Material & Methods

2.1. Fly husbandry

Fly lines were raised on a cornmeal based standard medium at room temperature (RT) and weekly transferred to fresh medium. Virgin females were crossed to mated males of the desired phenotype and incubated at the respective temperature and a 12 h dark/light cycle. Crossings with *esgReDDM* flies were kept at 18 °C. All other crossings were kept at 20 °C. Temperature sensitive genotypes were induced by shifting flies to 29 °C. The F1 generations were shifted to 29 °C 5-7 days post eclosion to induce the expression of UAS-dependent genes. Only mated female flies were used in assays.

Table 2.1: Used *Drosophila melanogaster* fly strains.

Name	Genotype	Origin
<i>EGT;Luc2</i>	+, <i>p{Esg-Gal4}</i> , <i>p{UAS-GFP}</i> , <i>p{tubulin-Gal80^{ts}}</i> ; <i>p{UAS-Luciferase at atp2}</i>	Michelle Markstein (126)
<i>esgReDDM</i>	+, <i>esg-Gal4</i> , <i>UAS-mCD8::GFP/CyO</i> ; <i>tubulin-Gal80^{ts}/TM6</i> , <i>UAS-H2B::RFP</i>	Maria Dominguez (153)
<i>UAS-RAF^{gof}</i>	<i>y,w,p{UAS-RAF^{gof},w+}</i> ; +; +	Michelle Markstein (126)
<i>w¹¹¹⁸</i>	<i>w[1118]</i>	Bloomington (5905)

2.2. Fly food

All assays were conducted on low-melt fly food (126) containing 1.5% agar-agar, 2% bacto yeast extract and 7% corn syrup (NM). The medium was boiled and supplemented with 1% propionic acid (10% in _{dd}H₂O) and 3% nipagin (10% in 70% EtOH) to prevent microbial growth. For the high fat diet (HF) 10% cocoa butter was added, for dietary restriction (DR) the amount of bacto yeast was reduced to 0.1%.

A standard cornmeal based medium was used for all stock flies and crossings.

Cornmeal Medium (for 500 ml)

31.25 g brewer's yeast

31.25 g cornmeal

Material & Methods

5 g	agar-agar
10 g	D-glucose, monohydrate
15 g	molasses
15 g	sugar beet syrup

Mix well and add 500 ml cold $\text{d}_2\text{H}_2\text{O}$. Bring to a boil and simmer for 15 min, autoclave and let cool to 60 °C. Add 1% propionic acid (10% in $\text{d}_2\text{H}_2\text{O}$) and 3% nipagin (10% in 70% EtOH). Pour medium into *Drosophila* culturing vials and air-dry. Store at 4 °C.

2.3. Microscopy

Microscopy was performed on dissected whole intestines and sections of vibratome-cut midguts. The Axio Imager.Z1 (Zeiss) was used for image capturing. Images were further analyzed using AxioVision (version SE64 Rel. 4.9) and ImageJ (version 1.49v) (186) software.

2.4. Luciferase assay

The Luciferase assay was performed as previously described (187) with minor modifications. After induction at 29 °C 3 adult flies per replicate were collected in 150 μl Glo Lysis Buffer (Promega, #E2661) and homogenized using a bead mill homogenizer for 2 min at 3.25 m/s. The homogenate was transferred to new reaction tubes and centrifuged for 3 min at 12.000 $\times g$ to pellet debris. Subsequently, the clear supernatant was transferred to fresh tubes and stored at -20 °C until further processing. For Luciferase measurement samples were thawed on ice and 50 μl were transferred to a white 96-well plate with flat, white bottom with at least one empty well between treatments. The samples were mixed with the same amount of substrate provided by the One Glo Luciferase Assay System (Promega, #E6110) right before signal detection. Luciferase signal was detected using a Tecan plate reader (Tecan, Infinite M200 Pro). A defined control was used on every plate to normalize treatments across plates.

2.5. Gut length

Whole intestines of flies induced at 29 °C for 3 days were dissected and mounted onto microscope slides. DIC pictures were taken using a fluorescence microscope (Zeiss, Axio Imager.Z1). The lengths of the guts were measured from the endodermal part of the cardia, R0, to the midgut-hindgut junction of the R5 region (147). Measurements were assessed using ImageJ (version 1.49v) (186).

2.6. Vibratome sectioning

Flies were dissected on day 3 or 10 after induction at 29 °C. After removing the head, vaginal/anal plate, wings and legs flies were fixed in 4% PFA (in S2) for at least 12 h. Flies were embedded in 7% agarose by bringing the agarose to a boil until no turbidity remained and pouring it into flexible molds. The fixed flies were directly embedded and adjusted in the agarose. Up to 4 flies were embedded into one mold. After hardening the agarose blocks were again fixed for at least 12 h and subsequently sectioned into 100 µm thick slices using a vibratome (with frequency = 80 Hz and amplitude = 0.5 mm). The sections were stained with phalloidin by applying a 1:1000 dilution (in PBS, for recipe see appendix) for 10 min and 3 times 5 min washing with PBS. The sections were mounted onto microscope slides and microscopic analyses were performed. The overall gut volume, the cell mass and the lumen volume were measured using ImageJ (version 1.49v)(186). The lumen to gut ratio was calculated subsequently.

2.7. Fecal output measurements

Fecal output was analyzed as previously described (188) with minor adjustments. Aslope fly vials were filled with NM supplemented with Brilliant Blue FCF food dye (E133, Ruth GmbH & Co.KG). Groups of three flies were collected in each vial and trapped in between the medium, a microscope cover slip and the vial's Styrofoam plug (Fig. 2.1). The flies were then incubated for 48 hours at 29 °C. The cover slips with the defecation spots were scanned, cropped to the appropriate size (Inkscape 0.92.1-64x-1) and analyzed using T.U.R.D. software (188) with Offset = 15, Min size = 50, Max size = 1000 and default settings (if not stated

Material & Methods

otherwise). Fecal spot counts were visually inspected for accuracy of analysis. The individual fecal spot sizes and quantities were assessed and used to calculate the total fecal output per fly per 24 h.

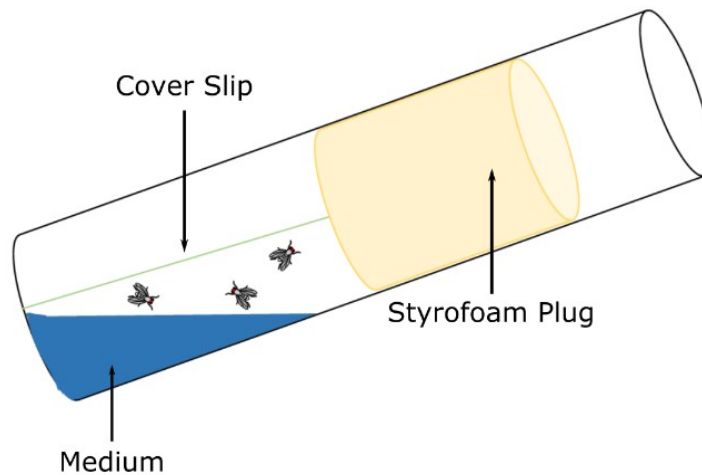


Fig. 2.1: Setup of fecal spot measurement. Flies are trapped in between medium, a microscope cover slip and a Styrofoam plug. The defecation spots on the cover slip are measured using T.U.R.D. software (188).

2.8. Transit time assay

The wells of 24-well plates were each loaded with a 16–25 mm² chunk of NM supplemented with Brilliant Blue FCF food dye (E133, Ruth GmbH & Co.KG). Individual flies, induced at 29 °C, were added to the wells and monitored every 15 min for 3 h. The appearance of the first dyed fecal spot determined the time from food ingestion to egestion per individual fly, which is referred to as transit time.

2.9. Gut integrity

Age matched fly populations of 20 individuals per replicate were incubated at 29 °C while feeding on NM supplemented with Brilliant Blue FCF food dye (E133, Ruth GmbH & Co.KG). The medium was changed every other day. Individuals with impaired gut integrity displayed leaking of the food dye into the body cavity resulting in blue colored flies. The number of the Smurf- and non-Smurf individuals (189, 190) was determined daily. Smurf

Material & Methods

phenotype was not categorized but analyzed as a binary output. Smurf as well as dead flies were removed from the population.

2.10. Bacterial DNA profiling

Flies for 16S data analyses were co-cultivated in modified cell culture flasks. Flies with a tumor phenotype and control flies were maintained in separate culture flasks joined by gauze, thereby providing an interface for bacterial exchange and homogenous access to bacteria prior to the experiment. Control and *RAF^{gof}* expressing flies were then separated for induction at 29 °C and split into vials with the respective food source. Food was exchanged according to the alternating food phases without changing the culturing flask, thereby making sure not to dilute microbial abundance through multiple passages into new vials. After days 3, 6 and 10, the midguts of 5 individuals per replicate were dissected, transferred to sterile S2 medium and homogenized for 2 min at 3.25 m/sec using a bead mill homogenizer (OMNI International, OMNI Bead Ruptor 24). DNA was extracted with the DNeasy Blood & Tissue Kit (Qiagen, #69504) following the manufacturer's protocol for *Pretreatment for Gram-Positive Bacteria*, followed by the protocol for *Purification of Total DNA from Animal Tissues*. DNA was eluted in 100 µl sterile AE buffer and stored at -20 °C until sequencing. The bacterial variable regions 1 and 2 of 16S rRNA genes were amplified as described by Rausch et al. (191). The amplicates were sequenced using the Illumina MiSeq with 2x300 bp paired-end sequencing. After assembling the reads using SeqPrep, Chimera were identified with ChimeraSlayer (192) and manual verification, Chimera were removed from the data set after manual verification. The sequences were further analyzed using QIIME 1.9.0 (193).

2.11. Dechoriation and recolonization

The parental generation of the desired F1 flies was allowed to lay eggs on a 10% apple juice agar plate glazed with a yeast/water solution. The parental generation was transferred to fresh medium and dead individuals were removed from the agar plate. The eggs were dechorionated by incubation in a 6% NaClO solution for 5 min directly on the agar plate. Eggs were loosened from the plate by gentle stroking with a sterile Drigalski spatula. Subsequently, the dechorionated eggs were washed with 99% EtOH for 2 min and sterile

Material & Methods

ddH₂O three times for 5 min. The eggs were then transferred to a sterile food vial containing the standard cornmeal-based fly food.

Culturing of *Lactobacillus plantarum*^{WJL}, *Lactobacillus brevis*^{EW}, *Acetobacter pomorum*, *Commensalibacter intestini*^{A911T} and *Enterococcus faecalis* (all received as a kind gift from Carlos Ribeiro) was performed exactly as previously detailed by Ribeiro *et al.* (194). The bacteria were then adjusted to their respective inoculation density in 50 µl PBS. For the recolonization each fly vial was provided with 50 µl of bacterial suspension. The steps including all culture media, incubation times and inoculation densities can be found in Ribeiro *et al.* (194) and online at www.protocols.io/view/growing-drosophila-gut-bacteria-hheb33e.

2.12. Survival

Age matched fly populations of 20 or 30 flies per replicate were transferred into modified cell culturing flasks and incubated at 29 °C while being submitted to the respective food regime. Dead, alive and escaped flies were counted every 2nd day, dead flies were removed from the population. Fresh food was provided at least every 4th day. Populations were monitored until all flies had deceased.

2.13. Body composition

Flies were incubated at 29 °C for the stated number of days before groups of 5 flies per replicate were collected into 2 ml screw cap tubes. Fly weight was assessed using a microbalance (ABS 80-4, Kern & Sohn GmbH). Subsequently, 1 ml of 0.1% Triton-X 100 in PBS was added and the flies were homogenized using in a bead mill homogenizer (OMNI International, OMNI Bead Ruptor 24) with three zirconium beads per tube. The homogenate was centrifuged for 3 min at 12.000 xg to pellet fly debris. The clear supernatant was transferred to new tubes and stored at -20 °C until further processing. The supernatant was used in the coupled colorimetric assay (CCA) for body fat assessment and the bicichonic acid assay (BCA) for body protein assessment. CCA was conducted as previously described (195). In a nutshell, the fly homogenate was heated to 70 °C for 5 min to inactivate enzymatic activity. Per replicate 50 µl homogenate were transferred to a 96-well plate with at least one

Material & Methods

empty well between treatments and 200 µl triglycerides (Thermo Fisher Scientific, TR22421), pre-warmed to 37 °C, was added into each well. Absorbance at 540 nm was measured before adding triglycerides and after 30 min incubation at 37 °C using a standard plate reader (LEDetect 96, Labexim Products). The protein assessment was conducted using the Pierce™ BCA Protein Assay Kit (Thermo Fisher Scientific, #23227) as directed by the manufacturer's protocol. In brief, 25 µl of the fly homogenate were transferred into a 96-well plate leaving at least one well empty between treatments. 200 µl of the working reagent (provided within the assay kit) were added into each well. The absorbance at 540 nm was measured after 30 min incubation at 37 °C using a standard plate reader (LEDetect 96, Labexim Products).

2.14. Metabolic rate assay

The basic metabolic rate was calculated using the method described by Yatsenko *et al.* (196) with minor adjustments. A chamber was set up with multiple fly respirometers. Each respirometer was composed of a microcapillary air tightly attached to a 1 ml micropipette tip. Inside the tip, slightly moistened soda lime was placed between two Styrofoam plugs. Groups of 3 flies were placed on top of the second Styrofoam plug in each respirometer. The respirometers were then sealed with plasticine and placed in a glass chamber filled with water. Two respirometers without flies were added as an atmospheric control. The CO₂ produced by the flies was absorbed by the soda lime. The subsequent low-pressure resulted in the ascend of water inside the respirometers' microcapillaries. Brilliant Blue FCF food dye (E133, Ruth GmbH & Co.KG) was used to enhance visibility of the water columns. The basic metabolic rate was quantified by measuring the ascension of the water column over two hours, which is proportional to the CO₂ produced by the flies in the respirometer during this time. The CO₂ production was calculated using the following formula:

$$\frac{(\pi * R^2) * (\Delta d - \Delta c) * 1000}{n * h}$$

R: radius of microcapillary

Δd: upper water level of sample

Δc: mean upper water level of negative controls

n: number of flies in respirometer

h: duration of assay in hours

2.15. Activity monitoring

Fly activity was measured using the *Locomotor Activity Monitor* (TriKinetics, LAM25) as previously described (197) with slight modifications. Individual flies, induced at 29 °C for 3 days, were placed in the LAM glass tubes filled with the respective medium (either NM, HF or DR). The tubes were then sealed with a Styrofoam plug and mounted into the LAM system. The LAM was set up in an undisturbed climate chamber at 29 °C with a 12 h light : 12 h dark rhythm. The flies were monitored for four days with the LAM light beam assessing the activity of the flies by detecting the number of beam crosses. The data of the first experimental day was discarded to exclude altered activity patterns due to fly handling. The data was preprocessed using the DAMFileScan software (DAMFileScan 110 Libs) prior to downstream analyses.

2.16. Feeding behavior

The ingestion rate of flies was measured using the FLIC system as previously described (198) with minor modifications. The FLIC system was assembled with 12 individual food arenas per unit, each arena providing access to the same 5% glucose solution. Single flies were placed into each arena and monitored for 2 hours. In summary, each arena consists of a food reservoir surrounded by a signal pad. Flies have to stand on the signal pad to reach the food source, thereby closing an electric circuit. Subsequently, the electric current is recorded for every individual fly, giving an exact representation of the fly's contact with the food source. The data was preprocessed using the DAMFileScan software (DAMFileScan 110 Libs) prior to downstream analyses.

2.17. RNA isolation

For RNA isolation 15 midguts per treatment were dissected in S2 medium, immediately transferred to a 2 ml screw cap tube containing 1 ml RNA Magic (Bio-Budget, #56-1000-100) and homogenized for 2 min at 3.25 m/sec using a bead mill homogenizer with 3 zirconium beads per tube. The homogenate was incubated for 5 min at RT and stored at -20 °C until further processing. Samples were thawed on ice for subsequent RNA isolation. 200 µl

Material & Methods

chloroform were added into each tube. Tubes were inverted (not vortexed) several times to provide homogenous mixing and incubated for 5 min at RT prior to 15 min centrifugation at 12.000 xg and 4 °C. The upper aqueous phase was transferred into a new tube (about 500 µl) and 500 µl 99% EtOH were added. The samples were centrifuged for 45 min at 17.000 xg and 4 °C after vigorously inverting the tubes for 30 sec. The supernatant was carefully removed and the RNA containing pellet was washed by adding 200 µl 99% EtOH and centrifuging for 5 min at 12.000 xg and 4 °C. The supernatant was completely removed and the pellet was air-dried for 3 min. The pellet was subsequently resuspended in 13 ml RNase-free ddH₂O. RNA was quantified using the Qubit 4 Fluorometer (Thermo Fisher Scientific).

2.18. Transcriptomic profiling

Flies for RNA profiling were co-cultivated in modified cell culture flasks joined by gauze prior to experimental dispatching. Upon tumor induction flies were kept in separate cell culture flasks with food being exchanged according to the feeding regime. 15 guts per replicate were dissected at day 13 after tumor induction. Subsequently, RNA was isolated as described in chapter 2.17. With TopHat (version 2.1.1) (199) quality filtered reads were mapped to the *Drosophila melanogaster* reference BDGP6. Subsequently, the Python script HTSeq (version 0.10.0) (200) was used to calculate read counts per transcript based on the gene annotation BDFP6.92. The significance of differentially expressed genes was calculated in 'R' using DeSeq2 (version 1.21.16). Euclidean distances between samples were calculated using the 'R' function "dist" and used in multidimensional scaling by the 'R' function "cmdscale". Heatmaps were generated with the 'R' function "heatmaps.2". Hierarchical clustering was used in dendrograms of heatmaps. Networks were generated using the String database (201) for protein-protein interactions (interaction score > 0.4). Venn diagrams were created using an 'R' script from Jan Taubenheim (unpublished), which is based on DeSeq2 and uses DeSeq matrices as input to calculate vector dis-/similarities. Diagrams were customized with eulerAPE on eulerr.co (202).

2.19. Bodipy staining

Intestines of flies were dissected and fixed in 4% PFA (in S2) for 1 h. After washing with 0.1% Triton-X 100 in PBS 3 times for 10 min, BodipyTM 493/503 (Thermo Fisher Scientific, #D3922) staining solution in a 1:1000 dilution (in 0.1% Triton-X 100 in PBS) was applied. The samples were incubated in the dark for 30 min at RT to avoid photobleaching of the fluorophore. The samples were washed 3 times with PBS for 5 min each and subsequently mounted onto microscope slides.

2.20. Statistics

Data were tested for normality using Shapiro-Wilks test and for homogeneity of variance using Levene test. Depending on the outcome unpaired t-test or Welch's t-test was chosen for parametric data, or Wilcoxon rank-sum test was performed for non-parametric data and datasets with low sample sizes. False discovery rate was used to correct for multiple testing. Data were either represented as boxplots or as means \pm standard error of the mean (SEM, represented by error bars in linegraphs). P-values below 0.05 were considered statistically significant. All statistics were performed using RStudio (version 1.1.453).

3. Results

3.1. Verification of the HF and DR model in healthy flies

Drosophila melanogaster is highly sensitive to nutritional interventions and has extensively been researched with studies highlighting the importance of the nature and origin of macro- and micronutrients in unison. I therefore investigated the effects of a balanced diet (NM), a 10% cocoa butter-based high fat diet (HF) and 0.1% protein limited dietary restriction (DR) for three consecutive days on metabolic parameters to validate the used nutritional model. An analysis of the flies' body compositions revealed a slight reduction in wet weight upon feeding on HF and a more severe reduction by about 25% after subjection to DR (Fig. 3.1 A). Proportional body fat, as measured by μg triacylglyceride per μg fly, was not significantly altered throughout upon either feeding regime (Fig. 3.1 B). However, changes became obvious upon staining the lipid droplets inside the intestinal cells with Bodipy. While HF fed flies displayed an increase in intracellular lipids (Fig. 3.1 E''), DR subjected flies stored less fat than NM fed controls (Fig. 3.1 E''' and E', respectively). The protein content of the flies was not altered by HF dieting but did significantly decrease upon subjection to DR (Fig. 3.1 C). Interestingly, the protein to fat ratio remained at a constant level of about 1.2 for all three tested food regimes (Fig. 3.1 D).

I further investigated the impact of HF dieting and DR subjection on physical activity by monitoring the circadian rhythm in a Locomotor Activity Monitor (LAM) (197) with a 12 h dark/light rhythm gated at 08:00 and 20:00 o'clock. Flies feeding on NM exhibited a typical circadian rhythm with one distinct morning activity peak and one evening activity peak, while minimal activity was detected throughout the rest of the day (Fig. 3.2 B). HF fed flies showed a smoothed activity pattern with higher activity throughout the day and reduced activity during peak times. Therefore, the total activity over 24 h was not altered in HF fed flies in comparison to NM fed flies (Fig. 3.2 A) albeit the shifted rhythmicity of HD fed flies. In contrast to that, the total activity over 24 h of DR subjected flies was significantly increased (Fig. 3.2 A) with activities being augmented during peak time as well as throughout the day (Fig. 3.2 B).

Results

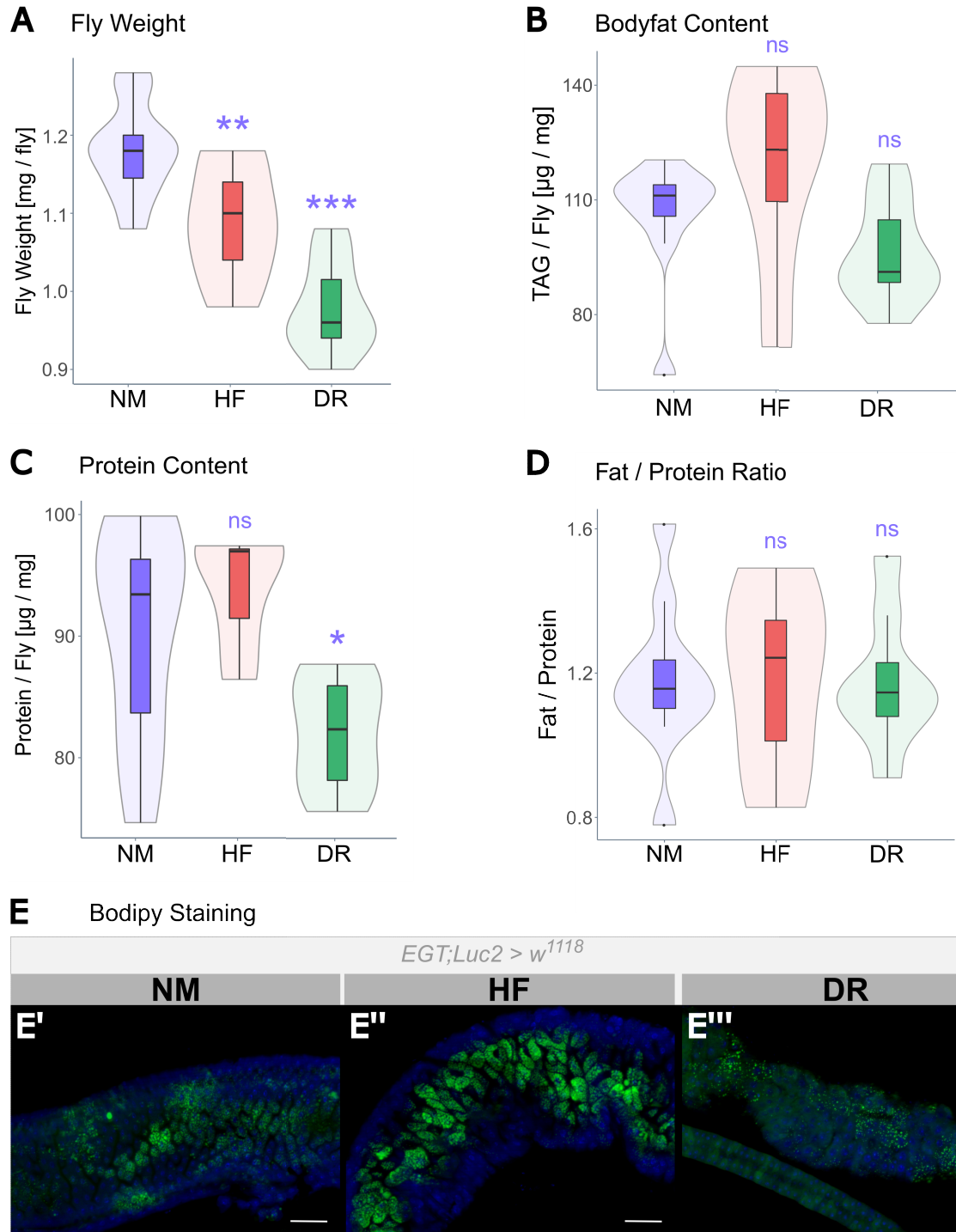


Fig. 3.1: Analysis of body composition of flies after submission to HF or DR. (A) The individual weight, (B) body fat content and (C) protein content of flies was determined 3 days after subjection to NM, HF or DR (n = 7-10). (D) The fat to protein ratio was subsequently calculated (n = 7-10). (E) Bodipy was used to stain lipid droplets in the midguts of flies 3 days after subjection to NM, HF or DR (n = 7-10). Genotype: *EGT;Luc2 > w¹¹¹⁸*, NM = normal medium, HF = high fat medium, DR = dietary restriction medium, TAG = triacylglyceride. ns = not significant, * p < 0.05, ** p < 0.01, *** p < 0.001. Asterisks' colors represent partner for comparison.

Results

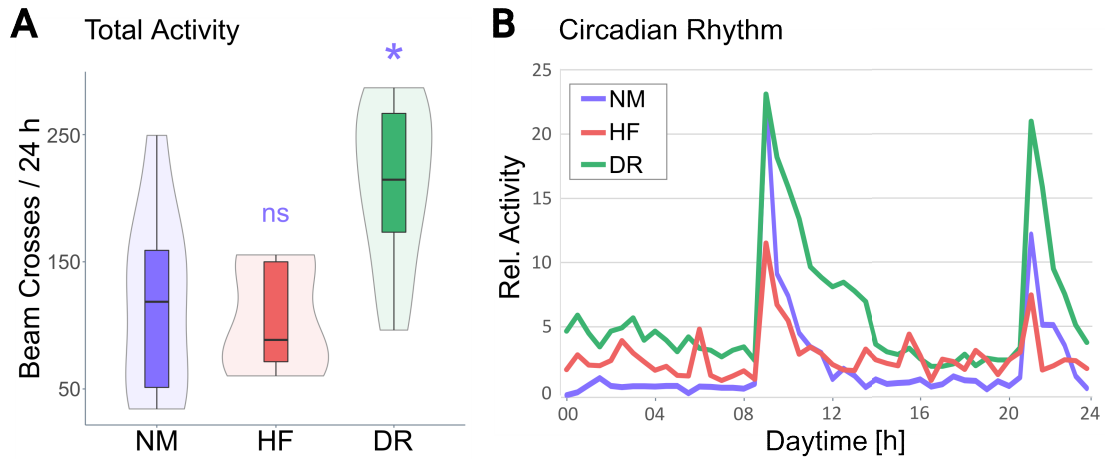


Fig. 3.2: Activity and circadian rhythm of flies after submission to HF or DR. Flies were subjected to NM, HF or DR and monitored for 3 consecutive days. (A) The total activity was calculated and (B) the circadian rhythm recorded (n = 5-11). Genotype: *EGT;Luc2 > w¹¹¹⁸*, NM = normal medium, HF = high fat medium, DR = dietary restriction medium. ns = not significant, * p < 0.05. Asterisks' colors represent partner for comparison.

DR is defined as a reduction in nutritional available protein, which directly influences nutrient-mediated cell proliferation. Therefore, I tested a range of protein concentrations (provided *via* yeast) on intestinal overproliferation to validate the DR regime. The used *Drosophila* model induces proliferation by ectopically expressing *RAF^{gof}* in intestinal stem cells (ISCs) and enteroblasts (EBs) with co-expressed *Luciferase* enabling the quantification of the overproliferation. Control flies showed an equal amount of proliferation when fed with 0.1% and 2% of yeast and a significantly higher proliferation when fed with 5% and 7.5% yeast. In flies with overproliferating ISCs and EBs an increase of the nutritional yeast content was directly reflected by an increase in proliferation with one steep increase from 0.1% to 2% and one from 5% to 7.5% yeast content (Fig. 3.3). The flies ectopically expressing *RAF^{gof}* in ISCs and EBs exhibited a higher level of intestinal proliferation in regard to every tested yeast concentration with about a 5- to 9-fold increase from 0.1% to 7.5% yeast, respectively (Fig. 3.3).

Results

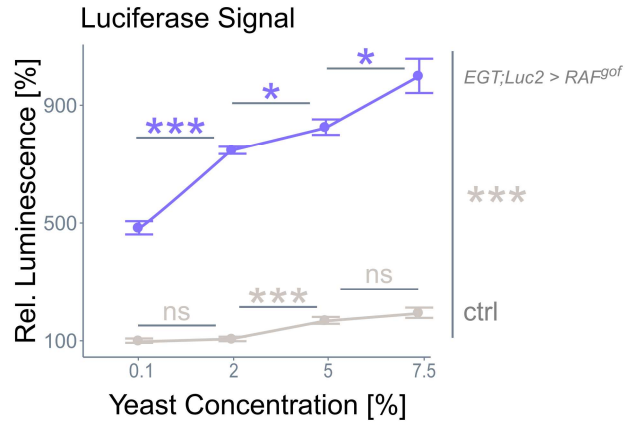


Fig. 3.3: Luciferase signal of esg^+ cells in control flies and flies with intestinal overproliferation after subjection to different yeast concentrations. The effect of nutritional yeast content on midgut intestinal stem cell proliferation was measured *via* esg^+ cells ectopically expressing Luciferase. The proliferation was assessed for control and tumor bearing flies ($n = 8$). ctrl = $EGT;Luc2 > w^{1118}$, ns = not significant, * $p < 0.05$, *** $p < 0.001$. Asterisks' colors represent partner for comparison.

3.2. The effects of HF and DR on the development of intestinal tumors

3.2.1. Gut morphology upon RAF^{gof} induction in ISCs and EB

Previous studies have established a gain-of-function isoform of the human *RAF* gene (RAF^{gof}) to induce overproliferation of intestinal cells when expressed in *Drosophila* intestinal progenitor cells (ISCs and EBs which are marked by the expression of *esg*) (126). I used the ReDDM cell lineage tracing system (153) to visualize the progress of the overproliferation induced by RAF^{gof} expression in these intestinal progenitor cells. The system makes use of two fluorescent proteins with dissimilar half-lives. Upon temperature sensitive induction, the *esg*-Gal4 driver leads to the accumulation of GFP in the cytoplasm and RFP in the nucleus of ISCs and EBs. During differentiation GFP fades over time and RFP remains in the differentiated intestinal cells for up to 3 weeks (203). The ReDDM system thereby not only enables tracing of cell ancestry but also reports on the cells' ability to differentiate or maintain stem cell properties.

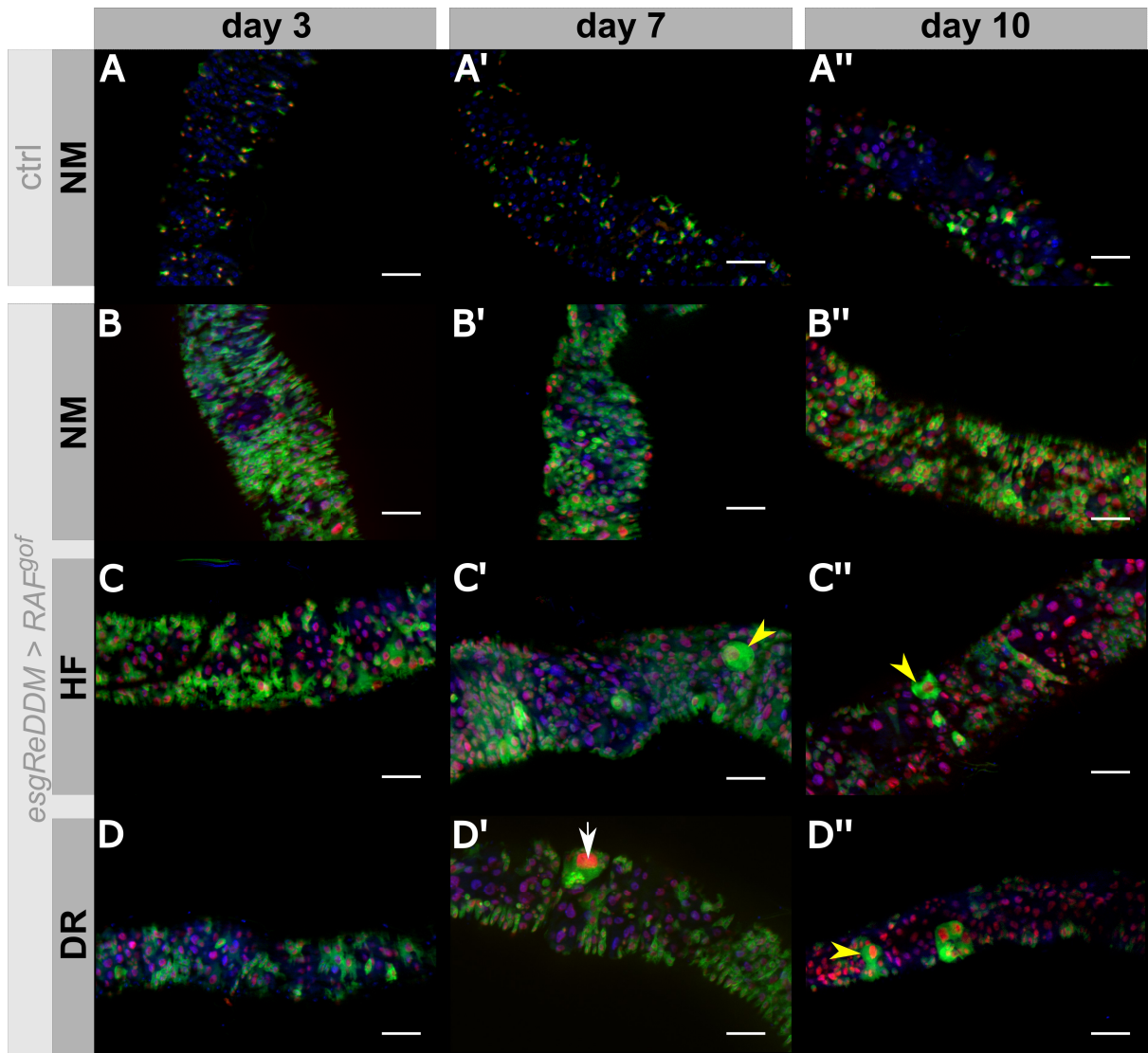


Fig. 3.4: Lineage tracing in the R2 midgut region of control flies and flies expressing RAF^{gof} in ISCs and EBs. Control flies and flies expressing RAF^{gof} were shifted to 29 °C to induce overproliferation and dissected on days 3, 7 and 10 (depicted region: R2, scale bar 50 μ m). The ReDDM system (153) identifies ISCs and EBs with nuclear RFP as well as cytoplasmic GFP. During differentiation the short lived GFP fades, therefore, differentiated cells retain only RFP. Note the formation of large individual cells in HF and DR subjected flies (yellow arrowheads) as well as the oversized nuclei in DR subjected flies (arrow). ctrl= control ($esgReDDM > w^{1118}$), ISC: intestinal stem cell; EB: enteroblast; NM: normal medium; HF: high fat medium; DR: dietary restriction medium; GFP: green fluorescent protein, green; RFP: red fluorescent, red protein; DAPI: nuclei, blue.

I used the ReDDM reporter system to monitor the development of RAF^{gof} -induced overproliferation in ISCs and EBs in 3 different regions of the intestine. While basic homeostatic proliferation was visible as interspersed ISCs and EBs in midguts of control flies (Fig. 3.4 A-A''), overproliferation was obvious in flies expressing RAF^{gof} in esg^+ cells (Fig. 3.4 B-B''). The accumulation of progenitor cells was observed in all feeding regimes (NM, HF and DR), at all time points and across all examined intestinal regions (Fig. S1, Fig. S2). It

Results

is noteworthy, that within the esg^+ cell accumulations single progenitor cells stood out by their massively increased cell size (Fig. 3.4 C-D'', yellow arrowheads) and nucleus size (Fig. 3.4, D', white arrow). This phenotype was observed only in flies subjected to HF or DR. The fluorescent signal was strongest on day three and slightly regressed in HF and DR subjected flies over time (Fig. 3.4, C-D''). All treatments displayed cells with RFP but without GFP indicating the maintained ability of progenitor cells to differentiate into ECs or EEs.

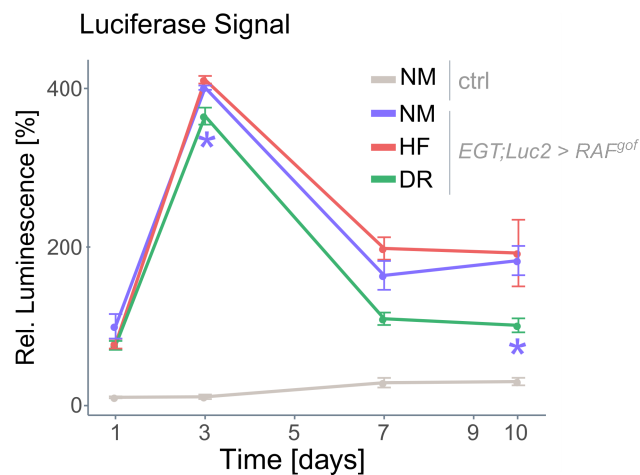


Fig. 3.5: Quantification of RAF^{gof} co-expressed Luciferase. The amount of the esg^+ cell mass was measured in control and RAF^{gof} expressing flies via co-expressed Luciferase (n = 5). ctrl = control ($w^{1118} > EGT;Luc2$), NM: normal medium; HF: high fat medium; DR: dietary restriction medium. * $p < 0.05$. Asterisks' colors represent partner for comparison.

The used *Drosophila* model for intestinal overproliferation was first established by Markstein *et al.* in 2014 (126). It induces the overproliferation of ISCs and EBs of the intestine by expressing RAF^{gof} in these cells. The co-expression of *GFP* and Luciferase facilitates the microscopic as well as molecular quantification of the proliferation. The proliferation was induced for 1, 3, 7 or 10 days and measured accordingly. As depicted in Fig. 3.5 the Luciferase signal was about four times higher on day 3 than on the other days measured. Subjection to DR significantly reduced proliferation over time while feeding on NM or HF resulted in similar Luciferase signal strength. It is noteworthy, that Luciferase signal was about 100 to 400 times stronger in RAF^{gof} expressing flies than in control flies reflecting the highly proliferative state of the tissue (Fig. 3.5).

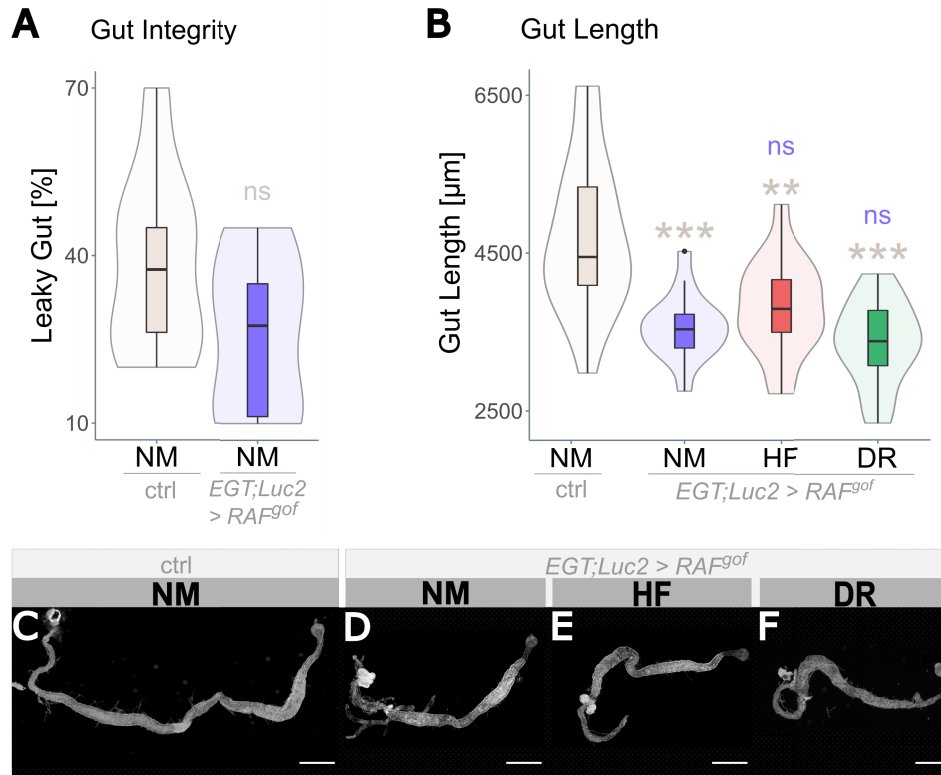


Fig. 3.6: Effects of RAF^{gof} induction in ISCs and EBs on gut length and integrity. (A) The smurf-assay (189) was performed to investigate whether RAF^{gof} -induced overproliferation of ISCs and EBs leads to a compromised gut integrity (n= 10). (B) The gut length of control flies and flies expressing RAF^{gof} in ISCs and EBs after subjection to NM, HF or DR (n = 17-19), (C-F) exemplary images of the whole intestines are displayed. ISC: intestinal stem cell; EB: enteroblast; ctrl = control ($w^{1118} > EGT;Luc2$); NM: normal medium; HF: high fat medium; DR: dietary restriction medium. ns: not significant; ** p < 0.01; *** p < 0.001. Asterisks' colors represent partner for comparison.

Uncontrolled cell proliferation can lead to the disruption of cellular structures and the evasion of cells into surrounding tissues. Flies expressing RAF^{gof} in progenitor cells were fed with NM supplemented with a blue dye to monitor the development of the gut integrity over time. Upon disruption of the intestinal epithelial monolayer, the blue dye leaked into the body cavity, resulting in blue colored flies referred to as “Smurf” flies (189). The observed populations of flies expressing RAF^{gof} in progenitor cells as well as the control populations did not exhibit significant differences in the percentage of “Smurf” flies (Fig. 3.6 A), indicating, that gut integrity was maintained albeit the massive intestinal overproliferation in flies expressing RAF^{gof} in ISCs and EBs. However, flies with the overproliferative phenotype displayed a significant shortening of the midgut independent of the food source (Fig. 3.6 B-F).

Results

Since the induction of the proto-oncogene *RAF* in intestinal progenitor cells induced massive proliferation (Fig. 3.4 B-D'', Fig. 3.5) and gut shortening at the same time (Fig. 3.6 B-F), I further explored the impact of the cell accumulations on the gut structure. Flies were embedded and cross sectioned after inducing *RAF^{gof}*-driven proliferation in progenitor cells for 3 consecutive days.

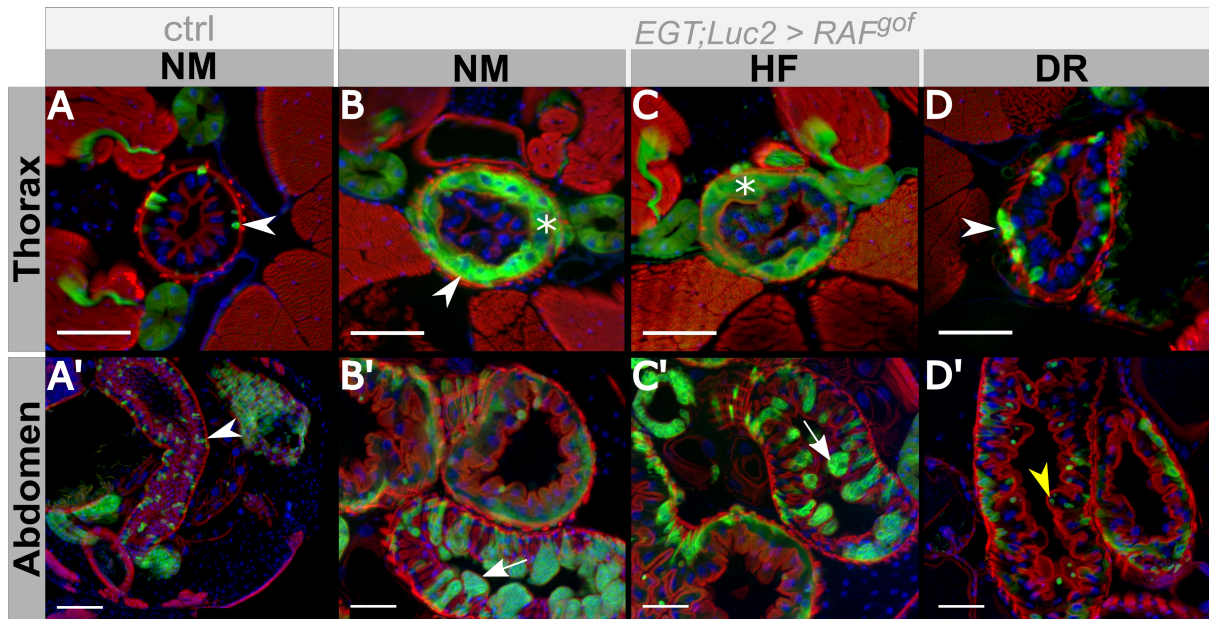


Fig. 3.7: The expression of *RAF^{gof}* in *e sg⁺* cells results in a tumor phenotype. Control and *RAF^{gof}* expressing flies were sectioned 3 days after induction. (A-D) Sagittal sections through the thorax of control and *RAF^{gof}* expressing flies. Note the ISCs and EBs attached to the basal membrane (white arrowheads) and the excessive *e sg⁺* cell mass (asterisk). (A'-D') Sagittal sections through the abdomen of control and *RAF^{gof}* expressing flies. Note the cell accumulations protruding into the lumen (arrows) and the *e sg⁺* cells detached from the basal membrane (yellow arrowheads). ISC: intestinal stem cell; EB: enteroblast; ctrl: control (*w¹¹¹⁸ > EGT; Luc2*); NM: normal medium; HF: high fat medium; DR: dietary restriction medium. GFP: *e sg⁺* cells, green; DAPI: nuclei, blue; Phalloidin: actin, red.

Thoracic sections of control flies displayed a rather homogenous cellular structure of large *e sg⁻* cells regularly interspersed with small *e sg⁺* cells attached to the basal lamina (Fig. 3.7 A, white arrowhead). In contrast, the sections through *RAF^{gof}* expressing intestines of flies feeding on NM or HF showed a clear deviation from this distinct structural layout. The *e sg⁺* cell mass formed an additional outer cell layer superseding the *e sg⁻* cells into the intestinal lumen (Fig. 3.7 B and C, asterisk). It appears that the *e sg⁻* cell mass was no longer in direct contact with the basal membrane. Interestingly, flies subjected to DR did not exhibit the formation of excessive cell mass to the same extent as NM fed flies (Fig. 3.7 B' and D)

Results

although the phenotype was highly diverse. The abdominal intestine of flies expressing *RAF^{gof}* in ISCs and EBs depicted a largely heterogenic phenotype. However, the intestines were clearly distinguishable from control intestines. While intestines of control flies again exhibited limited numbers of regularly spaced *esg⁺* cells, the *esg⁺* cell mass was unproportionally increased in *RAF^{gof}* expressing flies. These flies displayed proliferative tissue pushing into the gut lumen in tight cell clusters when feeding on NM or HF (Fig. 3.7 B' and C'). However, the phenotype was less severe in *RAF^{gof}* expressing flies subjected to DR where only singularized cells lost contact to the basal membrane and translocated towards the gut lumen (Fig. 3.7 D', yellow arrowhead).

The extent of protrusion of the additional cell mass in the thoracic intestine of *RAF^{gof}* expressing flies was quantified by measuring a) the overall gut volume, b) the lumen volume, c) the cell mass and d) the lumen to gut ratio. As indicated by the microscopic analysis of the intestinal cross sections, the gut volume as well as the cell mass was significantly increased in flies expressing *RAF^{gof}* in intestinal progenitor cells when feeding on NM or HF (Fig. 3.8 A and C). The subjection to DR reduced both parameters back to the level of control flies (Fig. 3.8 A and C). The mean luminal volume, a measure for the absolute gut diameter and thus for general intestinal passability, was slightly but not significantly reduced in flies with an overproliferation phenotype regardless of the food source (Fig. 3.8 B). Interestingly, the lumen to gut ratio, which served as a measure for relative gut obstruction was reduced in NM and HF feeding flies upon induction of overproliferation, whereas the obstruction was normalized to the control level by subjection to DR (Fig. 3.8 D).

In summary, the expression of *RAF^{gof}* in ISCs and EBs of the *Drosophila* midgut results in disproportionate proliferation of *esg⁺* cells (Fig. 3.4 , Fig. 3.5, Fig. 3.7) and the protrusion of the excessive cell mass into the gut lumen (Fig. 3.7, Fig. 3.8). 3 days after induction of overproliferation the intestines of tumor bearing flies are significantly shorter than intestines of control flies (Fig. 3.6 B-F) with protruding cell mass leading to a relative obstruction of the thoracic midgut (Fig. 3.7 D). Therefore, flies of the overproliferative genotype *EGT;Luc2 > RAF^{gof}* will further on be referred to as tumor bearing flies.

Results

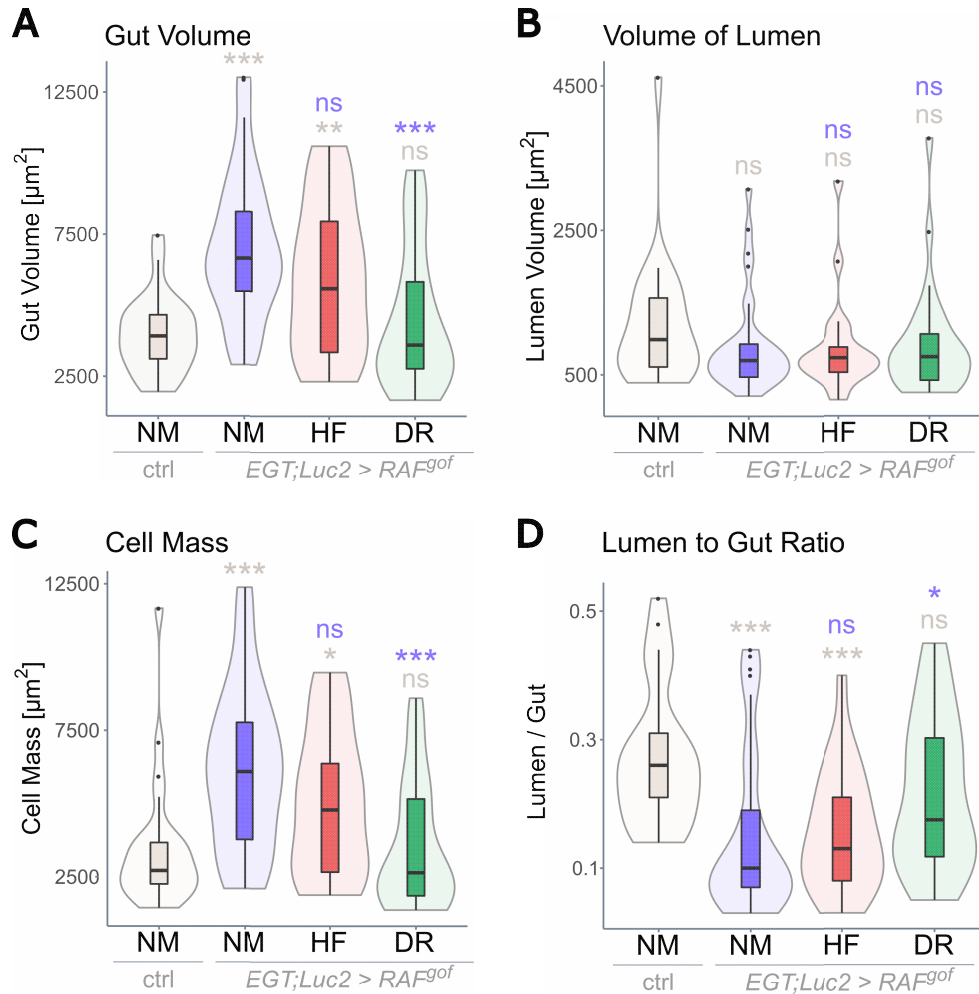


Fig. 3.8: Volume and relative obstruction of the intestine through excessive cell mass. The sagittal sections through the thorax of control and tumor bearing flies subjected to NM, HF or DR were used to measure (A) the total outer gut volume, (B) the volume of the gut lumen, (C) the total cell mass and (D) the lumen to gut ratio (n = 21-33). While the lumen volume displays the absolute intestinal constriction, the lumen to gut ratio represents the relative obstruction after 3 days of tumor induction. ctrl = control ($w^{1118} > EGT;Luc2$), NM = normal medium, HF = high fat medium, DR = dietary restriction medium. ns = not significant, * $p < 0.05$, ** $p < 0.01$, *** $p < 0.001$. Asterisks' colors represent partner for comparison.

3.2.2. Effects of RAF^{gof} -induced tumors on digestion

The expression of RAF^{gof} in intestinal progenitor cells resulted in the formation of solid tumors in the midgut of *Drosophila melanogaster* which inherently implies a possible impairment of intestinal functionality. Therefore, I investigated the effects of subjecting tumor bearing flies to NM, HF and DR on digestive parameters. The feeding behavior of tumor bearing and control flies was measured using the Fly Liquid-Food Interaction Counter (FLIC) (198). Flies were subjected to their respective feeding regime and tumors were induced for 3 consecutive days prior to the assay. During the assay all flies were supplied with the same 5%

Results

D-glucose solution to provide an evenly attractive food source for all feeding regimes. Tumor bearing flies showed an unaltered feeding behavior when fed with NM or HF but fed significantly more often when subjected to DR prior to the experiment (Fig. 3.9 A). Since the excessive tumor mass led to a shortening and a relative obstruction of the intestines of tumor bearing flies (Fig. 3.6, Fig. 3.8), the transit time through the gut was assessed. The experiment was set up similarly to the FLIC analysis with flies feeding on their respective food regimes for 3 days during tumor induction. They were subsequently entered into the transit time assay where all treatments were supplied with the same blue dyed food source. The time from starting the experiment until the first excretion of blue fecal spots was defined as gut transit time. While tumor induction did not affect the transit time of NM or HF fed flies in comparison to NM fed control flies, DR significantly increased the gut transit time of tumor bearing flies (Fig. 3.9). The T.U.R.D. software was used to assess the fecal output of control and tumor bearing flies. The software automatically assesses the fecal spot abundance (called fecal spot quantity) as well as individual fecal spot sizes and calculates the overall excretion (called total fecal output). Tumor bearing flies exhibited reduced numbers of fecal spots with normal fecal spot sized after feeding on NM or HF (Fig. 3.9 D and E). Subjection of tumor bearing flies to DR rescued fecal spot quantity but decreased fecal spot size (Fig. 3.9 D and E). Consequently, all tumor bearing flies exhibited lower total fecal output which was due to lower fecal spot quantity in NM and HF subjected flies and due to smaller fecal spot sizes in DR subjected flies (Fig. 3.9 F).

Results

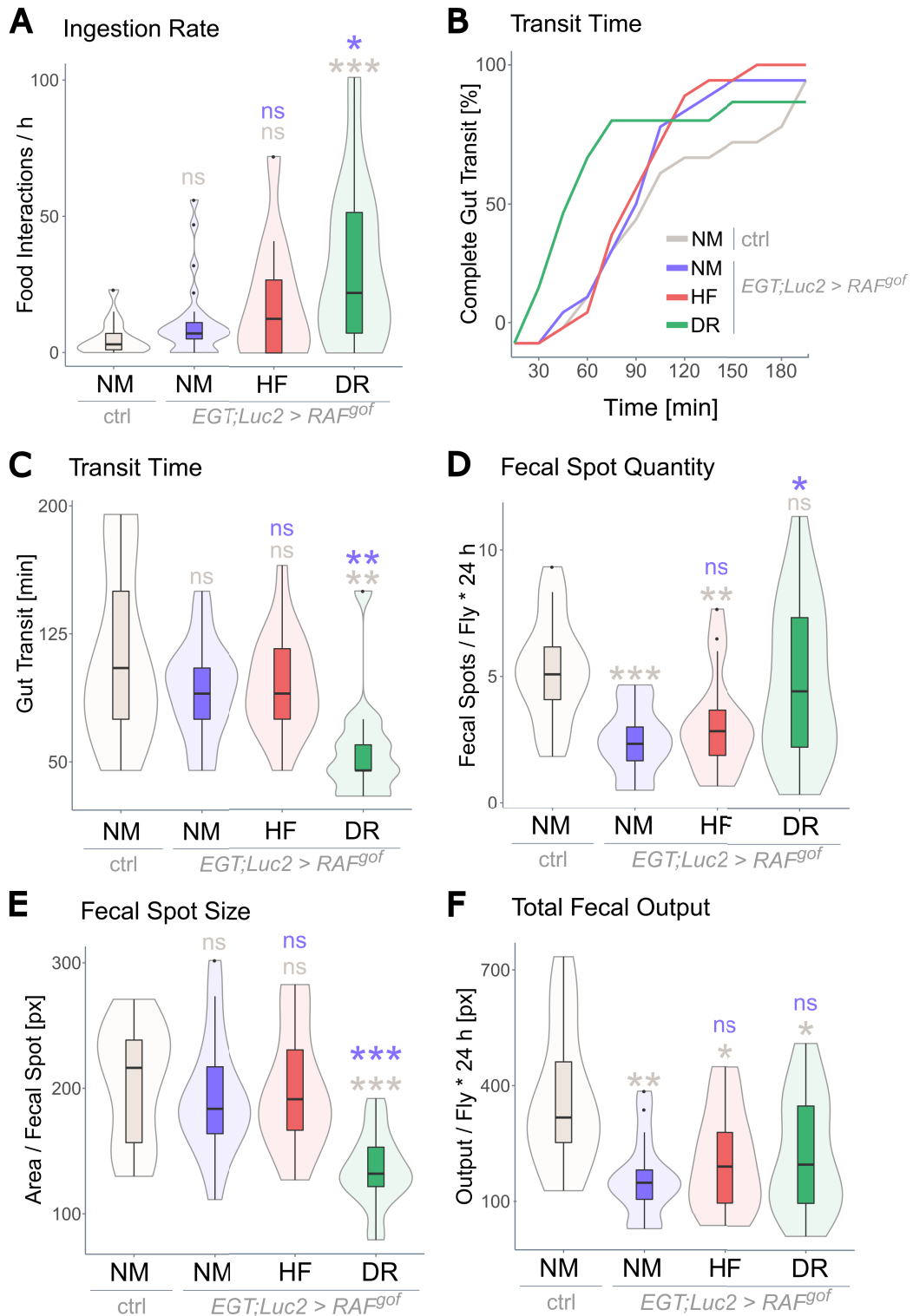


Fig. 3.9: Impact of nutritional interventions on the digestion of tumor bearing flies. (A) Food intake was measured in control and tumor bearing flies subjected to either diet. (B, C) The transit time, defined as the time from food ingestion to egestion, was assessed by providing blue colored food and monitoring the time until excretion of blue colored feces. Flies were monitored individually for 3 hours (n = 13-18). The T.U.R.D. software (188) was used to measure (D) the fecal spot quantity, (E) the individual fecal spot size and (F) the total fecal output of control and tumor bearing flies after 3 days of tumor induction (n = 9-10). ctrl = control (*w¹¹¹⁸ > EGT;Luc2*), NM = normal medium, HF = high fat medium, DR = dietary restriction medium. ns = not significant, * p < 0.05, ** p < 0.01, *** p < 0.001. Asterisks' colors represent partner for comparison.

Results

3.2.3. The impact of nutrition on the lifespan of tumor bearing flies

The excessive proliferation of ISCs in the midgut of *Drosophila melanogaster* led to the formation of cell mass protruding into the gut lumen (Fig. 3.7, Fig. 3.8 C) which in turn resulted in the relative obstruction of the intestine (Fig. 3.8 D). Additionally, the digestive functionality of tumor bearing flies was impaired irrespective of the food regime as reflected by the reduced total fecal output (Fig. 3.9 F).

Since the described obstructive phenotype was rescued by submission to DR and gut functionality was altered depending on the provided food, I monitored the effect of subjection to NM, HF or DR on the viability of flies during tumor induction.

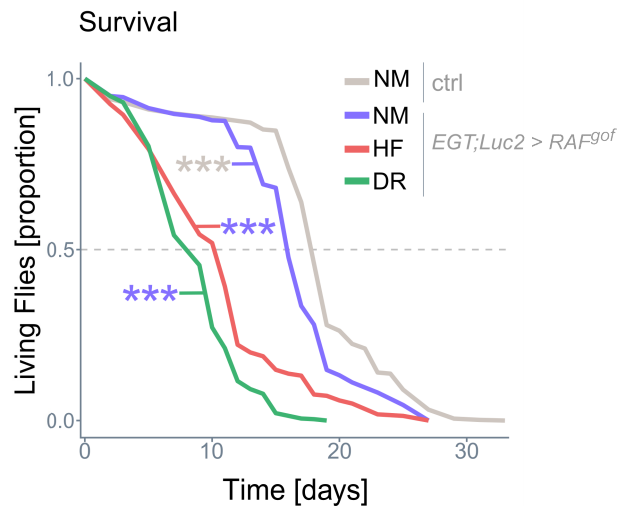


Fig. 3.10: Survival of tumor bearing flies subjected to different nutritional regimes. Flies were monitored upon tumor induction to evaluate the lifespans of control and tumor bearing flies subjected to NM, HF or DR (n = 15). ctrl = control ($w^{1118} > EGT;Luc2$), NM = normal medium, HF = high fat medium, DR = dietary restriction medium. *** p < 0.001. Asterisks' colors represent partner for comparison.

The lifespans of 15 populations of 30 individuals each were monitored until all individuals had deceased. The expression of RAF^{9of} in ISCs and EBs led to a significant reduction in lifespan with median lifespan being reduced from 19 days in controls to 16 days in NM fed flies (Fig. 3.10). The subjection to HF or DR resulted in a further reduction of median lifespan (Fig. 3.10, Tab. 3.1). Most interestingly, the submission of tumor bearing flies to DR resulted in a severe reduction of median lifespan to 9 days as compared to 16 days in NM fed flies

Results

(Fig. 3.10), albeit the observed reduction of tumor burden in DR subjected flies (Fig. 3.7 Fig. 3.8 A and C).

3.2.4. Intestinal tumors alter body composition and energy demands

The tested nutritional interventions clearly impacted tumor load and subsequently intestinal morphology of flies expressing *RAF^{gof}* in ISCs and EBs. While HF dieting neither ameliorated nor aggravated the tumor burden, subjection to DR significantly reduced tumor load (Fig. 3.7, Fig. 3.8 A and C). At the same time not only subjection to HF but also to DR drastically reduced lifespan in comparison to tumor bearing flies feeding on NM (Fig. 3.10). This observation implied a food mediated shift in metabolism. I therefore investigated the body composition of control and tumor bearing flies subjected to NM, HF or DR over the course of 10 days of tumor induction (Fig. 3.11 A).

The total wet weight per fly was measured on days 1, 3, 7 and 10 after tumor induction and revealed a mean weight of healthy flies of about 1.4 mg per fly with minor fluctuations across time. The subjection of tumor bearing flies to NM and HF both resulted in a slight decrease of fly weight over time with a weight loss of about 10% (Fig. 3.11 A). Tumor bearing flies subjected to DR exhibited a generally reduced wet weight across all measured time points as compared to NM fed flies and showed a final weight loss of about 15% after ten days of tumor induction (Fig. 3.11 A). The fat body acts as the main energy storage unit of the fruit fly. The measurement of total body fat revealed an initial reduction of body fat in NM fed tumor bearing flies upon tumor induction, followed by the normalization of the body fat content to the level of control flies over time (Fig. 3.11 B). Interestingly, subjection to HF and DR both resulted in a drastic loss of body fat at all measured time points until only about 5% body fat remained (Fig. 3.11 B). A similar pattern was detected for the flies' total protein levels (Fig. 3.11 C). While the protein content of tumor bearing flies feeding on NM was lower than that of healthy control flies on days 1, 3 and 7 it normalizes over the course of 10 days (Fig. 3.11 C). Subjection to HF or DR on the other hand, steadily reduced body protein content throughout the 10 days of tumor induction, although tumor bearing flies displayed a similar amount of protein at the beginning of tumor induction. The reduction of total protein content was most eminent in flies subjected to DR with about 50% total protein loss as compared to control and tumor bearing flies after feeding on NM for 10 days (Fig. 3.11 C).

Results

Interestingly the fat to protein ratio, which was calculated subsequently to body fat and protein measurements, drastically declined in all observed tumor fly populations with flies subjected to HF and DR exhibiting a 4-fold decline in fat to protein ratio (Fig. 3.11 D).

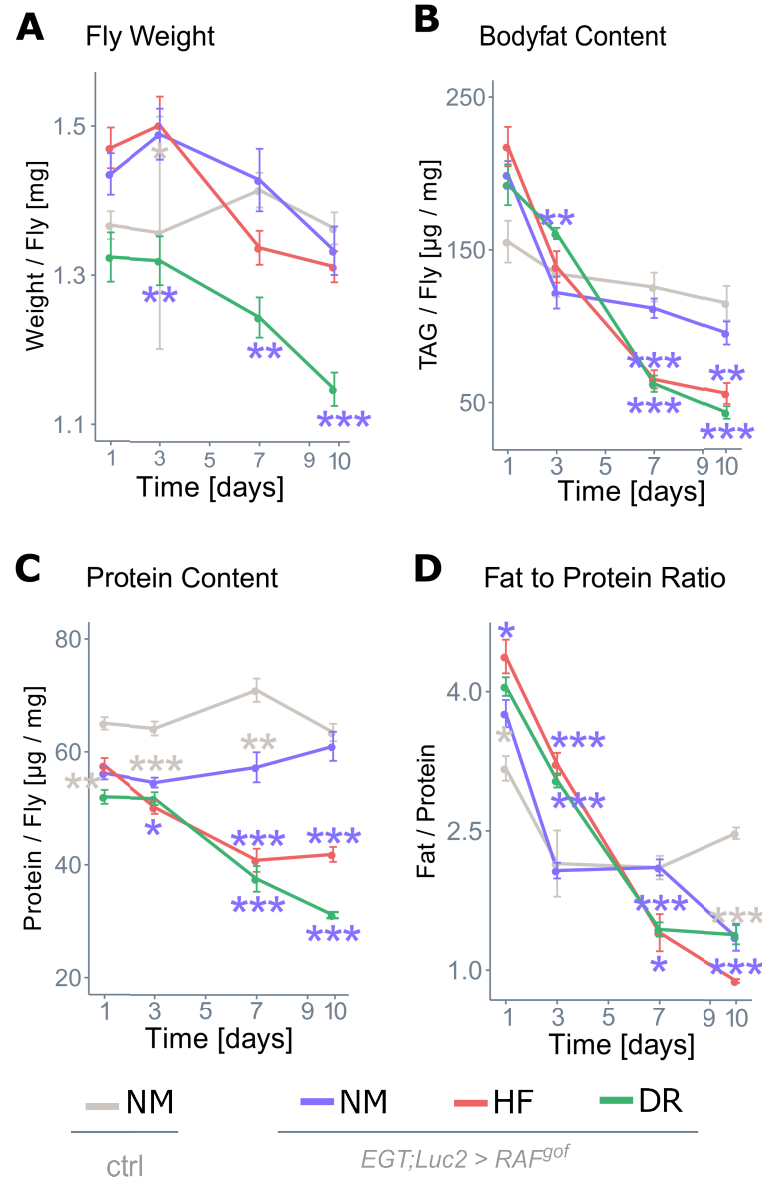


Fig. 3.11: Assessment of body composition of tumor bearing flies submitted to different nutritional interventions. The body composition of control and tumor bearing flies was measured at days 1, 3, 7 and 10 after induction. (A) The weight of control and tumor bearing flies was assessed (n = 14-17). (B) The whole body fat was analyzed *via* the triacylglyceride level (n = 14-18) as well as (C) the body protein content (n = 9-10). (D) The fat and protein levels were used to calculate the fat to protein ratios (n = 9-10). ctrl = control ($w^{1118} > EGT;Luc2$), NM = normal medium, HF = high fat medium, DR = dietary restriction medium. * p < 0.05, ** p < 0.01, *** p < 0.001. Asterisks' colors represent partner for comparison.

Results

The extensive loss of both body fat and protein implied that tumor bearing flies subjected to HF or DR experienced an accelerated energy demand. An increased energy demand can be compensated by changing the food source, increasing the food intake or lowering the energy expenditure. In this experimental setup flies could not influence their food source and only DR subjected but not HF fed flies showed compensatory feeding (Fig. 3.9 A). I therefore monitored the basic metabolic rate of control and tumor bearing flies subjected to NM, HF or DR.

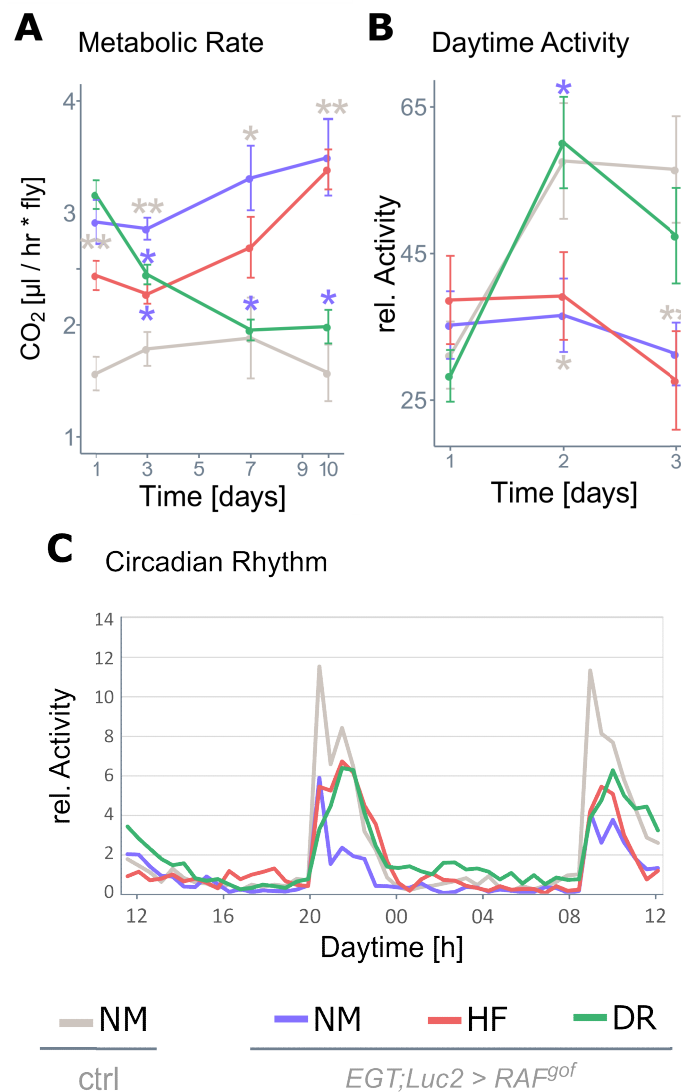


Fig. 3.12: Energy expenditure of tumor bearing flies subjected to different nutritional interventions. (A) The basic metabolic rate of control and tumor bearing flies was measured at days 1, 3, 7 and 10 after induction. Flies were shifted to 29 °C to induce tumor formation in *RAF^{gof}* expressing flies prior to activity monitoring for 3 consecutive days. (B) The total daytime activity was calculated and (C) the circadian rhythm was recorded (n = 14-42). ctrl = control (*w¹¹¹⁸* > *EGT;Luc2*), NM = normal medium, HF = high fat medium, DR = dietary restriction medium. * p < 0.05, ** p < 0.01. Asterisks' colors represent partner for comparison.

Results

Interestingly, the basic metabolic rate was higher in tumor bearing flies than in controls on day 1 after induction. However, the basic metabolic rate of NM and HF fed flies continuously increased over the 10 days of tumor induction, whereas it declined in tumor bearing flies subjected to DR and after 10 days was normalized to the control level (Fig. 3.12 A). The basic metabolic rate was measured in the afternoon during a resting phase of the flies. The flies' circadian rhythms during a 12 h dark/12 h light cycling were recorded over the course of 3 days to gain insight into the overall activity patterns and activity of tumor bearing flies subjected to NM, HF or DR. The total daytime activity measured the physical activity of individual flies during the 12 h light cycle including resting phases and activity peaks, and revealed a similar activity of all treatments at the beginning of the experiment upon 1 day of induction (Fig. 3.12 B). The daytime activity remained constant for tumor bearing flies feeding on NM or HF across the monitored time interval. In contrast, the daytime activity of control and tumor bearing flies subjected to DR was increased on days 2 and 3 after induction (Fig. 3.12 B). Analyzing the circadian rhythms of control and tumor bearing flies revealed that all flies maintained circadian rhythmicity with control flies showing the clearest distinction between high activity morning and evening peaks, and low activity resting phases throughout the rest of the day. All tumor bearing flies exhibited flatter activity peaks in the morning and in the evening compared to the controls. The tumor bearing flies subjected to DR displayed increased activity throughout the night time (from 8 pm to 8 am) and higher and longer lasting activity peaks in the morning and the evening in comparison to tumor bearing flies feeding on NM (Fig. 3.12 C).

In summary, the tumor phenotype results in substantial loss of both body fat and protein in flies subjected to HF or DR but not NM (Fig. 3.11 B and C). This points to an altered energy demand in these flies which has to be compensated for. The basic metabolic rate increased over time in HF fed tumor bearing flies, whereas it decreased in tumor bearing flies subjected to DR (Fig. 3.12 A).

3.3. The effects of a recurrent diet on the development of intestinal tumors

3.3.1. A recurrent diet prolongs the lifespan of tumor bearing flies

The expression of *RAF^{gof}* in ISCs and EBs of the midgut of *Drosophila melanogaster* produced a solid tumor with excessive cell mass protruding into the gut lumen. The tumorous cell mass led to the relative obstruction of the intestine 3 days after tumor induction and resulted in impaired gut functionality. Interestingly, the subjection of tumor bearing flies to DR rescued these phenotypes and partially restored gut functionality. However, the lifespan of tumor bearing flies was drastically reduced upon subjection to DR which can, at least in part, be attributed to the substantial loss of body fat and protein and implies an accelerated yet unmet energy demand in these flies or a deregulation of nutrition-dependent signaling.

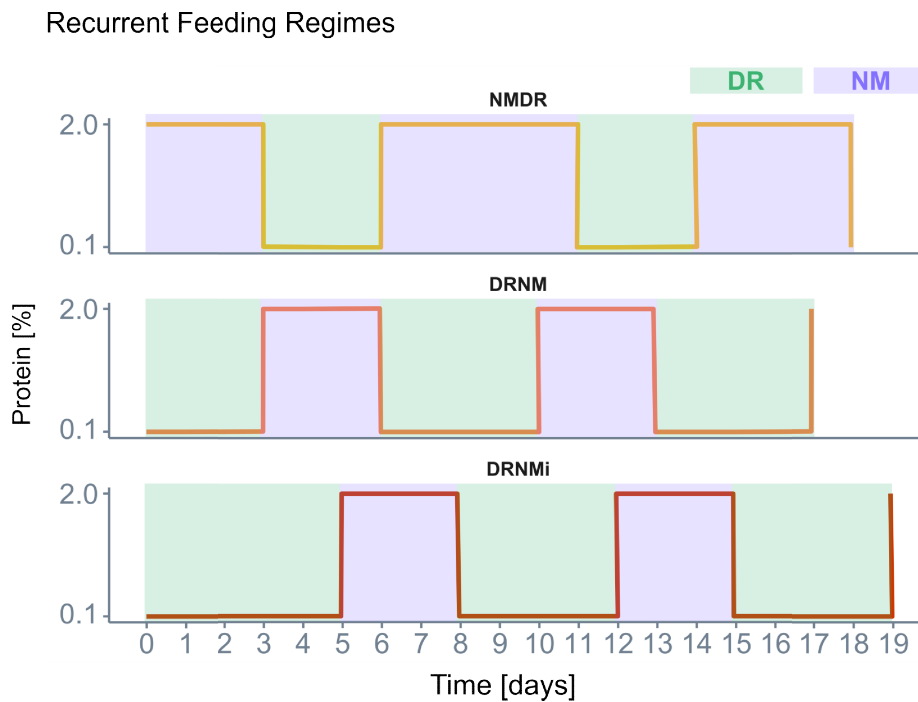


Fig. 3.13: Schematic of the investigated recurrent feeding regimes. NM = normal medium, DR = dietary restriction medium, NMDR = recurrent diet with 4 days NM + 3 days DR, DRNM = recurrent diet with 3 initial days DR followed by 3 days NM and 4 days DR, DRNMi = DRNM with 5 initial days of DR.

A recent study reported on a recurrent diet consisting of phases of protein restriction and feeding on fully nutritious medium, to be as effective in prolonging lifespan as lifelong DR (185). Therefore, I investigated the effect of 3 different diets (Fig. 3.13) on the lifespan of

Results

tumor bearing flies. The tested recurrent diets consisted of repeated cycles of i) 4 days NM, 3 days DR (referred to as NMDR), ii) 5 initial days DR, followed by cycles of 3 days NM and 4 days DR (referred to as DRNMI) or iii) 3 initial days DR, followed by cycles of 3 days NM and 4 days DR (referred to as DRNM). All 3 investigated recurrent diets significantly prolonged the median as well as the maximum lifespan of tumor bearing flies in comparison to tumor bearing flies fed with NM (Fig. 3.14 A and B, Tab. 3.1). It is noteworthy, that 5 initial days of DR resulted in a population decrease of about 30% within the first week (Fig. 3.14 A). However, the tumor bearing flies that survived the initial death phase exhibited the highest maximum lifespan of 27.2 ± 0.45 days (Fig. 3.14 B, Tab. 3.1). Tumor bearing flies subjected to DRNM restored survival back to the level of unimpaired control flies feeding on NM (Fig. 3.14 C). At the same time, control flies subjected to DRNM exhibited a 47.4% increase in median survival (median survival 28 days) as compared to control flies fed with NM (median survival 19 days) (Fig. 3.14 D, Tab. 3.1). DRNM was selected for further analyses since the regime drastically increased lifespan of control flies and rescued the lifespan of tumor bearing flies to the level of NM fed controls.

Tab. 3.1: Median and maximum lifespans of all nutritional regimes.

<i>Treatment</i>	<i>Food</i>	<i>Median lifespan [days]</i>	<i>Max. 10 % lifespan [days]</i>	<i>p-value (comparison with control NM)</i>	<i>p-value (comparison with tumor bearing NM)</i>
Control	NM	19	20.27 ± 0.44	na	0
	DRNM	28	37.71 ± 1.43	0	na
Tumor-bearing	NM	16	20.93 ± 0.86	0	na
	HF	11	16.29 ± 1.17	0	0
	DR	9	13.48 ± 0.71	0	0
	DRNM	17	23.8 ± 0.63	0.146	5.55E-16
	DRNMI	21	27.2 ± 0.45	0.421	1.13E-09
	NMDR	21	24.2 ± 0.43	0.838	0

Results

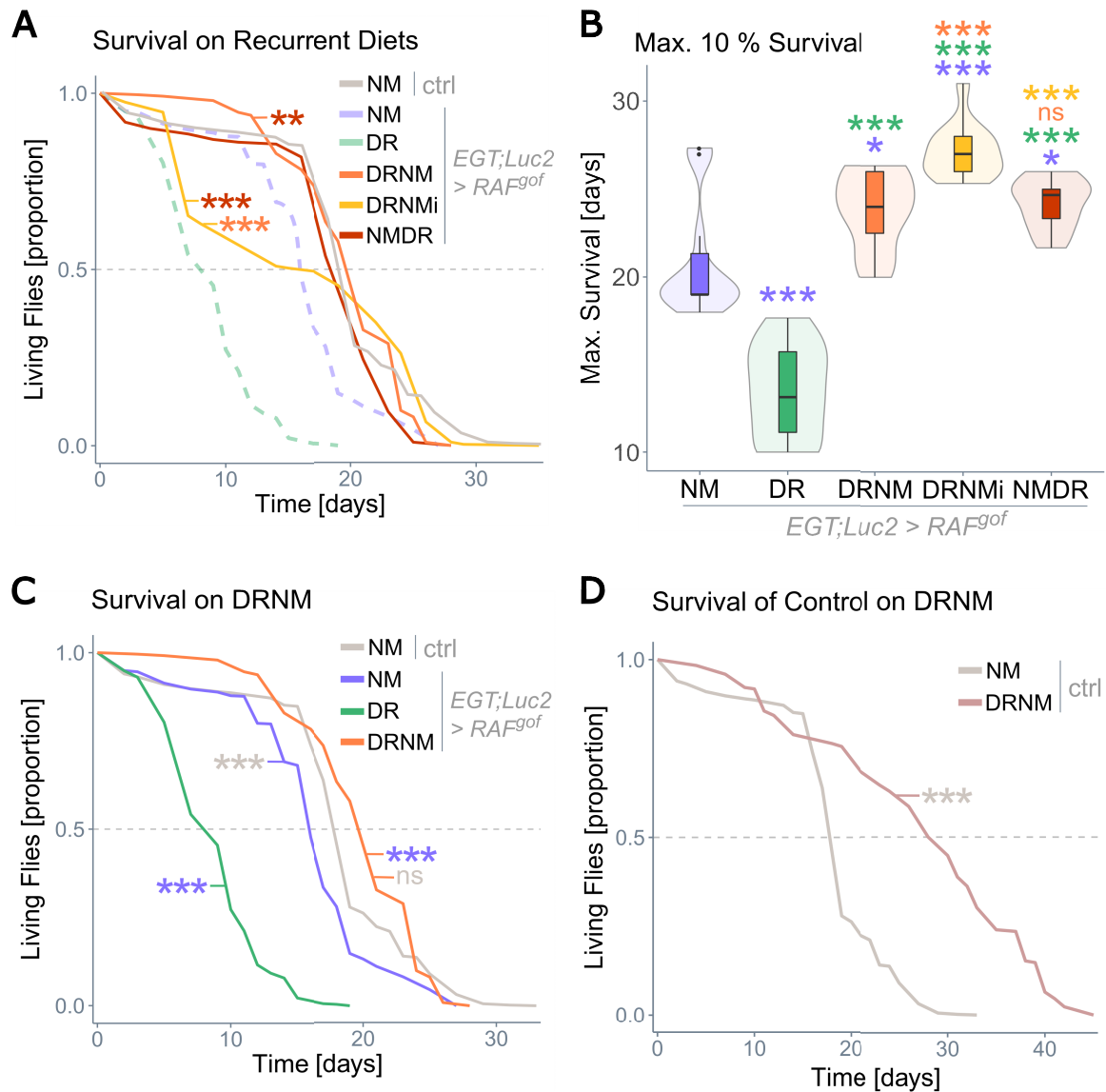


Fig. 3.14: Survival of tumor bearing flies on different recurrent diets. (A) The effect of 3 different types of recurrent feeding regimes was investigated in tumor bearing flies ($n = 12-15$). (B) The maximum lifespans were calculated by analyzing the oldest 10% of the population ($n = 12-15$). (C) A recurrent diet of phases of DR and feeding on a fully nutritious medium (DRNM) was applied to tumor bearing flies in comparison to controls and tumor bearing flies subjected to NM or lifelong DR ($n = 12-15$). (D) The effect of the recurrent diet DRNM on control flies ($n = 12-15$). ctrl = control ($w^{1118} > EGT;Luc2$), NM = normal medium, DR = dietary restriction medium, DRNM = recurrent diet with 3 initial days DR followed by 3 days NM and 4 days DR, DRNMI = DRNM with 5 initial days of DR, NMDR = recurrent diet with 4 days NM + 3 days DR. ns = not significant, * $p < 0.05$, ** $p < 0.01$, *** $p < 0.001$. Asterisks' colors represent partner for comparison.

3.3.2. The effects of a recurrent diet on gut morphology and functionality

The subjection of tumor bearing flies to the recurrent feeding regime DRNM resulted in the restoration of lifespan to the control level. Since DR was able to restore gut morphology and partially gut functionality in tumor bearing flies, I investigated the tumor load in effects of

Results

subjection to DRNM on gut morphology and functionality in comparison to control flies subjected to NM or DRNM, and tumor bearing flies subjected to NM, DR or DRNM. The subjection of control flies to DRNM did not reveal any obvious morphological changes neither in the thoracic nor the abdominal gut regions (Fig. 3.15 A-B'). Tumor bearing flies feeding on NM for 10 days exhibited massive protrusions of excessive cell mass into the intestinal lumen (Fig. 3.15 C, asterisk). While these flies exhibited a clear structuring of the intestinal cells into an outer esg^+ cell layer and an inner esg^- cell layer after 3 day of tumor induction (Fig. 3.7 B), the cellular layers were arbitrarily arranged after 10 days of induction (the equivalent of one completed cycle of the recurrent regime) and cells disintegrated from the basal membrane (Fig. 3.15 C and C', yellow arrowhead).

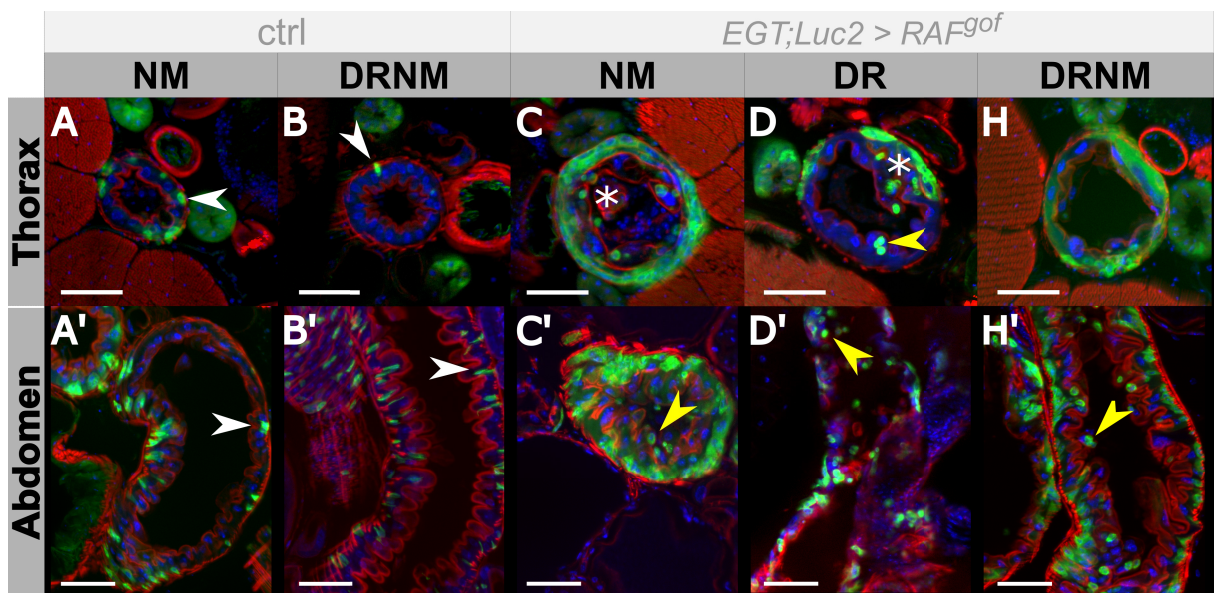


Fig. 3.15: Tumor load of flies subjected to a recurrent diet. Control and tumor bearing flies were sectioned after 10 days of subjection to NM, DR or the recurrent diet DRNM. (A-H) Sagittal sections through the thorax. Note the single esg^+ cells attached to the basal membrane (white arrowhead) and detached esg^+ cells in DR submitted tumor bearing flies (yellow arrowhead) as well as excessive tissue protruding into the intestinal lumen (asterisks) (A'-H') Sagittal sections through the abdomen. Note the esg^+ cells attached to the basal membrane (white arrowheads) in control flies and the detached esg^+ in tumor bearing flies submitted to NM, DR or DRNM (yellow arrowhead). ctrl = control ($w^{1118} > EGT; Luc2$), NM = normal medium, DR = dietary restriction medium, DRNM = recurrent diet with 4 days DR + 3 days NM. GFP: esg^+ cells, green; DAPI: nuclei, blue; Phalloidin: actin, red.

Flies subjected to DR for 10 days were very fragile and easily disintegrated upon sectioning. However, the thoracic and abdominal regions of the intestines of these flies displayed less esg^+ cells than tumor bearing flies feeding on NM (Fig. 3.15 C-D'). Nevertheless, DR

Results

subjected tumor bearing flies still displayed hyperplastic cell mass protruding into the gut lumen as well as esg^+ cells disintegrated from the basal membrane (Fig. 3.15 D, asterisk and yellow arrowhead, respectively). The subsection of tumor bearing flies to DRNM resulted in the formation of excessive esg^+ cell mass. The thoracic regions of the intestine showed only little cell mass protruding into the lumen (Fig. 3.15 H) as compared to NM fed tumor bearing flies (Fig. 3.15 C). The intestines resembled those from flies subjected to DR for 10 days but retained integrity upon sectioning. The abdominal regions of the intestines of tumor bearing flies subjected to DRNM displayed little additional esg^+ cell mass with esg^+ cells disintegrating from the basal membrane (Fig. 3.15 H').

The presented tumor model provides the opportunity to quantify esg^+ cells *via* RAF^{gof} co-expressed Luciferase and thus to directly monitor tumor growth. I used the Luciferase measurement to assess the esg^+ cell mass in control flies subjected to NM or DRNM, and tumor bearing flies subjected to NM, DR or DRNM for 10 days (equivalent to a completed cycle of the recurrent regime).

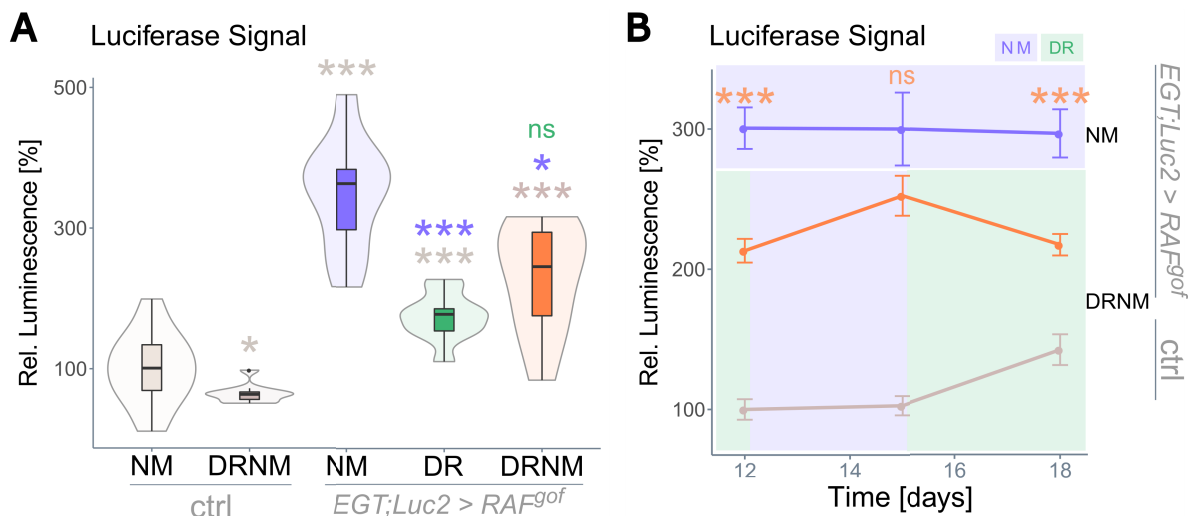


Fig. 3.16: Luciferase signal as measure for tumor mass in RAF^{gof} expressing flies after subsection to a recurrent diet. (A) The Luciferase co-expressed alongside RAF^{gof} in esg^+ cells was measured to quantify tumor load after 10 days of tumor induction (n = 10-20). (B) The fluctuation in signal strength of co-expressed Luciferase was measured in control and tumor bearing flies after phases of subsection to DR (green shading) or feeding on NM (blue shading) (n = 5-10). ctrl = control ($w^{1118} > EGT;Luc2$), NM = normal medium, DR = dietary restriction medium, DRNM = recurrent diet with 4 days DR + 3 days NM. ns = not significant, * $p < 0.05$, *** $p < 0.001$. Asterisks' colors represent partner for comparison.

Results

The submission of control flies to DRNM resulted in a slight reduction of *esg*⁺ cell mass compared to control flies feeding on NM (Fig. 3.16 A). The induction of the *RAF*^{gof}-dependent intestinal tumor led to a significant increase of co-expressed Luciferase in flies feeding on NM, the extent being similar to that seen after 3 days of tumor induction (Fig. 3.3). Tumor bearing flies subjected to DR for 10 days exhibited a drastic reduction in tumor mass compared to NM fed tumor bearing flies (Fig. 3.16 A). The submission of tumor bearing flies to DRNM resulted in a reduction of tumor mass to the same extent as DR alone, although this treatment exhibited a wider phenotypic range (Fig. 3.16 A). Interestingly, the tumor load fluctuated during the recurrent feeding regime with significantly less *esg*⁺ cell mass after DR phases and tumor loads similar to lifelong NM after NM phases (Fig. 3.16 B).

The additional cell mass in the intestines of tumor bearing flies can protrude into the gut lumen and lead to a relative as well as an absolute intestinal obstruction. I analyzed the saggital sections through the thoracic midgut in regard of a) the total gut volume, b) the cell mass, c) the volume of the intestinal lumen as a measure for intestinal passability, and d) the lumen to gut ratio as a measure for relative intestinal obstruction of controls and tumor bearing flies subjected to NM, DR or DRNM.

The total gut volume was decreased when subjecting control flies to DRNM but was unaffected in tumor bearing subjected to NM or DR (Fig. 3.17 A). The subjection to DRNM resulted in an increased total gut volume in respect to the DRNM subjected controls (Fig. 3.17 A). The intestinal cell mass was reduced in control flies subjected to DRNM, similarly to the total gut volume. The intestinal cell mass of tumor bearing flies on the other hand was significantly increased when feeding on NM but rescued to the control level by the application of DR (Fig. 3.17 B). The subjection of tumor bearing flies to DRNM did not rescue the phenotype but increased the cell mass in comparison to the respective cell mass of DRNM subjected control flies (Fig. 3.17 B). The intestinal lumen volume was significantly reduced due to the application of DRNM in control flies as well as in tumor bearing flies subjected to NM (Fig. 3.17 C). Subjection to DR or DRNM rescued the volume of the intestinal lumen of tumor bearing flies and restored it to the level of the respective control (Fig. 3.17 C). Interestingly, the subjection of control flies to DRNM resulted in overall narrowed intestines, which was reflected in all 3 measurements (Fig. 3.17 A-C) including the lumen to gut ratio which represents the relative obstruction of the intestine (Fig. 3.17 D). However, the relative obstruction due to tumor induction was more constricting in flies

Results

feeding on NM but was rescued by the subsection of tumor bearing flies to DR or DRNM (Fig. 3.17 D). Both of these feeding regimes restored the lumen to gut ratio back to the respective control level (Fig. 3.17 D). In summary, the application of DRNM in control flies resulted in downsized midguts whereas the induction of *RAF^{gof}*-dependent tumors resulted in flies having enlarged intestines (Fig. 3.17 A-C). Interestingly, subjecting tumor bearing flies to DR or DRNM rescued the passability of the intestinal lumen as well as the tumor-dependent relative intestinal obstruction to the same extents (Fig. 3.17 D).

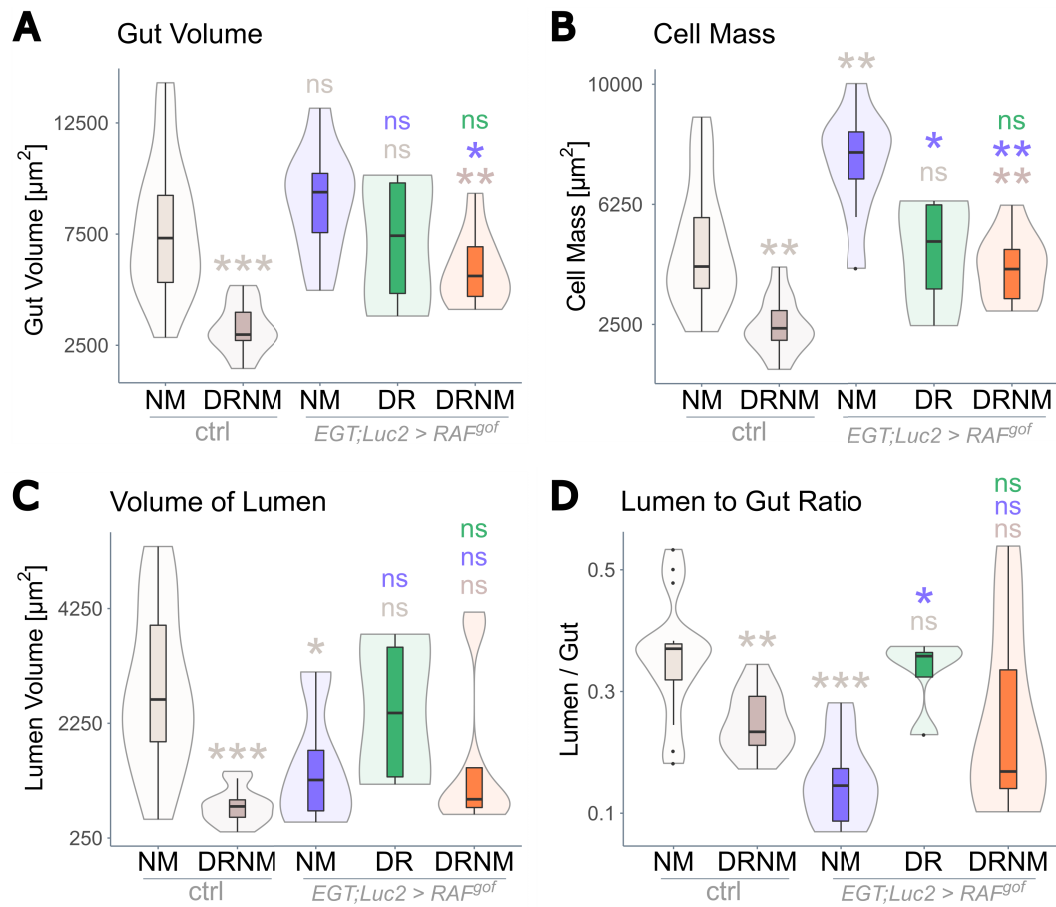


Fig. 3.17: Assessment of relative and absolute obstruction of midguts of control and tumor bearing flies subjected to DRNM. The sagittal sections through the thorax of control and tumor bearing flies subjected to NM, DR or DRNM were used to measure (A) the total outer gut volume, (B) the total cell mass, (C) the total volume of the gut lumen and (D) the lumen to gut ratio (n = 9-11, DR n = 4). While the lumen volume displays the absolute intestinal passability, the lumen to gut ratio represents the relative obstruction after 10 days of tumor induction. ctrl = control (*w¹¹¹⁸* > *EGT;Luc2*), NM = normal medium, DR = dietary restriction medium, DRNM = recurrent diet with 4 days DR + 3 days NM. ns = not significant, * p < 0.05, ** p < 0.01, *** p < 0.001. Asterisks' colors represent partner for comparison.

Results

Intestinal function is evidently linked to the gut morphology. Since the morphological analyses of control and tumor bearing flies subjected to NM, DR or DRNM revealed alterations of the midgut, the digestion of these flies was assessed by measuring the fecal output using the T.U.R.D. system (188). The total fecal output is a result of the sizes of the produced fecal spots and the number of produced fecal spots. The number of fecal spots produced per fly per 24 h was not altered due to tumor induction (Fig. 3.18 A). However, subjection to DRNM resulted in a higher fecal spot number in control flies as compared to control flies feeding on NM (Fig. 3.18 A).

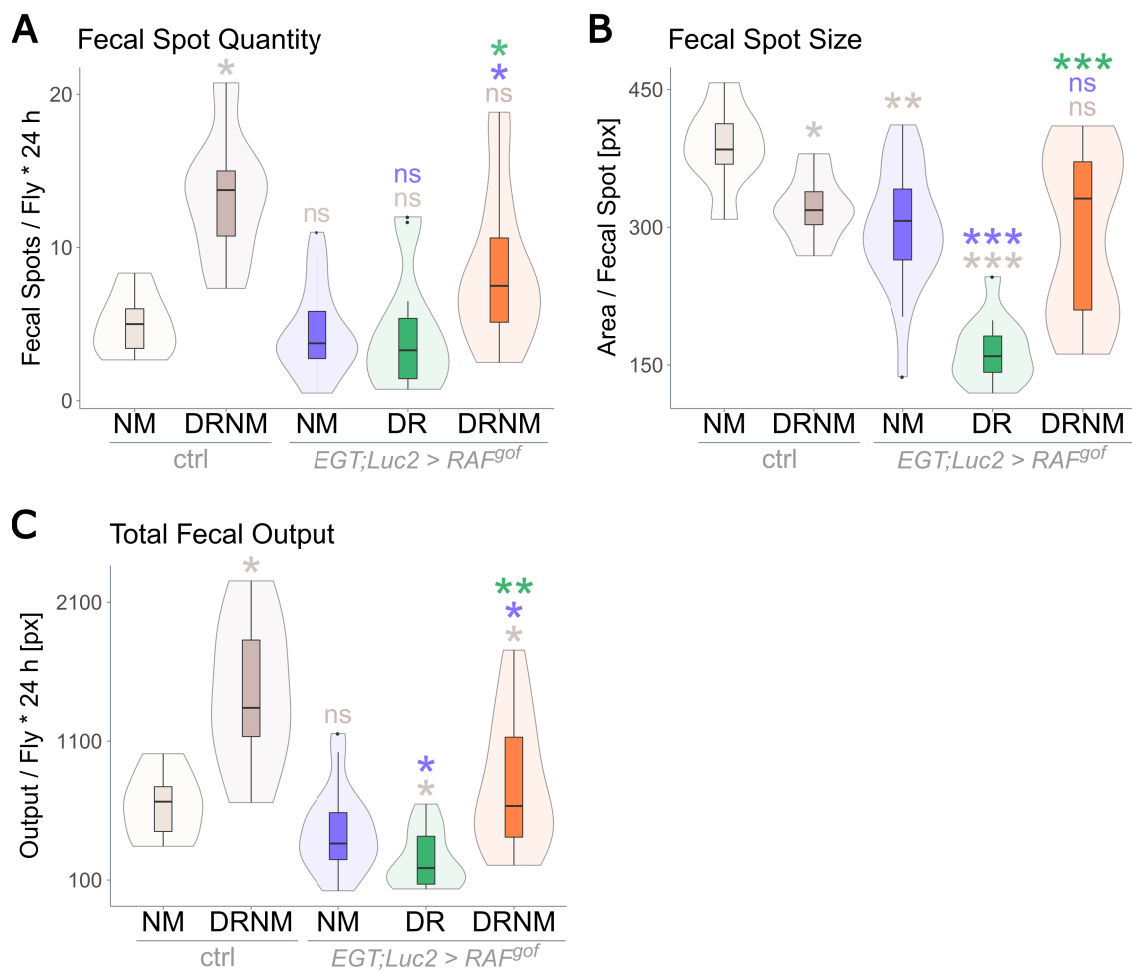


Fig. 3.18: Analysis of gut functionality of tumor bearing flies subjected to DRNM. The T.U.R.D. software (188) was used to measure (A) the fecal spot quantity, (B) the individual fecal spot size and (C) the total fecal output after 10 days of tumor induction of control and tumor bearing flies subjected to NM, DR or DRNM (n = 7-21). ctrl = control ($w^{1118} > EGT;Luc2$), NM = normal medium, DR = dietary restriction medium, DRNM = recurrent diet with 4 days DR + 3 days NM. ns = not significant, * p < 0.05, ** p < 0.01, *** p < 0.001. Asterisks' colors represent partner for comparison.

Results

In contrast, the size of the individual fecal spots was decreased in DRNM subjected control flies as compared to control flies feeding on NM (Fig. 3.18 B). Tumor induction *via* *RAF^{gof}* expression resulted in decreased fecal spot sizes in flies subjected to NM or DR. However, the fecal spot size was restored by subjecting tumor bearing flies to DRNM (Fig. 3.18 B). Both measurements, the fecal spot quantity and the individual fecal spot sizes were used to calculate the total fecal output of control and tumor bearing flies subjected to NM, DR or DRNM. The subjecting of control flies to DRNM resulted in the overall increase in fecal output compared to control flies feeding on NM (Fig. 3.18 C) which can be attributed to the increased number of fecal spots (Fig. 3.18 A). The tumor formation did not alter overall fecal output in flies feeding on NM as compared to the control flies, whereas the subjecting of tumor bearing flies to DR or DRNM significantly reduced total fecal output compared to their respective control (Fig. 3.18 C). In summary, fecal spot size was decreased due to two aspects, tumor formation and protein limitation. Additionally, DRNM increased fecal spot abundance. Since tumor bearing flies subjected to DRNM produced as many fecal spots of the same size as the DRNM control, it can be deduced that tumor formation did not further limit fecal output in these flies.

3.3.3. Body composition and energy demands after subjecting to a recurrent diet

The microscopic analyses as well as the measurement of the *RAF^{gof}* co-expressed Luciferase depicted the indubitable reduction of tumor mass in tumor bearing flies subjected to DR (Fig. 3.5, Fig. 3.7). Nevertheless, the strict protein limitation resulted in the premature death of flies and a substantial loss of body mass including body fat and protein (Fig. 3.11) which most likely occurred due to altered energy expenditure and an unmet energy demand (Fig. 3.12). Since the survival of tumor bearing flies was rescued by the subjecting to the recurrent feeding regime, I hypothesized that subjecting tumor bearing flies to DRNM would be less deleterious. Therefore, I studied the body composition and basic energy expenditure in control flies and tumor bearing flies subjected to NM, DR or DRNM. Subjecting control flies to DRNM resulted in a significant reduction in fly body weight (Fig. 3.19 A). Interestingly, subjecting tumor bearing flies to DRNM resulted in no further alteration of body weight. Tumor bearing flies subjected to DR exhibited a reduction in body weight while tumor bearing flies feeding on NM did not (Fig. 3.19 A). The TAG level assessment depicted a

Results

significant reduction in body fat after subjection to DRNM in control flies as well as due to tumor induction in all *RAF^{gof}* expressing flies (Fig. 3.19 B). The body fat reduction was stronger in DR subjected than in NM fed tumor bearing flies but was strongest in tumor bearing flies subjected to DRNM (Fig. 3.19 B). Similarly to the body fat, the protein level was significantly reduced upon subjection of control flies to DRNM (Fig. 3.19 C). It is noteworthy, that tumor induction did not exacerbate the protein loss but resulted in the same level of body protein content in control and tumor bearing flies subjected to DRNM. The same extend of protein loss was observed in tumor bearing flies subjected to DR whereas tumor bearing flies feeding on NM did not significantly loose whole body protein in regard to the control flies (Fig. 3.19 C).

The subsequently calculated body fat to protein ratio was slightly reduced in control flies subjected to DRNM in comparison to control flies feeding on NM; however, tumor induction resulted in a 2-fold reduction in flies feeding on NM or subjected to DR (Fig. 3.19 D). Interestingly, the subjection of tumor bearing flies to DRNM did not alter the fat to protein ratio. Nevertheless, a wide variation was observed in this treatment (Fig. 3.19 D). The measurement of the basic metabolic rate revealed that only tumor bearing flies subjected to NM experienced an increase whereas neither subjection of control nor tumor bearing flies to DRNM or DR resulted in an alteration of basic metabolic rate (Fig. 3.19 D).

In summary, subjecting control as well as tumor bearing flies to the recurrent feeding regime resulted in proportionate overall reduction of body fat and protein and therefore a similar fat to protein ratio in these treatments. In contrast, tumor induction resulted in disproportionate changes of the body composition in flies subjected to NM or DR and consequently resulted in a shift in fat to protein ratio.

Results

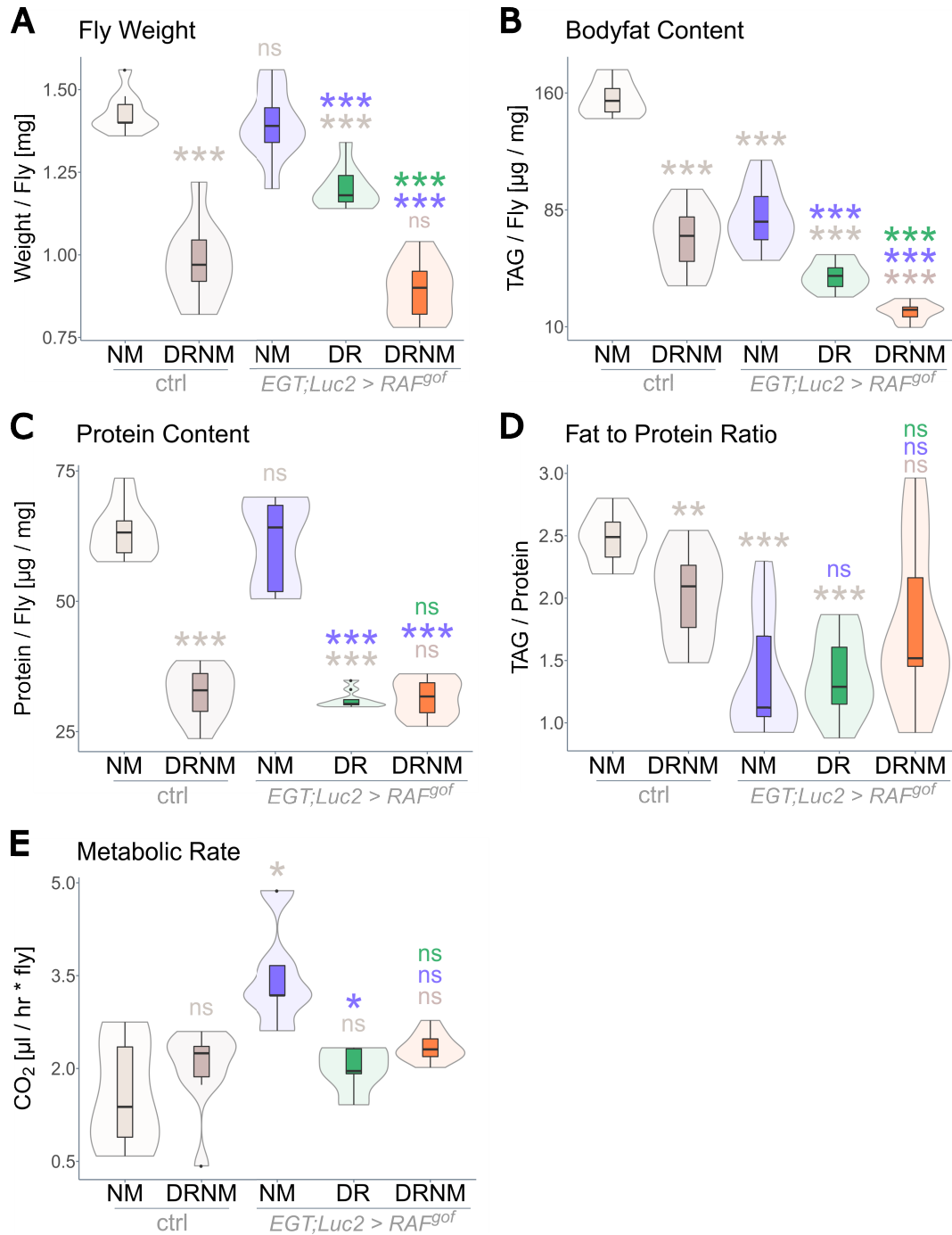


Fig. 3.19: Body composition and basic metabolic rate of control and tumor bearing flies subjected to DRNM. The body composition of control and tumor bearing flies subjected to NM, DR or DRNM for 10 days was evaluated by measuring (A) the individual fly weight (n = 10), (B) the body fat content *via* TAG levels (n = 10-25) and (C) the total body protein content (n = 9-19). (D) The fat to protein ratio was calculated subsequently (n = 9-10). (E) The basic metabolic rate of control and tumor bearing flies subjected to NM, DR or DRNM was measured (n = 5-10). ctrl = control ($w^{1118} > EGT;Luc2$), NM = normal medium, DR = dietary restriction medium, DRNM = recurrent diet with 4 days DR + 3 days NM, TAG = triacylglyceride. ns = not significant, * p < 0.05, ** p < 0.01, *** p < 0.001. Asterisks' colors represent partner for comparison.

Results

3.3.4. Transcriptome analysis of intestines of flies subjected to a recurrent diet

Subjecting flies to a recurrent feeding regime with phases of NM alternating with phases of subjection to DR resulted in the elongation of median lifespan to almost 50% in control flies. I analyzed the transcriptomes of control flies subjected to either lifelong NM or DR in comparison to subjection to the recurrent DRNM regime. The treatments were sampled after 13 days of either feeding regime. DRNM treated flies had completed a phase of feeding on NM at the time of sampling in order to identify transcription alterations that convey the effects of DR throughout refeeding periods and to potentially identify genes or gene clusters that are specifically regulated by alternating nutritional availability.

All differentially expressed genes (DEGs) of healthy flies feeding on NM, DR or DRNM with $p < 0.001$ and foldchange > 4 were used in K-means clustering to identify nutrition-dependent expression patterns (Fig. 3.20, Tab. 3.2) The heatmap illustrates the differential expression of 5 main gene clusters. The DRNM treatment group showed 2 clusters (clusters 3 and 4) that were regulated in a similar pattern as the NM treatment group. Subsequently, these genes responded quickly to fluctuating nutritional abundance. KEGG enrichment identified involvement of cluster 3 in *Other glycan degradation* and *Lysosome*, and of cluster 4 with *Neuroactive ligand-receptor interaction*. Clusters 1 and 2 showed a similar expression pattern in DRNM as observed in the DR treatment group. They therefore contain genes that responded slowly to nutritional changes. These clusters both showed enrichment trends (only before correcting for multiple testing) for *Toll and Imd signaling pathway*. Interestingly, Cluster 5 contained DEGs that showed a varying expression with part of the DRNM samples being similar to NM and the other part being similar to DR. These genes were KEGG enriched for *Toll and Imd signaling pathway*.

The transcriptomes of control and tumor bearing flies were analyzed after 13 days feeding continuously on NM, DR or DRNM. In order to identify long-lasting transcriptomic changes in response to DR, that are still regulated after switching to a non-limiting regime, the DRNM subjected flies were sampled after a period of feeding on NM. At the same time the effect of the different nutritional regimes was investigated to trace transcriptomic signatures that can be associated with the observed phenotypes of prolonged longevity in DRNM subjected control and tumor bearing flies as well as transcriptomic signatures that might be accountable for the severe wasting phenotype observed in tumor bearing flies when subjected to DR.

Results

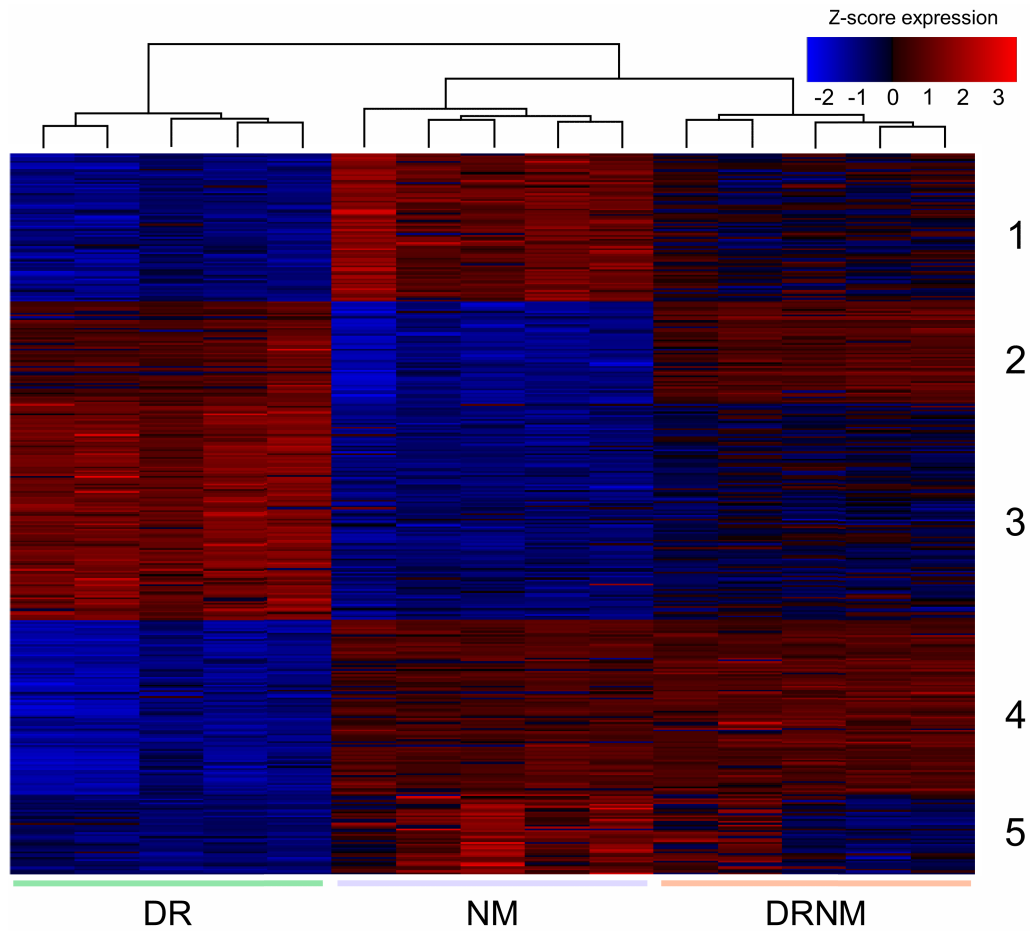


Fig. 3.20: Heatmap of mRNA expression profiles of control flies subjected to NM, DR or DRNM. K-means clustering of differentially expressed genes with $p < 0.001$ and foldchange > 4 are depicted ($n = 5$). control = $w^{1118} > EGT; Luc2$, NM = normal medium, DR = dietary restriction medium, DRNM = recurrent diet with 4 days DR + 3 days NM.

Tab. 3.2: Excerpt of KEGG enrichment analysis of differentially expressed genes within the clusters depicted in the heatmap of control flies subjected to different feeding regimes.

Cluster	Pathway ID	Pathway Name	# GiP	# DEG	p value	adj p-value
1	path:dme04624	Toll and Imd signaling pathway	67	3	0.002198595	0.29900892
2	path:dme00980	Metabolism of xenobiotics by cytochrome P450	69	3	0.001424435	0.064574387
	path:dme00982	Drug metabolism - cytochrome P450	68	3	0.001365102	0.064574387
	path:dme04624	Toll and Imd signaling pathway	67	3	0.001307366	0.064574387
3	path:dme00511	Other glycan degradation	22	4	1.65E-06	0.000223752
	path:dme04142	Lysosome	118	5	9.90E-05	0.006728973
4	path:dme04080	Neuroactive ligand-receptor interaction	56	4	0.000274793	0.037371902
5	path:dme04624	Toll and Imd signaling pathway	67	3	8.68E-05	0.011802699

Terms that were enriched only before correcting for multiple testing are depicted in grey. GiP = Genes in pathway, DEG = Differentially expressed genes, adj = adjusted

Results

Multi-dimensional scaling including all detected genes revealed a distinct clustering of the treatment groups for both the controls and tumor bearing individuals as well as for the 3 investigated nutritional regimes (Fig. 3.21). Samples of tumor bearing flies and control flies separated along the 1st dimension, which accounted for 40% of sample variety, while the samples of different feeding regimes separated along the 2nd dimension, which accounted for 21% of sample variety. All samples from DRNM subjected flies clustered closer to their respective NM counterpart whereas samples from flies subjected to DR formed clusters far from the respective NM or DRNM treatment.

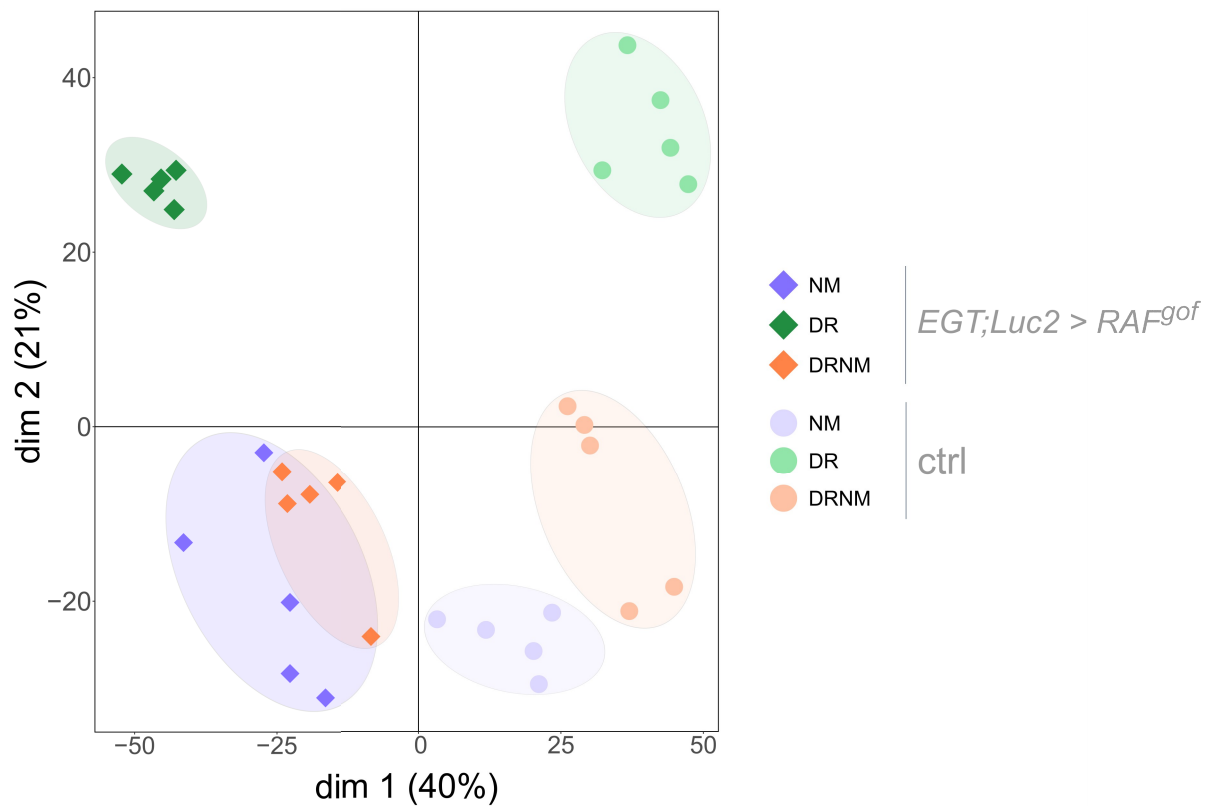


Fig. 3.21: Analysis of variation between and among samples using multi-dimensional scaling (MDS) based on all transcripts (unweighted). mRNA of tumor bearing and control flies was sequenced after 13 days of subjection to the respective feeding regime (n = 5). Ellipses were added manually. ctrl = control ($w^{1118} > EGT;Luc2$), NM = normal medium, DR = dietary restriction medium, DRNM = recurrent diet with 4 days DR + 3 days NM.

Analyses of the interactions between DEGs in healthy control flies feeding on DR, NM or DRNM identified a main network consisting of two subnetworks (Fig. 3.22). Both subnetworks were enriched for genes associated with the *Toll and Imd signaling pathway*

Results

(KEGG) (Tab. 3.3). While genes differentially expressed between NM and DRNM mainly belonged to the large subnetwork, DEGs of DR and DRNM showed unique interactions within the small subnetwork and adjacent nodes (Fig. 3.22). DEGs that were unique between DR and NM were not associated with either subnetwork but dispersed throughout the whole network. In contrast to that, the interactions of DEGs of tumor bearing flies subjected to either feeding regime revealed a single main network (Fig. 3.23) associated (non-significantly after correcting for multiple testing) with *Other glycan degradation* (KEGG) (Fig. 3.23, Tab. 3.4). DEGs between NM and DRNM were mainly associated with the core network (Fig. 3.23, red circle) whereas all other interactions were dispersed homogenously throughout the network.

In summary, two distinct subnetworks which exert similar functions with associations to the immune system are regulated in response to nutritional interventions in unimpaired control flies. Another network is active in tumor bearing flies with diets again accessing distinct components of the network.

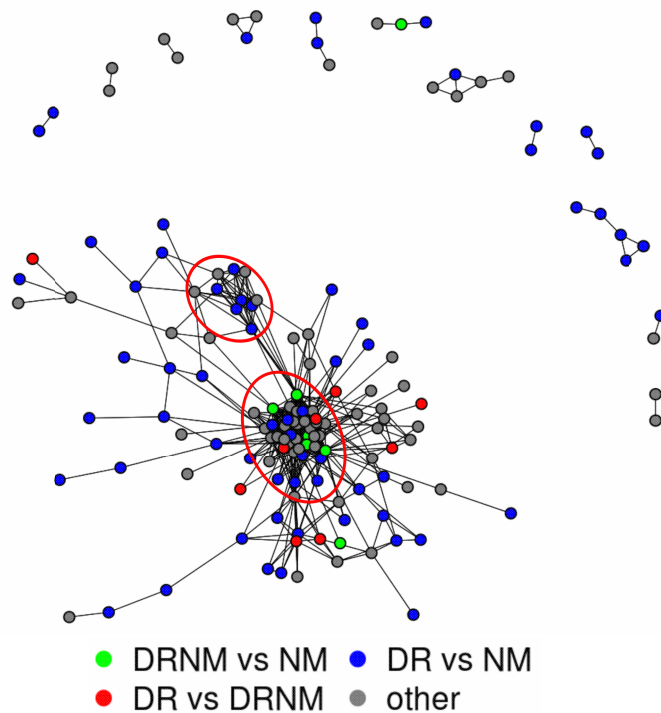


Fig. 3.22: Interaction network of differentially expressed genes in control flies. Only differentially expressed genes with $p < 0.001$ were used ($n = 5$). The red circles mark the small and the large subnetworks. Genotype = $w^{1118} > EGT; Luc2$, NM = normal medium, DR = dietary restriction medium, DRNM = recurrent diet with 4 days DR + 3 days NM.

Results

Tab. 3.3: Excerpt of KEGG enrichment analysis of interaction networks upon subsection to different feeding regimes in healthy control flies.

Subnetwork	KEGG ID	KEGG term	# GiP	# DEG	p-value	adj p-value
large subnetwork	path:dme04624	Toll and Imd signaling pathway	67	3	0.000294654	0.040072998
	path:dme04080	Neuroactive ligand-receptor interaction	56	2	0.006044684	0.411038532
	path:dme00511	Other glycan degradation	22	1	0.047477961	1
small subnetwork	path:dme04624	Toll and Imd signaling pathway	67	4	1.80E-07	2.45E-05

Displayed are enrichment analyses for both subnetworks. Terms that were enriched only before correcting for multiple testing are depicted in grey. GiP = Genes in pathway, DEG = Differentially expressed genes, adj = adjusted.

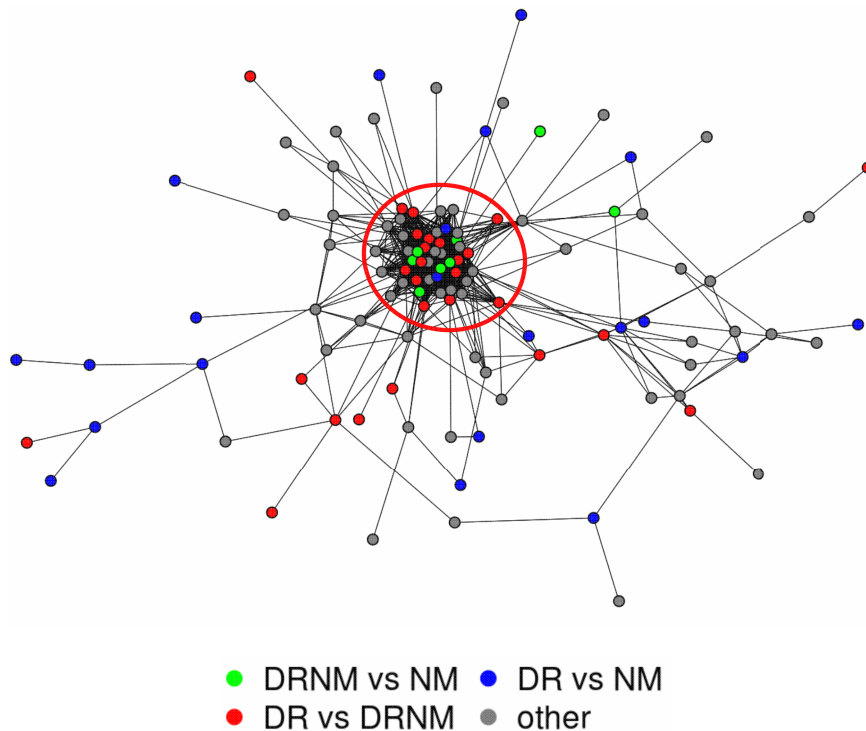


Fig. 3.23: Interaction network of differentially expressed genes in tumor bearing flies. Only differentially expressed genes with $p < 0.001$ were used ($n = 5$). The red circle marks the core network. Genotype = *EGT;Luc2 > RAF^{gof}*, NM = normal medium, DR = dietary restriction medium, DRNM = recurrent diet with 4 days DR + 3 days NM.

Results

Tab. 3.4: KEGG enrichment analysis of interaction network in tumor bearing flies upon subjected to different feeding regimes.

KEGG ID	KEGG term	# GiP	# DEG	p-value	adj p-value
path:dme00511	Other glycan degradation	22	1	0.0206179	1

Terms that were enriched only before correcting for multiple testing are depicted in grey. GiP = Genes in pathway, DEG = Differentially expressed genes, adj = adjusted.

In order to identify not only patterns but single genes that potentially contribute to the observed phenotypes, the DEGs of control and tumor bearing flies were categorized according to the condition that they were relevant to. Analyzing the overlaps of DEGs in control and tumor bearing flies identified the largest part of DEGs to be unique to subjection to DR (1977 and 2698 DEGs in controls and tumor bearing flies, respectively) (Fig. 3.24). The 2698 DEGs identified to be uniquely expressed in tumor bearing flies feeding on DR are likely involved in the severe wasting phenotype observed solely in these flies. Genes within this group were proliferation-associated like *armadillo* and *yorkie*, or associated with the insulin signaling pathway including the *Insulin-like receptor*, *S6KL*, and *Foxo*. Furthermore, immunity related genes like the pathway components *spätzle*, *Toll* and *Relish*, as well as multiple *Autophagy-related factors*, the *drop dead* gene and 21 *lethal* genes were unique to tumor bearing flies when subjected to DR.

1726 DEGs were attributable to both DR and DRNM in control flies and contained those genes that retained differential transcript levels throughout phases of refeeding (light ochre colored overlaps). These overlaps include those genes that represent long-lasting transcriptional changes and that therefore likely are key genes for the effectiveness of DRNM in terms of mimicking lifelong DR. Genes represented in this overlap included the insulin-binding protein *ImpL2*, the insulin receptor substrate *Chico*, the longevity gene *I'm not dead yet*, the amino acid transporter *slimfast*, the transcription factor *Foxo*, *S6KL* and the lipase *magro*. A subset of 888 DEGs was unique to DRNM treatment in control flies (orange colored crescents). The overlap represents genes that might be regulated specifically in response to alternating food abundances. Genes uniquely expressed in DRNM subjected control flies included proliferation regulators like *4E-BP*, the transcription factor *pointed*, energy stress sensor *AMPK alpha*, immune system components like *PGRP-LC* or the lipase *brummer*.

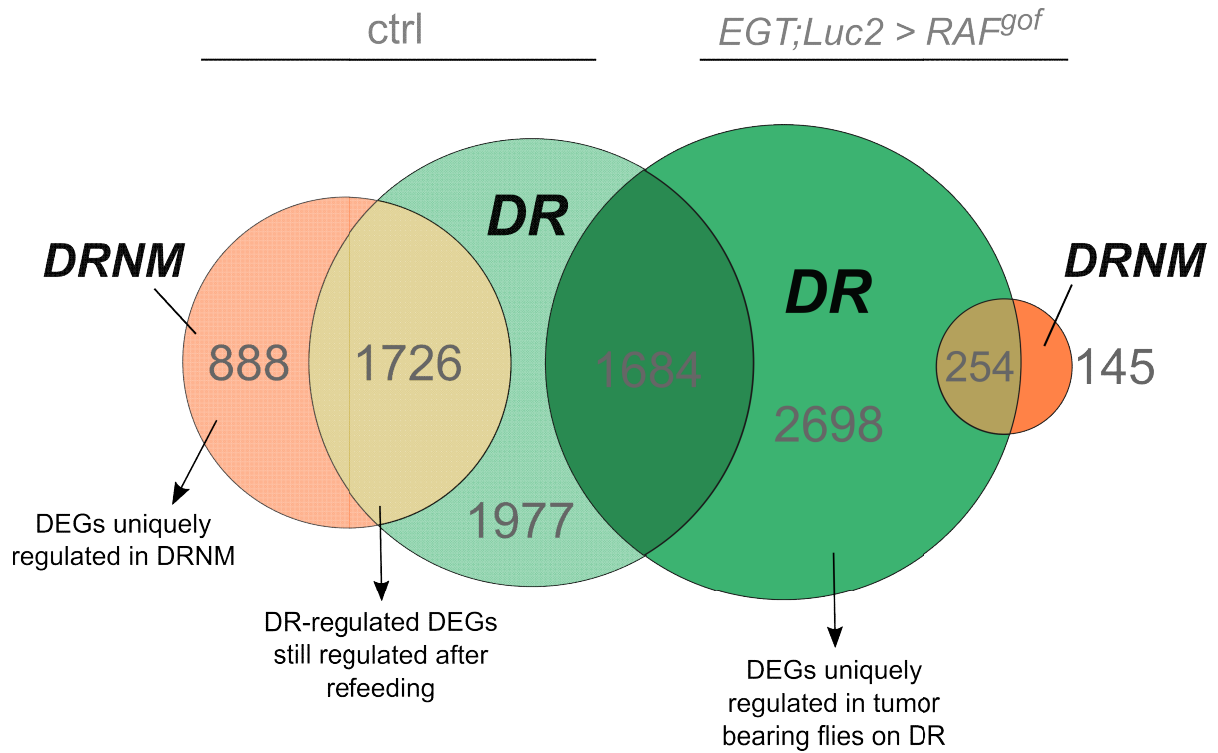


Fig. 3.24: Venn diagram of differentially expressed genes in either control or tumor bearing flies subjected to different feeding regimes. Differentially expressed genes (DEGs) in comparison to NM are displayed in each circle ($n = 5$). Overlaps represent genes differentially expressed in two conditions. ctrl = control ($w^{1118} > EGT;Luc2$), DR = dietary restriction medium, DRNM = recurrent diet with 4 days DR + 3 days NM.

3.3.5. Changes of the microbial composition after subsection to a recurrent diet

The microbiota is an important player in organismal health and well-being and functions as a central integrator of nutrition and epithelial homeostasis. The dietary input naturally shapes the intestinal microbiota and can foster the establishment of a “healthy” microbial community (204, 205). Diseases, including cancer, are often associated with a shift in the microbial community. Furthermore, single bacterial taxa have been identified to promote overproliferation in multiple model systems (extensively reviewed in (206–208)). In the presented tumor model, recolonized flies expressing RAF^{gof} in intestinal progenitor cells presented a significantly higher tumor load than germ free flies of the same genotype (Fig. 3.25).

Results

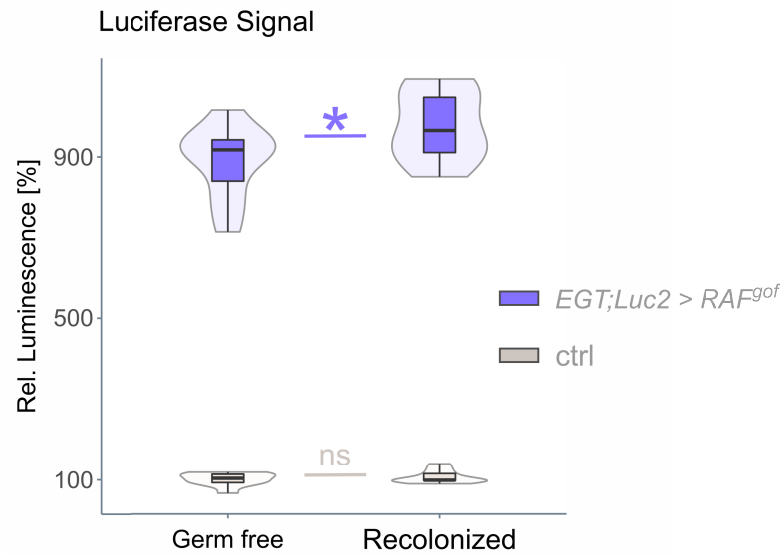


Fig. 3.25: Quantification of RAF^{gof} co-expressed Luciferase in germ free and recolonized flies. The amount of esg^+ cell mass was measured in control and RAF^{gof} expressing flies via co-expressed Luciferase (n = 10). All treatments were fed with NM. ctrl = control ($w^{1118} > EGT;Luc2$), NM = normal medium. ns = not significant, * $p < 0.05$.

I investigated the microbial composition on control and tumor bearing flies subjected to lifelong NM, DR or the recurrent feeding regime DRNM in order to identify how an alternating diet shapes the intestinal microbiota and to understand whether or not tumor bearing flies follow a similar pattern. Although no significant differences were detected, the α -diversity was slightly increased in NM fed control flies than in DR fed flies of the same genotype (Fig. 3.26 A). While the α -diversity of NM or DR subjected flies was rather constant over time, the taxonomic diversity of DRNM subjected control flies fluctuated with more operational taxonomic units (OTUs) observed after phases of feeding on NM and less OTUs observed after phases of feeding on DR. In contrast, the α -diversity of tumor bearing flies slightly decreased over the course of 10 days when feeding on NM or DR (Fig. 3.26 B). Most interestingly, subjecting tumor bearing flies to DRNM resulted in a fluctuation opposing the pattern observed in control flies with tumor bearing flies exhibiting less taxonomic units after phases of feeding on NM than after feeding on DR.

Results

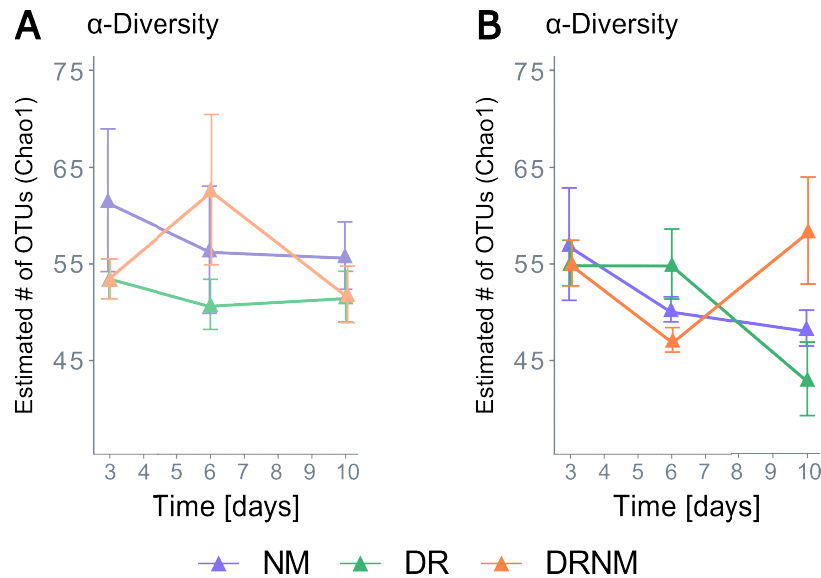


Fig. 3.26: α -diversity of control and tumor bearing flies over time. (A) α -diversity of control flies subjected to NM, DR or DRNM over time ($n = 5$). (B) α -diversity of tumor bearing flies subjected to NM, DR or DRNM over time ($n = 5$). NM = normal medium, DR = dietary restriction medium, DRNM = recurrent diet with 4 days DR + 3 days NM. OTU = operational taxonomic units. No significances within or between treatments were detected.

The β -diversity was analyzed over the course of 10 days in order to clarify which patterns of microbial shift are induced by subjection to the different diets and to identify pattern (dis-)similarities between control and tumor bearing flies. The bacterial community 3 days after switching the control flies to 29 °C was similar across all feeding regimes, with *Xanthomonadales* making up the majority of bacterial taxa (Fig. 3.27). The abundance of *Enterococcaceae* increased over the course of 10 days in NM and DRNM fed flies, whereas DR subjected flies exhibit a fluctuating pattern with *Enterococcaceae* transiently being the most abundant taxon after 6 days. After 10 days the microbial community of DRNM subjected flies showed great similarity to that of flies continuously feeding on NM.

Interestingly, the microbial community of tumor bearing flies after 3 days of tumor induction resembled the community observed in the respective controls (Fig. 3.27). All tumor bearing flies showed an increase in *Burkholderiales* after 6 days of tumor induction independent of the feeding regime. However, the abundance was normalized after 10 days. Both NM and DR subjection resulted in the increase of *Lactobacillaceae* after 10 days of tumor induction, whereas the microbial community of DRNM subjected flies after 10 days of tumor induction (after a phase of feeding on DR) shared great similarity with the original community after 3 days of tumor induction (also after a phase of feeding on DR).

Results

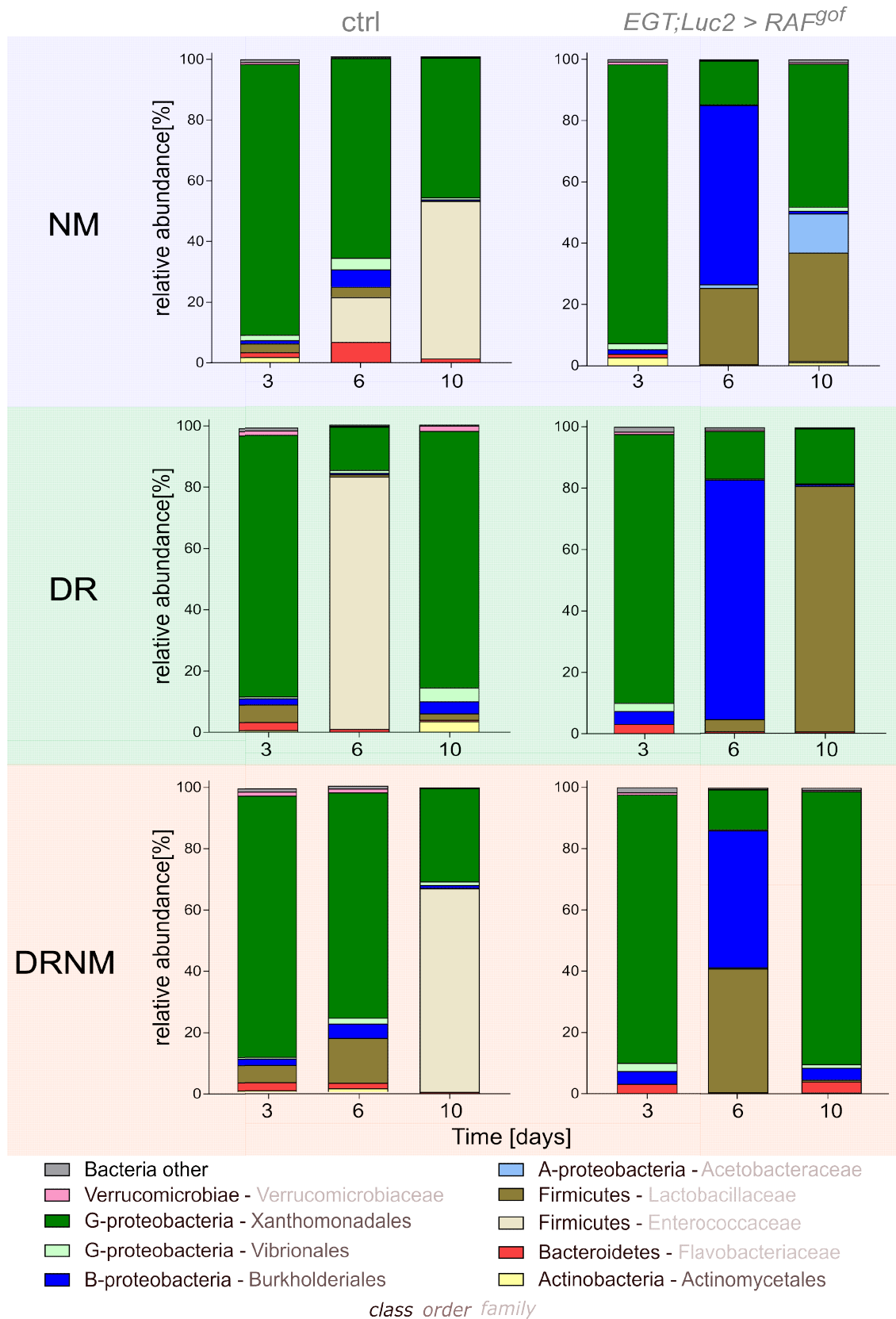


Fig. 3.27: Microbial composition of control and tumor bearing flies subjected to different feeding regimes. Flies were subjected to lifelong NM, DR or the alternating feeding regime DRNM and sampled after 3, 6 and 10 days of tumor induction (n = 5). ctrl = control ($w^{1118} > EGT;Luc2$), NM = normal medium, DR = dietary restriction medium, DRNM = recurrent diet with 4 days DR + 3 days NM.

Results

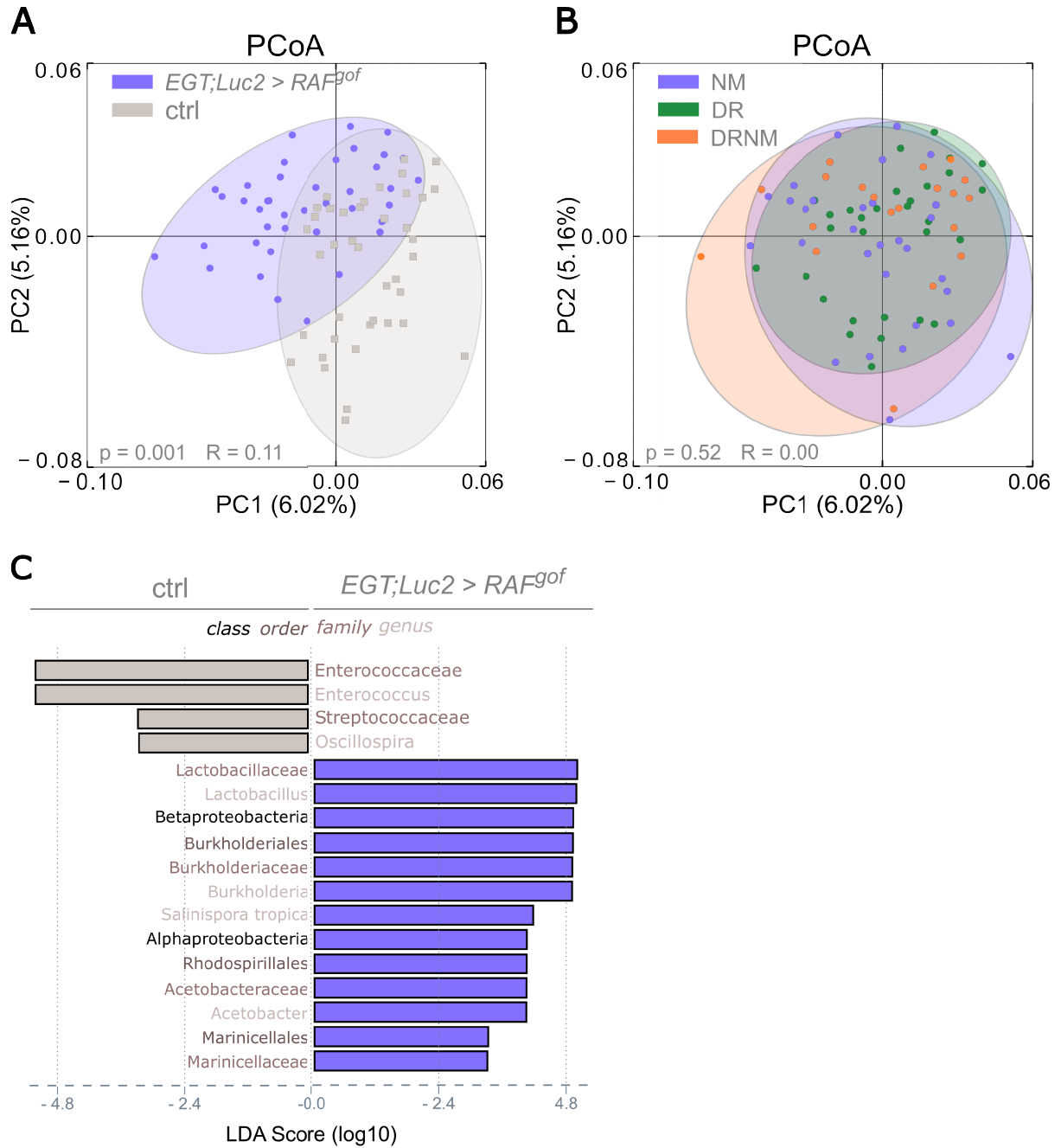


Fig. 3.28: Analysis of the microbial community in control and tumor bearing flies. (A) PCoA of Binary-Pearson matrix of control and tumor bearing flies. (B) PCoA of Binary-Pearson matrix of feeding regimes of control and tumor bearing flies. Ellipses were added manually. (C) Linear discriminant analysis of effect size (LEfSe) of control and tumor bearing flies. Bars represent taxa specifically associated with either genotype. ctrl = control ($w^{1118} > EGT;Luc2$), PCoA = Principal Coordinate Analysis, PC = Principal Coordinate.

The principal coordinate analysis identified distinct clusters for control and tumor bearing flies (Anosim, $p = 0.001$, $R = 0.11$) (Fig. 3.28 A) whereas the microbiota of the investigated feeding regimes did not cluster significantly (Anosim, $p = 0.52$, $R = 0.00$) (Fig. 3.28 B). Analyzing the taxa which were specific for either control or tumor bearing flies, revealed the

Discussion

association of the families *Enterococcaeae* and *Streptococcaceae* with control flies (Fig. 3.28 C). Tumor bearing flies on the other hand, were specifically associated with increased abundances of the classes *Alpha-* and *Betaproteobacteria*, as well as the families *Lactobacillaceae* and *Marinicellaceae* (Fig. 3.28 C).

4. Discussion

4.1. Model validation

Tumors are highly responsive to their nutritional environment and multiple nutritional regimes have been proposed to manipulate tumor growth. Among these nutritional regimes, interventions that use fat as a main source of calories and interventions that limit protein availability are the most consistently reported to limit tumor growth. However, results are varying and often contradicting, making further systematic studies irremissible. The study presented in this thesis uses a high fat model with 10% cocoa butter, making up 75% of the total caloric intake, and a protein limited DR model with 0.1% protein intake, to investigate the influences of different nutritional impacts on the development of *RAF^{gof}*-induced intestinal tumors. The models were validated by analyzing whether subsection of healthy control flies to either regime (HF or DR) induces archetypal phenotypes, in regards of body composition and activity patterns.

Flies that were fed a HF diet exhibited an initial drop in body weight (Fig. 3.1 A) which can be attributed to the change to a calorically dense food source which frequently results in the reduction of wet weight due to less frequent feeding and subsequently reduced uptake of water, if water is not supplied separately (92). A slight, but non-significant increase in body fat was observed after 3 days while stable protein levels were maintained (Fig. 3.1 B, C). However, an increase in lipid droplets in the cells of the intestinal epithelium of HF fed flies in comparison to NM fed flies became evident upon Bodipy staining (Fig. 3.1 E', E''). The accumulation of fat and the establishment of an obesity phenotype are gradually achieved over time with significant weight gain being delayed rather than an initial symptom (209). Nevertheless, the accumulation of fat in intestinal cells provides evidence, that cocoa fat is digested and taken up by cells of the *Drosophila* intestinal tract which, after a given time, results in increased fat storage and an obesity phenotype (210). Additionally, the circadian

Discussion

rhythm is altered flies fed 10% HF (Fig. 3.2 B). While flies still exhibited peak activities in response to light stimuli, the amplitude of activity during peak times was reduced whereas the activity amplitude during resting times increased (Fig. 3.2 B). These alterations of circadian rhythm and activity are a hallmark in obesity models in *Drosophila* and mammals (209–211).

Flies subjected to DR for three days exhibited weight loss (Fig. 3.1 A) which was accompanied by a significant reduction in total protein content (Fig. 3.1 C). At the same time flies maintained a stable fat to protein ratio (Fig. 3.1 D) which reflects a balanced reduction of body mass. Although there was no significant loss of total body fat after 3 days of DR, the lipid content in the intestinal cells was clearly reduced (Fig. 3.1 E'''), which is relatable to an initial compensatory fat mobilization from the gut and a delay in fat mobilization from the fat body. Fats in the form of TAGs are mobilized from the fat body upon nutrient scarcity by multiple ways that often act in parallel. One possibility is the translocation of the transcription factor Foxo, which is induced by multiple pathways including the insulin and Tor signaling pathway, as well as the adipokinetic hormone receptor pathway (212). Translocation of Foxo into the nucleus induces the expression of target genes like the growth arrest-inducing translational inhibitor *4E-BP* or the lipases *brummer* and *magro* which mobilize stored fats (182, 212, 213). Beside the physiological alterations in body composition, DR fed flies also exhibited altered activity patterns and increased overall activity (Fig. 3.1) which is in consent with previous studies of DR in *Drosophila* (214, 215).

In summary, both tested nutritional interventions induce archetypal phenotypes observed under these feeding regimes and are thus suitable as models to investigate the effects of HF and DR on human disease development including tumor progression.

4.2. Expression of *RAF^{gof}* results in the formation of excessive *esg*⁺ tissue

The intestine of *Drosophila melanogaster* is comprised of pluripotent ISCs and EBs, that further differentiate into absorptive ECs or secretory EEs. The epithelial monolayer shares great structural and functional similarities with its mammalian counterpart (Fig. 1.7) and the majority of disease associated genes has a homolog in the fruit fly (118). The fruit fly's intestine has successfully been used as a model to elucidate the molecular underpinnings of various diseases including multiple cancers. In this study, I used a model that induces excessive overproliferation of intestinal progenitor cells, which serve as cells of cancer origin

Discussion

in most CRCs (26, 27), by the induction of RAF^{gof} , a constitutively active isoform of the EGFR pathway component RAF. The EGFR signaling pathway and its MAPK cascade downstream components are frequently mutated in CRC including mutations in the genes *RAS* and *RAF* with up to 31.8 and 10.1% incidence, respectively (216). Interestingly, the MAPK pathway is not only responsive to extracellular growth factors, but also integrates nutritional growth cues (164, 217, 218). The tumors induced in the used model system are transplantable and self-sufficient to sustain growth in a non-tumor environment (126). Furthermore, the tumorous esg^+ tissue co-expresses *GFP* and Luciferase, which enable microscopic as well as molecular tracing, and quantification. Since intestinal tumors are highly responsive to nutritional interventions, I used this model to assess the effects of HF dieting and protein limited DR on the progression of RAF^{gof} -induced, ISC-derived intestinal tumors.

The expression of RAF^{gof} in esg^+ cells resulted in an increased Luciferase signal in all feeding regimes at all time points measured, with the strongest signal 3 days after induction (Fig. 3.5). The intestine is a very plastic organ that quickly responds to environmental changes and stressors in order to sustain homeostasis or to regenerate in response to tissue damage. The strong and fast increase in the Luciferase signal is likely due to an overall increase of *esg* promoter activity during stem cell proliferation. The increased Luciferase signal after elongated periods of RAF^{gof} induction, on the other hand, resulted from an overall increase in esg^+ cell mass (Fig. 3.4) rather than solely increased promoter activity. The excessive proliferation further resulted in the formation of an additional esg^+ cell layer in the thoracic midgut and in dense cellular accumulations protruding into the abdominal midgut (Fig. 3.7 A, A' and B, B'). The additional cell mass resulted in the relative obstruction of tumor bearing flies (Fig. 3.8 A, C, D) and an impaired intestinal function (Fig. 3.9 D, F), which is frequently observed in cancer patients (219). Furthermore, these tumor bearing flies exhibited a significantly decreased lifespan (Fig. 3.10). Therefore, the induction of RAF^{gof} in *Drosophila* ISCs and EBs results in the formation of mildly aggressive solid tumors that alter gut morphology, impair intestinal functionality and decrease survival.

4.3. HF diet does not affect tumor load but promotes cachexia-like wasting

The nutritional intake has long been known to influence tumor progression (88, 220, 221). Since treatment options are limited and high rates of tumor recurrence as well as treatment

Discussion

resistance are reported (21, 22), nutrition has once again come into focus as sustentative cancer treatment. The influence of nutritional uptake affects tumor progression in at least two different ways. Firstly, macromolecules directly promote tissue growth through local and systemic growth pathways including insulin, TOR and EGFR signaling. Secondly, nutrition indirectly influences tumor progression by affecting overall organismal health and energy supply. A state of excessive fat and muscle tissue wasting, termed cachexia, occurs in the majority of patients with advanced cancers and contributes to up to 45% of cancer related deaths (222). Tumor growth is a vastly energy demanding process, therefore, a high caloric nutritional intake is needed to maintain tissue homeostasis besides the tumor growth itself. I investigated the effects of HF dieting on tumors induced by the expression of *RAF^{gof}* in *esg⁺* ISCs and EBs of *Drosophila melanogaster* to elucidate the HF-dependent development of intestinal tumors and its potential to affect cachexia-like wasting. Sagittal cross sections through tumor bearing flies fed with NM or HF revealed the formation of excessive cell mass in the thorax as well as in the abdomen in all feeding regimes (Fig. 3.7, Fig. 3.8 C). While control flies exhibited *esg⁺* cells randomly interspersed throughout the intestinal epithelium (Fig. 3.7 A and A', white arrowheads), tumor bearing flies feeding on NM or HF showed the accumulation of additional *esg⁺* cell mass that formed a solid layer around the *esg⁻* cells in the thorax (Fig. 3.7 B and C, asterisks) and dense *esg⁺* cell accumulations that protruded into the abdominal lumen (Fig. 3.7 B' and C', white arrows). The additional thoracic cell mass increased the overall gut volume and resulted in a relative intestinal constriction of the anterior midgut in tumor bearing flies fed with NM or HF (Fig. 3.8 A and D). Food is digested during its passage through the intestinal tube, linking gut morphology to function. In the used model, the total fecal output was reduced and could be directly attributed to a reduction in fecal spot quantity (Fig. 3.9 D, F). This effect was stringent in tumor bearing flies fed with HF as well as with NM and reflects symptoms that are frequently experienced by CRC patients. Poor digestion and impaired bowel peristalsis of CRC patients often result in constipation and diarrhea, as well as alterations in stool size and shape (219, 223–225).

I could demonstrate that the presented model induced solid tumors that altered intestinal morphology by altering cell mass and cell type composition, and impaired gut functionality by reducing fecal output. However, these differences were observed in tumor bearing flies feeding on either NM or HF. In *Drosophila*, animal- as well as plant-based fats lead to an obesity phenotype and diabetes (210, 226), both of which were previously linked to tumor progression (227, 228). Although caloric intake is usually high in fat enriched diets, it has

Discussion

been shown that the specific composition of dietary fats is rather critical to its effects on tumor progression than sheer overeating (229–231). For example, while safflower and corn oil exhibit tumor promoting effects, other fats, like coconut or olive oil, do not alter tumorigenesis or, like fish oil, even have anti-tumorigenic properties in colon cancer (231–233). This study used cocoa butter which is composed of approximately 60% saturated fatty acids, 30% monounsaturated fatty acids and 3% polyunsaturated fatty acids. The fatty acids are composed of 34.5% stearic (saturated) and oleic acids (monounsaturated) each, 26% palmitic acids (saturated), 3.2% linoleic acid (polyunsaturated), as well as 1.8% other fatty acids. Both stearic and oleic acids have been demonstrated to inhibit cell proliferation and tumor progression (234, 235). In contrast, high intake of polyunsaturated fats increases tumor proliferation while palmitic acid promotes tissue evasion and metastasis (229, 236). This study shows that cocoa butter HF dieting neither increased nor reduced tumor load in flies expressing *RAF^{gof}* in intestinal progenitor cells although calorically dense fat was digested and incorporated into the tissue, and induced an obesity-like phenotype (Fig. 3.1 E, Fig. 3.2). This effect might be due to the specific fatty acid composition of cocoa butter, which contains high rates of both tumor inhibiting and tumor promoting factors. Therefore, this study highlights the diverse functions of fats in tumor progression and illustrates, that increased caloric intake through fats is not sufficient to promote tumor growth in fruit flies.

Interestingly, tumor bearing flies fed a HF diet exhibited a significant reduction in median life span by 31% on HF compared to NM (Fig. 3.10, Tab. 3.1), although the tumor phenotype did not differ in the microscopic and the molecular quantification, nor in the digestive functionality between NM and HF fed tumor bearing flies (Fig. 3.5, Fig. 3.7 B, B', C and C', Fig. 3.8, Fig. 3.9 B-F). However, after 7 days of tumor induction, dense *esg⁺* cell accumulations and atypical single cells with drastically enlarged nuclei formed in HF but not NM fed tumor bearing flies (Fig. 3.4 B' and B'', C' and C'', yellow arrowheads). The shape and size of nuclei is tightly regulated in order to allow for proper rearrangement and function during and after mitosis. Cancer cells often exhibit morphological alterations of the nucleus and it has been recognized that increased nucleus size is directly linked to decreased overall survival probability (237, 238). I analyzed the body composition of tumor bearing flies subjected to NM and HF in order to elucidate the physiological underpinnings of the observed premature death in HF fed flies. The largest part of the body mass consists of fat and protein. In tumor bearing flies fed with a HF diet, both of these components were drastically reduced over the course of 10 days until only approximately 5% of each remained (Fig. 3.11 B, C). At

Discussion

the same time, a basic metabolic rate similar to NM fed tumor bearing flies was maintained (Fig. 3.12 A). The loss of fat and muscle tissue is one of the main indicators of tumor-induced cachexia (108, 109). Providing optimal nutritional intake to patients with advanced colorectal cancer is often problematic since patients frequently experience loss of appetite as well as nutrient malabsorption. However, cachexia is not only an unmet energy demand but is characterized by a distinct set of alterations that induce wasting to large parts independently of the nutritional intake (239, 240). In multiple *Drosophila* cachexia models, Ecdysone-inducible gene L2 (ImpL2) has been identified to impair insulin signaling by scavenging Dilps, resulting in a tumor-induced insulin resistance (110, 241). It is possible that tumor-induced insulin resistance is additive to the insulin resistance that is observed due to HF intake and obesity (242, 243). Therefore, a diet high in fats might exponentiate the tumor-induced insulin resistance in *RAF^{gof}* expressing flies and result in a cachexia-like wasting of fat and protein mass alike.

4.4. DR limits intestinal tumor growth but promotes cachexia-like wasting

Limiting food regimes are consistently linked to health benefits and longevity and have been shown to reduce tumor growth in multiple tumor models (88, 89, 91, 98, 99, 244, 245). A reduction of the overall caloric intake is the most widely used approach. However, DR which is characterized by the sole reduction of protein, was proven to be superordinate to caloric restriction (94–96) and was therefore investigated in this study. Benefits of DR are mediated in large parts by TOR signaling, a main integrator of nutritional sensing and growth regulation (101, 102, 246) with mutations along the signaling cascade often being observed in cancers (247–250).

In this study the application of strict DR for 3 consecutive days in flies expressing *RAF^{gof}* in ISCs and EBs resulted in the reduction of the tumor load as measured by co-expressed Luciferase (Fig. 3.5). Cross sections through the thorax and abdomen of tumor bearing flies fed with NM exhibited massive accumulation of *esg⁺* cell in the thoracic midgut with the formation of a second cell layer surrounding the fully differentiated *esg⁻* cells (Fig. 3.7 B, asterisk). On the other hand, tumor bearing flies subjected to DR exhibited significantly less excessive tissue mass with *esg⁺* cells being interspersed in the epithelial monolayer, similarly to the phenotype in control flies (Fig. 3.7 A and D, white arrowhead). NM fed *RAF^{gof}*

Discussion

expressing flies formed large esg^+ cell nests detached from the basal lamina and protruding into the lumen of the abdominal gut (Fig. 3.7 B', white arrow), whereas DR fed tumor bearing flies exhibited no such protrusions but only single esg^+ cells detached from the basal membrane (Fig. 3.7 D', yellow arrowhead). In total, the latter displayed only slightly increased amounts of esg^+ cells in comparison to healthy control flies (Fig. 3.7 A' and D'). The total gut volume, cell mass and relative gut obstruction further support the reduced tumor load and morphological recovery of tumor bearing flies subjected to DR (Fig. 3.8). In order to test the gut functionality of tumor bearing flies in response to DR, I examined the fecal output after feeding on the different nutritional regimes. When feeding on fully nutritious NM, tumor bearing flies exhibited significantly less fecal output in comparison to unimpaired controls due to less fecal spots while maintaining regular fecal spot size (Fig. 3.9 D-F). Upon subjection to DR, tumor bearing flies still exhibited a reduced fecal output. However, the reduction was solely due to a decrease in the size of individual fecal spots while fecal spot quantity was rescued (Fig. 3.9 D-F). Consequently, DR seems to restore gut functionality of tumor bearing flies, as the food passes through the intestine with the same regularity as in healthy control flies.

DR was shown to reduce tumor progression in a variety of models (100, 251–253). The main signaling pathway that integrates nutritional cues is the insulin signaling pathway, which mediates growth in response to nutrient abundance through the MAPK, PI3K/AKT and the TOR pathways (164) (Fig. 1.10). When nutrients are abundant, Dilp2, 3 and 5 are released from the *Drosophila* IPCs into the hemolymph from where they are accessible for distant tissues (Fig. 1.9). Dilps bind to the IR which leads to a phosphorylation cascade that activates both the MAPK pathway and Pi3K/Akt signaling *via* Chico. The MAPK cascade promotes tumor growth through the expression of target genes involved in cell survival, proliferation and angiogenesis (45, 137, 254). The Pi3K/Akt pathway, on the other hand, leads to the phosphorylation of the transcription factor Foxo which subsequently translocates from the nucleus into the cytoplasm where it no longer exerts target gene expression (178). However, Pi3k/Akt also activates Tor by inhibiting its inhibitor Tsc1-2. In parallel, free amino acids are imported into cells *via* Slimfast and also activate Tor to induce expression of target genes involved in cell size, ribosome biogenesis, proliferation and differentiation (255–257). Although protein intake generally correlates with growth, it seems that the role of protein quality is not to be overlooked, since replacing animal protein with the same amount of plant based protein reduces tumor growth significantly (251). Interestingly, the tumor growth

Discussion

reducing effect of plant protein is threshold-limited and seems to be subordinate to overall protein quantity independent of protein quality (251). However, the abovementioned pathways are not only inactive when nutrients are scarce, but induce the expression of target genes specifically enhancing cell stress resistance and rest in order to survive nutrient limitations. Low insulin signaling results in dephosphorylated Foxo shuttling into the nucleus to induce target gene expression which includes expression of the translational inhibitor 4E-BP (105, 182, 258), the cell cycle inhibitor p27 (259, 260) and the pro-apoptotic death receptor ligand Fas (178). Thereby, DR actively mediates stress resistance, cell growth arrest and survival, rather than solely lacking growth promotion through minimal signaling. Furthermore, the state of differential stress resistance, which describes a resting stage of unimpaired cells, cannot be induced in tumor cells, which are largely insensitive to extrinsic cues and remain in a highly proliferative state throughout nutrient scarcity. Therefore, healthy cells are better facilitated to endure stresses whereas cancer cells remain vulnerable. This effect was successfully exploited during chemotherapy which was shown to be more efficient and have less side effects when reducing or prohibiting nutritional input prior to drug admission (261–265).

Since DR is undoubtedly linked to longevity and due to the DR mediated drastic reduction of the tumor load of flies expressing *RAF^{gof}* in ISCs and EBs, I surveyed the lifespan of tumor bearing flies feeding on NM or DR. Surprisingly, the median lifespan of tumor bearing flies was radically reduced by 43% when feeding on DR in comparison to NM (Fig. 3.10, Tab. 3.1) albeit the reduced tumor mass. In addition, enlarged nuclei formed in single cells of DR fed tumor bearing flies after 7 days of tumor induction (Fig. 3.4 D' and D'', yellow arrowhead, white arrow, respectively). Interestingly, misshaped and amorphous nuclei are frequently observed in advanced cancers and are indicative of poor prognosis of patient survival (237, 238).

Upon investigating the body composition of the prematurely deceasing flies, a massive loss of fat and protein mass was observed (Fig. 3.11 B, C). Moreover, tumor bearing flies fed with DR exhibited approximately 15% weight loss (Fig. 3.11 A), a phenotype that is often observed in patients that suffer from advanced cancers and have entered into a cachectic state (109, 266). Cachexia is characterized by 3 metabolic phases: the first phase is considered preclinical and does not induce obvious changes in the metabolic rate, the second phase is a short hypermetabolic response, whereas the third phase is described by severe hypometabolism (267). The metabolic rate of flies expressing *RAF^{gof}* in ISCs and EBs was

Discussion

drastically reduced over time in DR subjected animals compared to flies of the same genotype lacking tumorigenesis (Fig. S3). This effect is not attributable to a decreased metabolic turnover mediated by DR alone, since flies subjected to DR have been shown to have unimpaired postprandial and resting energy consumption (268). The metabolic rate of tumor bearing flies fed with DR was at the control level on day 1 which can be considered the preclinical phase. However, flies were already hypometabolic on day 3 and metabolic rate further decreased. The 3 metabolic phases were described by a study using a cachexia-inducing tumor model in rats. It has to be considered that *Drosophila* metabolism and lifespan are substantially faster than those of rats. Therefore, it is likely that the 3 metabolic phases of cachexia proceeded within a fraction of the time resulting in flies suffering considerably faster from hypometabolism. The hypermetabolic phase described by Zylitz *et al.* (267) is likely missed in this experimental setup due to the tight time frame of cachexia staging in flies.

The extensive tissue loss in cachectic individuals implies an increased energy demand. Indeed, tumor bearing flies in this study exhibited increased rates of food interactions when submitted to DR (Fig. 3.9 A). These interactions display the number of contacts between a fly and the food source but neither reflect the amount of food that has been ingested nor the absorption rate of ingested nutrients. Furthermore, these rates are not necessarily consistent during tumor progression. The phenomenon of protein leverage, which describes the ingestion of protein low food until a threshold protein uptake is achieved (269) has to be taken into account when conducting experiments with *ad libitum* access to food. However, the strict protein limitation used in this study deems compensatory feeding to be unlikely to reach the protein uptake of the NM feeding regime. Interestingly, cachexia is not only conferred by an unmet energy demand but is characterized by distinct modes of action that impair insulin signaling through the scavenging of insulin by ImpL2, which results in insulin resistance (110). This implies the possibility that the application of DR, which sensitizes cells to insulin signaling by upregulating critical pathway components like the insulin receptor itself (105), may counteract tumor-induced cachexia. However, this hypothesis did not hold since DR subjected flies exhibited extensive wasting, whereas NM fed flies did not, although DR fed flies developed significantly less tumor mass. Therefore, there has to be a cachexia-promoting interaction between the tumor and the protein restriction. One explanation might be the expression of insulin scavenging proteins by Foxo. Brunet *et al.* (178) discovered a Foxo binding site in the promoter region of the insulin-like growth factor-binding protein 1, which is the mammalian structural homolog of *Drosophila's* ImpL2 (270). Therefore, instead of

Discussion

preventing cachexia by improving insulin signaling, the low insulin signaling during DR might induce a negative feedback loop of insulin scavenging proteins in addition to tumor-induced insulin scavenging and thus may result in the observed cachexia phenotype.

In summary, subjecting tumor bearing flies to DR significantly reduced the tumor growth and tumor-dependent intestinal obstruction, and restored gut functionality. However, DR subjection promoted fat and muscle wasting of tumor bearing flies which resulted in their premature death albeit the reduced tumor load. This form of tumor induced wasting is characterized by an altered metabolism of cancer cells as well as an independence of anabolic stimuli combined with a resistance to catabolic stimuli (239). While DR induces a state of growth arrest and resource conservation in healthy cells, tumor cells are resistant to those inputs and seem to promote wasting in order to enable further tumor growth. Therefore, tumor growth under DR conditions is reduced but not eliminated and is kept up at the expense of distant tissues. Based on these findings I focused my research on finding a nutritional regime that promotes the tumor reducing effects of DR while maintaining nutritional input necessary for the preservation of healthy tissues.

4.5. A recurrent diet limits tumor growth and restores lifespan

Although dietary restriction has been shown to positively influence tumor development, it has not yet found broad application as a sustentative cancer treatment. Compliance with permanent DR is low and is not universally applicable, as shown in this study, depending on the metabolic state of a patient. Therefore, research has focused on finding substances that effectively mimic DR while avoiding actual nutritional restrictions. Metformin, a drug that is considered the first line treatment in type 2 diabetes, has continuously been associated with reduced cancer risk and tumor formation (271, 272). Metformin mimics DR and limits growth in a bipartite way. Firstly, Metformin decreases insulin levels, thereby reducing growth promotion through PI3K/AKT and TOR (273). Secondly, Metformin supposedly shifts the cellular AMP/ATP ratio through interaction with mitochondrial respiratory chain complex 1 and thereby induces AMP-activated protein kinase (AMPK) (274). AMPK in turn induces catabolic processes and apoptosis (275), and inhibits TOR by activating its inhibitor TSC2 as well as by inhibiting the TOR scaffold protein RAPTOR (276, 277). Resveratrol, another DR mimetic, also reduces tumor growth and induces apoptosis by addressing the TOR pathway

Discussion

through the activation of AMPK (278). Aside from DR mimetics, alternative nutritional regimes are being investigated in order to provide a form of dietary limitation that increases compliance while conveying the effects of permanent DR.

Feeding regimes that consist of a fasting-mimicking diet and short phases of feeding on a fully nutritious diet have recently been shown to exhibit health promoting effects in terms of reduced insulin signaling, visceral fat reduction, rejuvenation of the immune system and reduced cancer risk (279, 280). Furthermore, a recurring diet consisting of DR alternating with refeeding on a fully nutritious diet is also able to mimic permanent DR in terms of lifespan extension and reduction in insulin signaling (185). The same study suggests, that the observed effects increase with the length of time of feeding on DR and that translational alterations induced by DR persist throughout short phases of feeding on a nutrient rich diet. Therefore, I applied 3 different recurrent feeding regimes, differing in the time periods spend on DR and NM, in order to find a recurrent diet that reduces tumor load in flies expressing *RAF^{gof}* in ISCs and EBs while circumventing the effects of tumor-induced wasting (Fig. 3.11 B and C). Applying NMDR, a recurrent diet that rhythmically alternated 4 days of feeding on NM followed by 3 days of feeding on DR, resulted in an increased maximum lifespan (Tab. 3.1) and the extension of the lifespan of tumor bearing flies to the level of healthy control flies (Fig. 3.14 A). The reverse regime of 4 days DR followed by 3 days NM, termed DRNMI, including an initial phase of 5 days DR also restored lifespan to the control level and exhibited the highest maximum lifespan throughout all tested regimes (Fig. 3.14 B, Tab. 3.1). However, DRNMI resulted in a fast decrease of tumor bearing flies within the 1st week of tumor induction (Fig. 3.14 A). Therefore, the initial phase was reduced to 3 days DR followed by the same rhythm of 3 days NM and 4 days DR, termed DRNM. DRNM effectively restored lifespan of tumor bearing flies to the level of healthy control flies (Tab. 3.1, Fig. 3.14 A, B). Furthermore, subjecting healthy control flies to DRNM resulted in a lifespan extension of 47.4% (Fig. 3.14 D). Both the analysis of *RAF^{gof}* co-expressed Luciferase as well as microscopic analysis of saggital sections through the thorax and abdomen of tumor bearing flies revealed a significant reduction in *esg*⁺ tumor mass similar to the reduction observed in DR alone (Fig. 3.15, Fig. 3.16 A). Furthermore, subjecting tumor bearing flies to DRNM restored gut morphology and intestinal functionality (Fig. 3.17, Fig. 3.18).

Surprisingly, the body composition of DRNM fed flies is strikingly similar to the body composition of DR subjected tumor bearing flies (Fig. 3.19). However, while DR induced a

Discussion

cachexia-like metabolic state which subsequently resulted in the flies' premature death, DRNM subjected tumor bearing flies experience lifespans similar to those of healthy controls. DRNM subjected flies seemed not to suffer from tumor-induced wasting although they still experienced substantial body mass catabolism (Fig. 3.19 A-D). This paradox might be explained by the cycling of the investigated physiological phenotypes between the limits of NM and DR. Measurements of the *RAF^{gof}* co-expressed Luciferase, which was used as a measure for the tumor cell mass, revealed fluctuating Luciferase levels depending on the food provided previous to the assessment (Fig. 3.16 B). The Luciferase measurement clearly illustrates a cycling of the tumor mass with levels being similar to NM fed tumor bearing flies after feeding on NM and significantly reduced levels after periods of feeding on DR. Since all experiments on DRNM subjected flies were performed after a period of feeding on DR, the observed phenotypes likely represent the lower extreme values of a plastic phenotype that responds to its nutrient environment. McLeod *et al.* demonstrated that the midgut of *Drosophila* quickly responds to nutrient abundance and within 4 days completely restores ISCs ablated during protein starvation (281). Furthermore, refeeding after protein depletion quickly resulted in the retrieval of organ size and the loss of atrophy markers in mice (280). A compensatory increase in *Drosophila* ISCs is achieved after 24 h of refeeding (282), thus it can be hypothesized that intestinal recovery is further accelerated in tumor bearing flies due to the already increased number of active ISCs. The long-lasting translational changes induced by DR (185) continuously promote health parameters while the tissue loss observed during phases of DR most likely recovers during periods of feeding on NM, preventing the premature death of tumor bearing flies when subjected to DRNM in comparison to subjection to lifelong DR.

In summary, subjecting flies with *RAF^{gof}*-induced tumors to a recurrent diet consisting of phases of feeding on strict DR and on fully nutritious NM, resulted in the significant reduction of tumor load, the resumption of physiological gut functionality and rescued survival to the level of healthy control flies. The tumor bearing flies exhibited loss of body mass during subjection to DR which was most likely restored during refeeding and thus prevented tumor-induced wasting. The recurrent diet presented in this study did not completely inhibit tumor growth but rescued lifespan to the level of healthy controls. To eliminate malignant cells, treatment options would need to be joined, for example by combining surgery and chemotherapy with DRNM. Interestingly, it was shown that fasting prior to chemotherapeutic interventions induces differential stress resistance in healthy but not

Discussion

cancer cells (261, 262, 283, 284). Differential stress resistance is largely conferred by proto-oncogene downregulation. Since tumor cells are largely independent of growth signaling they remain activated upon nutrient limitations whereas healthy cells enter into a state of stress resistant growth rest (283, 285). However, differential stress resistance is not only conveyed by fasting, but was also shown to be accomplished by strict DR (286). The health benefits of the presented recurrent regime with phases of strict DR likely expand beyond the level of moderate DR and, similarly to fasting, promote health benefits faster while inducing stronger physiological responses at the same time (285). The presented recurrent diet therefore is of considerable medical relevance not only as subsidiary cancer treatment but in a variety of diseases that are responsive to DR, including but not limited to obesity, diabetes and cardiovascular diseases. At the same time, this form of recurrent diet presents as an endurable form of nutritive intervention and thus will increase patient compliance considerably.

4.6. DR induces long-lasting transcriptional alterations

Many of the health benefits that are elicited by continuous DR, including lifespan extension, sensitized insulin signaling and reduced metabolic rate, were reproducible through subjection to a recurrent feeding regime (185). I analyzed the transcriptomic profiles of healthy flies in order to categorize transcriptomic patterns that are responsible for the health benefits induced by DR and to identify key genes that enable recurrent diets to mimic lifelong DR. Therefore, flies subjected to DRNM were sampled after a period of refeeding and compared to their age matched counterparts continuously feeding on NM or DR.

Clustering of the DEGs of control flies subjected to either feeding regime identified 5 gene clusters with distinct expression patterns that were opposing in their expression pattern between DR and NM (Fig. 3.20, Tab. 3.2). Out of these, 2 clusters displayed an expression pattern shared between DRNM and NM (clusters 3 and 4). Since the DRNM treated flies were sampled after a period of feeding on NM these 2 clusters contain genes that react fast to fluctuating nutrient abundance. In contrast, the clusters 1 and 2 showed similar expression patterns between DRNM and DR and contain genes that remain differentially expressed throughout short periods of refeeding. Interestingly, 3 clusters (clusters 1, 3 and 5) were in between the opposing expression extremes of DR and NM. These clusters, together with the clusters that were similar to DR even after refeeding, contain genes that respond slowly to an

Discussion

increase of nutritional input and are most likely responsible for the growth arrest and the cellular resting stage observed upon dietary limitation (180, 182, 258). Therefore, they are prime candidates for genes that enable DRNM to mimic continuous DR. These clusters were KEGG enriched for *Toll and Imd signaling pathway* (Tab. 3.2) and are potentially involved in effectuating the immune system alterations observed after phases of nutrient scarcity, and the long-lasting health benefits of DR and DRNM (287–289).

This finding is further substantiated by the interaction networks based on the DEGs from control flies subjected to NM, DR or DRNM which identified a main network composed of two subnetworks. Both the small and the large subnetwork were enriched for *Toll and Imd signaling pathway* (Fig. 3.22, Tab. 3.3). Genes that were differentially expressed between NM and DRNM, genes that react fast to nutrient fluctuations, belonged to the large subnetwork whereas DEGs of DR and DRNM, genes that react slowly to nutrient fluctuations, mainly contributed to the small network (Fig. 3.22). Interactions of DEGs between DR and DRNM largely overlapped with those of DR and NM with the latter additionally dispersing throughout the whole network. This highlights the distinct expression profile activated by the recurrent diet, which accesses the similar metabolic functions through dissimilar pathway component interactions. At the same time, the interaction network of tumor bearing flies subjected to either regime was reduced to one reduced main network (Fig. 3.23) which can be attributed to an impaired ability of tumorous cells to adequately access cellular signaling components in order to respond to extrinsic input, and therefore reflects the molecular degeneracy of the intestines of tumor bearing flies.

Health benefits through DRNM are conferred by the regulation of specific target genes. I investigated the DEGs of healthy and tumor bearing flies feeding on NM, DR or DRNM in order to address 3 main questions: A) Which genes are liable to long-lasting transcriptional changes and are potential targets to confer DR related health benefits throughout periods of refeeding? B) Are there target genes that are specifically regulated by the recurrent feeding regime but not in lifelong DR or NM? C) Are there genes specifically expressed in tumor bearing flies subjected to DR that can explain the severe wasting phenotype observed solely in these flies? To answer these questions, I generated a Venn diagram based on the DEGs between the feeding regimes for both control and tumor bearing flies and additionally merged the DR regulated DEGs (Fig. 3.24). The overlap of the control samples revealed 1726 genes to be regulated by DR as well as by DRNM, and thus contained genes that remained

Discussion

differentially expressed throughout the refeeding period. Both DR and DRNM induced the differential expression of *I'm not dead yet*, a gene that leads to lifespan extension (290–292). Prime candidates for the long-lasting health benefits of DR and DRNM are the transcription factor *foxo* and the ribosomal protein kinase *S6K*, which were both upregulated in DR and DRNM. The two genes are affected through insulin and Tor signaling and induce stress resistance and cell growth arrest by activating target genes downstream of the insulin signaling (105, 180, 181) and inhibiting ribosome biosynthesis (293). Insulin signaling was further boosted by upregulation of the insulin receptor substrate *Chico*. At the same time, the insulin binding protein *ImpL2* was downregulated in DR as well as in DRNM. Since *ImpL2* is a Dilp scavenging protein (110, 270), its downregulation additionally maximizes insulin signaling during times of nutrient scarcity but also throughout phases of refeeding. Refeeding after nutrient scarcity can result in a boost and rejuvenation of multiple physiological aspects like cognition, the immune system and cell proliferation (287–289). In this study 888 genes were identified to be uniquely regulated after refeeding in DRNM (Fig. 3.24). Interestingly, these genes included *AMPK alpha* and *4E-BP* both of which are known to induce stress resistance and cell cycle arrest (275, 276). Furthermore, AMPK also induces catabolic processes and suppresses TOR signaling by activating its inhibitor TSC (276, 294).

DR and the recurrent regime presented in this study were able to reduce tumor growth and reinstate gut functionality. However, while DRNM rescued the lifespan of tumor bearing flies, DR drastically reduced lifespan (Fig. 3.14, Tab. 3.1). I investigated the DEGs uniquely regulated in tumor bearing flies after submission to DR and identified 2698 genes (Fig. 3.24) exclusive to the observed wasting phenotype. Most interestingly, these genes contained 21 *lethal* genes as well as several *autophagy-related factors*. Autophagy is a catabolic mechanism that degrades cytosolic constituents during starvation and entails the loss of lean body mass in patients suffering from cancer-induced wasting (295, 296). It has been hypothesized that tumors release starvation-mimicking factors that induce systemic autophagy in order to access nutrients and sustain tumor growth (295, 297). Intriguingly, both defective and excessive regulation of autophagy contributes to severe muscle atrophy (296), making it obscure to disentangle their distinct modes of action within the cachexia network. However, the hypothesis of DR induced tumor-associated cachexia is further substantiated by the upregulated expression of *Yki* solely in DR fed tumor bearing flies. Activated *Yki* induces ISC proliferation and has previously been established to induce cachexia in *Drosophila* (110, 111). Most interestingly, tumor bearing flies exhibited down regulation of *drop dead* when

Discussion

subjected to DR. Truncation of *drop dead* results in gross intestinal phenotypes in *Drosophila* including intestinal dysfunction and severe loss of body fat, which eventually results in premature death (298). The gene is only induced in tumor bearing flies and not control flies subjected to DR. Thus it most likely represents a link between abnormal proliferation and dietary intake and greatly contributes to tumor-induced wasting.

In summary, the transcriptomic analyses identified separate genetic networks in response to DR and refeeding. A number of genes induced by DR slowly responds to refeeding and therefore most likely contributes to the DR-like health benefits and lifespan extension in DRNM. In contrast to that, refeeding during a recurrent diet induces a distinct subset of genes that additionally confers stress resistance. The recurrent feeding regime thus not only mimics DR but introduces additional beneficial genetic alterations that further prolong health- and lifespan. Additionally, the wasting phenotype observed solely in tumor bearing DR subjected flies could be related to the induction of autophagy related genes which seemingly result in a disbalance of catabolic and anabolic processes and subsequent lean tissue wasting. Additionally, the downregulation of *drop dead*, a gene that induces intestinal malfunction and enhanced loss of storage metabolites, not only contributes to the tumor-induced cachexia-like phenotype observed in DR subjected flies, but also directly links tumor-diet interactions to systemic loss of intestinal functionality.

4.7. Intestinal tumors result in a dysbiotic shift of the intestinal microbiota

A functional microbiota is an important player in individual well-being and provides multiple health benefits including protection from pathogens (299) and detoxification of otherwise harmful toxins (300). Furthermore, bacteria can induce proliferation and shape the intestine by influencing its cellular composition (301). The intestines of germ free mice and flies show slower cell turnover than their conventionally reared counterparts, indicating a role of the microbiota not only as invasive pathogens that induce tissue regeneration but also in physiological intestinal homeostasis (302–304). Inducing intestinal tumors by expressing *RAF^{gof}* in *Drosophila* ISCs and EBs resulted in a higher tumor load in recolonized flies in contrast to germ free flies of the same genotype (Fig. 3.25). Bacteria can induce overproliferation, for example by stimulating intrinsic growth signaling pathways or by inducing DNA damage through the release of toxins or reactive oxygen species (305–307).

Discussion

The intestinal microbiota is an essential part of the digestive system with bacteria altering amino acid availability and providing essential amino acids (308–310), breaking down complex carbohydrates (311, 312) or providing vitamins to the host (313, 314). The complex microbial system is vastly responsive to environmental factors like drug administration (315–318) and diet (205, 319–321) which sustains microbial growth and acts as a reservoir to introduce microbial species. For example, it has been demonstrated that a high fat diet induces microbial dysbiosis (322). Furthermore, the shifted microbiota of obese mice is able to induce obesity in previously lean mice upon fecal transplantation (323). However, it remains largely unclear whether the shifted microbiota marks consequence or causality of obesity. Although the role of protein intake on the intestinal microbiota is largely unexplored, recent studies provide first insights into the association between protein intake and its effects on the microbial community. Interestingly, overall protein intake correlates with taxonomic diversity (324, 325) which could also be demonstrated in the present study (Fig. 3.26 A). In opposition, specific restriction of tryptophan has recently been demonstrated to increase taxonomic richness (326, 327). Beside the contradictory results on taxonomic diversity, protein restriction reproducibly increased the intestinal barrier function in pigs and resulted in the establishment of a presumably beneficial microbiota (328, 329). Furthermore, since the microbiota directly affects amino acid availability in the intestine, it might be accountable for DR-dependent health benefits and consequently improved longevity. Interestingly, the microbial community in intestines of flies subjected to DRNM fluctuated in terms of taxonomic diversity with higher diversity after periods of feeding on NM (Fig. 3.26 A). Microbial amendment following the dietary saltations might help establish a health-promoting microbial community. Indeed, recent studies on intermittent fasting demonstrated that diet-induced restructuring of the intestinal microbial community reduced obesity and retinopathy in mice (330, 331). During an alternating recurrent feeding regime, times of limited food access potentially thin out opportunistic bacterial taxa and enrich those taxa that are required for optimal nutrient metabolization and uptake, whereas times of nutrient abundance might serve to increment the bacterial pool. Therefore, a recurrent diet might over time maximize the inter-coordinated symbiosis between microbiota and host. Interestingly this mechanism seems to be impaired in tumor bearing flies independent of the feeding regime. Suggesting that the effect of the tumor development on the intestinal microbiota is superior to effects generated through varying nutritional intake. The intestinal microbiota is not only passively selected through gut acidity and niche availability but is actively regulated by the host through

Discussion

the actions of the host immune system and the release of antimicrobial peptides (AMPs). It is likely that tumor bearing flies lose part of the selection mechanism since Foxo, which is regulating the expression of various AMPs (332) and is sensitive to a variety of stress factors, is dysregulated during tumor development. At the same time, Foxo is a target of the insulin and Tor signaling pathway. Therefore, the misregulation of Foxo due to tumorigenesis might mask the effects of different food regimes on the development of the microbiota, resulting in a dysbiotic shift in tumor bearing flies with little respect to the underlying nutritional regime.

A shifted microbiota has been associated with a multitude of diseases including inflammatory bowel disease (333–335), asthma (336, 337), obesity and diabetes (323, 338, 339), or even psychiatric diseases (340, 341). Analysis of the microbial composition of control and tumor bearing flies revealed a distinct microbial shift after tumor induction *via* *RAF^{gof}* overexpression (Fig. 3.27). The tumor tissue was associated with high abundances of α - and β -*Proteobacteria* as well as *Lactobacillaceae* (Fig. 3.28). Interestingly, all feeding regimes showed a distinct transient increase in *Burkholderiales* after 6 days of tumor induction. It is noteworthy, that the order of *Burkholderiales* is frequently found and significantly enriched in colorectal tumors in humans (342–344). After 10 days of tumor induction the microbiota of flies feeding on either medium was quite dissimilar to the respective controls without tumors (Fig. 3.27). Solely tumor bearing flies that had been subjected to the recurrent DRNM regime exhibited a microbiota that was similar to that observed after 3 days and, most interestingly, similar to the microbiota observed in healthy control flies when subjected to DR. This similarity might reflect the overall improved health status of the DRNM fed flies even after 10 days of tumor induction.

In summary, lifelong subjection of control or tumor bearing flies to NM or DR resulted in the establishment of distinct microbial communities over time. The identification of *Burkholderiales*, an order that is frequently enriched in human CRCs, as a transiently flourishing bacterial unit in tumor bearing flies especially highlights the relevance of *Drosophila* as a model to investigate the molecular and microbial underpinnings pertinent to CRC. Most interestingly, an alternating recurrent feeding regime potentially maximizes host-microbe mutualism by specifically selecting advantageous bacterial taxa during nutrient scarcity, and renewing and replenishing the microbial reservoir when food is abundant. Therefore, the health benefits and life prolongation through DRNM not only rely on the host itself but on the whole metaorganismic entity.

5. Conclusion & Outlook

Tumors are very sensitive to their nutrient environment and nutrition directly affects two major prognostic factors, which are tumor growth and systemic organismal wasting. Different nutritional regimes positively influence tumor development. Diets that provide 80-90% of calories *via* fats have been proposed to limit tumor growth while nurturing healthy cells by limiting the available carbohydrates which are the main source of energy for tumor cells. In this study I subjected *Drosophila melanogaster* that express RAF^{gof} in ISCs and EBs and produce a solid intestinal tumor to a diet high in cocoa fat. The intestinal tumors were largely unaffected by the diet and developed similarly to those in flies feeding on a control diet. Interestingly, the HF fed flies experienced extensive tissue wasting and died significantly faster than the controls. In contrast to that, healthy flies subjected to HF diet show reduced lifespan which is accompanied by a gain of body mass (345, 346) (summarized in Fig. 5.1). However, in tumor bearing flies, the HF diet likely induces insulin resistance in healthy cells and thus increases the level of circulating carbohydrates and fostering tumor growth. Furthermore, tumors themselves have been shown to release factors that reduce systemic insulin signaling, thus the organismal wasting observed in HF fed tumor bearing flies might be provoked by fat-mediated insulin resistance that is enhanced by tumor-induced insulin insensitivity.

Protein limited DR is the only regime that consistently results in decreased tumor mass in a multitude of tumor models. Additionally, DR increases insulin sensibility and therefore might counteract wasting. Subjecting tumor bearing flies to DR resulted in a drastic reduction in tumor mass but at the same time, in extensive organismal wasting and subsequent premature death. Consequently, I designed a recurrent diet with phases of feeding on a fully nutritious diet alternating with phases of strict DR, to exploit the reduced tumor growth due to DR while circumventing extensive wasting. Indeed, the tumors of flies subjected to DRNM showed reduced growth to the same extent as tumors after subjection to lifelong DR and rescued lifespan to the level of healthy controls (summarized in Fig. 5.2). Although not all tumors are equally sensitive to nutritional limitations (252), the regime potentially still positively influences treatment outcome by boosting organismal health in a twofold manner. Firstly, upon experiencing nutrient scarcity healthy cells enter a state of protection called differential stress resistance. Due to their independence of external growth signals, tumor cells do not enter this protective state and remain vulnerable to chemotherapeutic treatment, while healthy

Conclusion & Outlook

cells largely evade destruction. Strict nutrient restriction prior to chemotherapy sessions has been shown to limit side effects and to ameliorate patients' subjective well-being (264, 347).

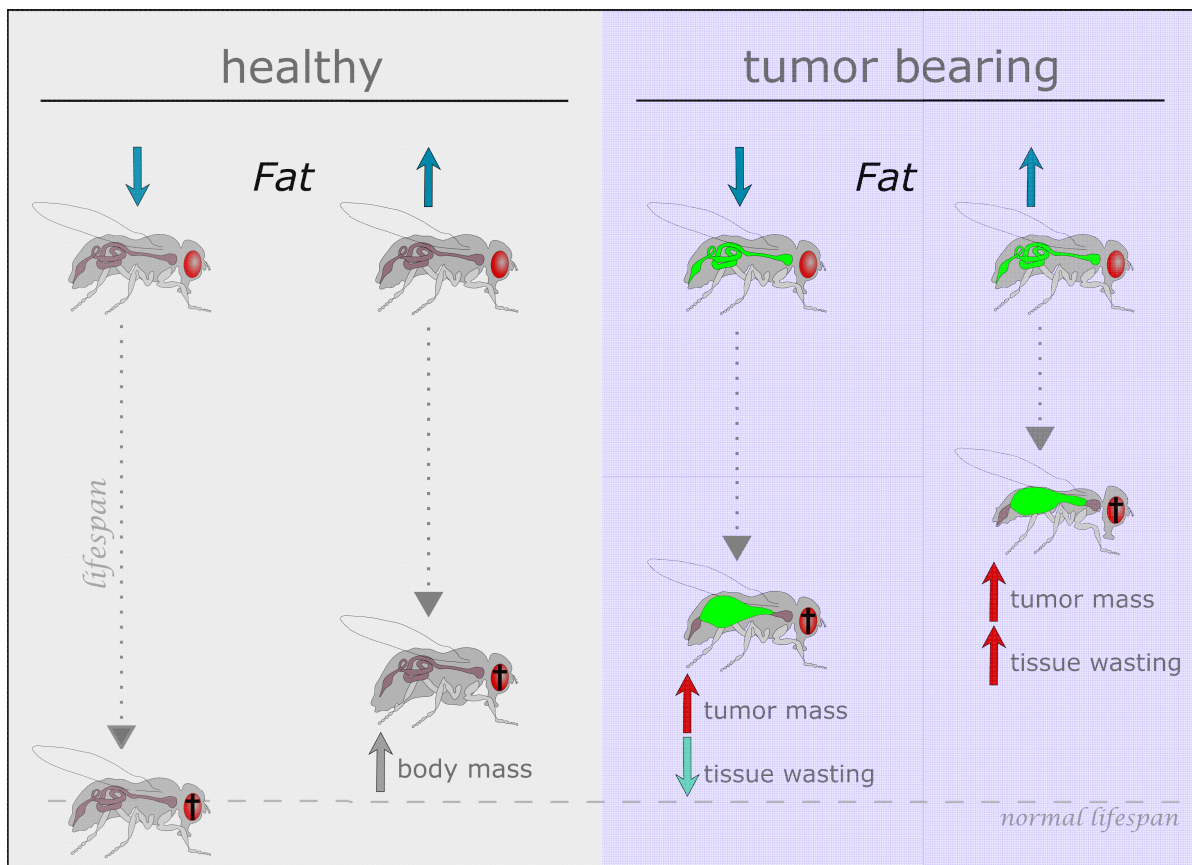


Fig. 5.1: Scheme representing the effects of high fat dieting on lifespan and tissue wasting in healthy and tumor bearing flies. High fat intake shortens lifespan and leads to increased body mass in healthy flies (left). Tumor induction reduces the lifespan of flies on low fat diets, but does not induce wasting. However, the lifespan of tumor bearing flies is dramatically shortened when feeding on a high fat diet with flies additionally experiencing extensive tissue wasting (right).

Secondly, not only DR confers health benefits, but refeeding after subsection to a restrictive feeding regime has proven to increase tissue regeneration and to rejuvenate the immune system. Indeed, RNA profiling identified a subset of genes that was specifically regulated upon refeeding. Therefore, a recurrent diet combines the limitation of tumor growth and increased sensitivity to chemotherapy conferred by protein restriction with systemic rejuvenation and an immune system boost after refeeding.

In summary, the application of the presented recurrent diet that effectively mimics lifelong DR is of great medical relevance since it combines the benefits of tumor limiting DR with an

Conclusion & Outlook

endurable feeding regime that likely will increase patient compliance with nutritional limitations. It will be critical to determine the required phase lengths in order to optimize the induced health benefits. Additionally, it has to be determined whether it is sufficient to limit specific amino acids instead of their overall amount, since not all amino acids seem to be equally relevant for DR (348, 349). In the long-run subjecting patients to personalized therapy plans including conventional treatments and a sustentative recurrent feeding regime might become a powerful tool to optimize colorectal cancer prognosis and overall survival.

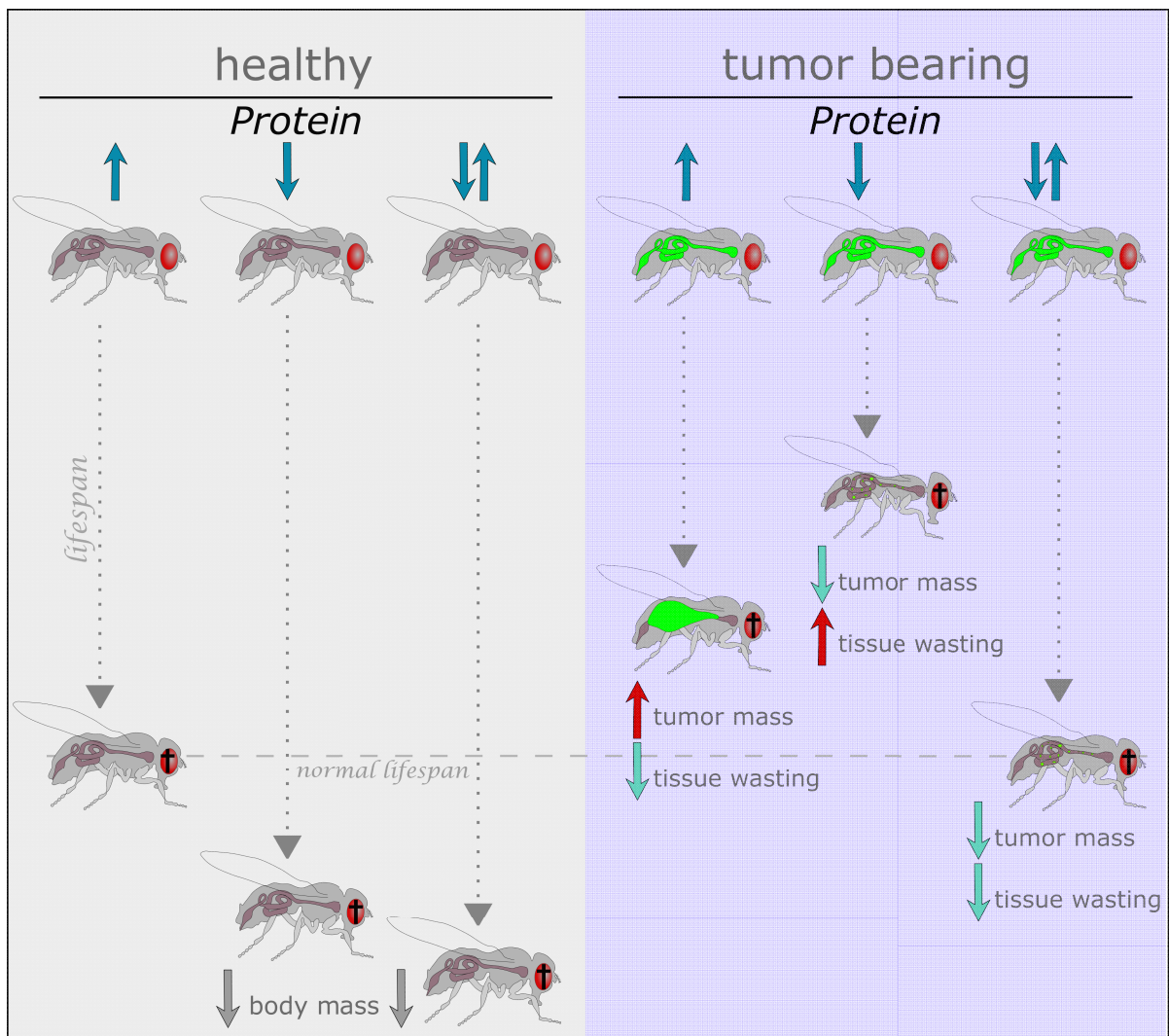


Fig. 5.2: Scheme representing the effects of protein restriction and recurrent protein restriction on lifespan and tissue wasting in healthy and tumor bearing flies. Low protein intake prologs lifespan and leads to decreased body mass, recurrent protein restriction further prologs lifespan in healthy flies (left). While lifespan is reduced in tumor bearing flies on fully nutritious diets and is dramatically shortened by feeding on a low protein diet. Additionally, low protein fed tumor bearing flies experience extensive tissue wasting. Subjection to recurrent protein restriction restores the life expectancy of tumor bearing flies back to the level of healthy controls feeding life-long on the fully nutritious medium, and does not promote tissue wasting (right).

6. References

1. Ferlay J, Soerjomataram I I, Dikshit R, Eser S, Mathers C, Rebelo M, Parkin DM, Forman D D, Bray F (2015) Cancer incidence and mortality worldwide: sources, methods and major patterns in GLOBOCAN 2012. *Int J Cancer* 136(5):E359-386.
2. Gandomani HS, Yousefi SM, Aghajani M, Mohammadian-Hafshejani A, Tarazoj AA, Pouyesh V, Salehiniya H (2017) Colorectal cancer in the world: incidence, mortality and risk factors. *Biomed Res Ther* 4(10):1656.
3. Granados-Romero JJ, Valderrama-Treviño AI, Contreras-Flores EH, Barrera-Mera B, Herrera Enríquez M, Uriarte-Ruiz K, Ceballos-Villalba JC, Estrada-Mata AG, Alvarado Rodríguez C, Arauz-Peña G (2017) Colorectal cancer: a review. *Int J Res Med Sci* 5(11):4667.
4. Bardou M, Barkun AN, Martel M (2013) Obesity and colorectal cancer. *Gut* 62(6):933–947.
5. Deng L, Gui Z, Zhao L, Wang J, Shen L (2012) Diabetes Mellitus and the Incidence of Colorectal Cancer: An Updated Systematic Review and Meta-Analysis. *Dig Dis Sci* 57(6):1576–1585.
6. Lee K-J, Inoue M, Otani T, Iwasaki M, Sasazuki S, Tsugane S (2007) Physical activity and risk of colorectal cancer in Japanese men and women: the Japan Public Health Center-based prospective Study. *Cancer Causes Control* 18(2):199–209.
7. Zisman AL, Nickolov A, Brand RE, Gorchow A, Roy HK (2006) Associations between the age at diagnosis and location of colorectal cancer and the use of alcohol and tobacco: Implications for screening. *Arch Intern Med* 166(6):629–634.
8. PDQ Adult Treatment Editorial Board (2002) *Colon Cancer Treatment (PDQ®): Patient Version* Available at: <http://www.ncbi.nlm.nih.gov/pubmed/26389319> [Accessed July 13, 2018].
9. Heerboth S, Housman G, Leary M, Longacre M, Byler S, Lapinska K, Willbanks A, Sarkar S (2015) EMT and tumor metastasis. *Clin Transl Med* 4(1):6.
10. Kalluri R, Weinberg R a (2009) The basics of epithelial-mesenchymal transition. *J Clin Invest* 119(6):1420–1428.
11. National Cancer Institute (2015) Cancer Staging. *Natl Inst Heal*. Available at: <https://www.cancer.gov/about-cancer/diagnosis-staging/staging> [Accessed July 16, 2018].
12. Edge SB, Byrd DR, Compton CC, Fritz AG, Greene FL, Trotti III A (2010) *AJCC Cancer Staging Manual Seventh Edition* Available at: <http://www.cancer.gov/cancertopics/factsheet/detection/staging>.
13. Bowel Cancer Australia (2017) Bowel Cancer Staging. Available at: <https://www.bowelcanceraustralia.org/bowel-cancer-staging> [Accessed August 1, 2018].
14. Smith D, Ballal M, Hodder R, Soin G, Selvachandran S, Cade D (2006) Symptomatic Presentation of Early Colorectal Cancer. *Ann R Coll Surg Engl* 88(2):185–190.
15. National Cancer Intelligence Network (2009) Colorectal cancer survival by stage. (June):1–2.
16. Cancer.Net Editorial Board (2013) Understanding Radiation Therapy. *Cancer.net Artic*. Available at: <https://www.cancer.net/navigating-cancer-care/how-cancer-treated/radiation-therapy/understanding-radiation-therapy> [Accessed July 13, 2018].
17. Cancer.Net Editorial Board (2012) Colorectal Cancer: Treatment Options. *Cancer.net Artic*. Available at: <https://www.cancer.net/cancer-types/colorectal-cancer/treatment-options> [Accessed July 13, 2018].
18. National Comprehensive Cancer Network Board (2017) *NCCN Guidelines for Patients: Colon Cancer* Available at: <https://www.nccn.org/patients/guidelines/colon/index.html#2>.
19. The American Cancer Society medical and editorial content team (2018) Targeted Therapy Drugs for Colorectal Cancer. *Cancer.org*. Available at: <https://www.cancer.org/cancer/colon-rectal-cancer/treating/targeted-therapy.html> [Accessed July 13, 2018].

References

20. Cancer.Net Editorial Board (2012) Understanding Immunotherapy. *Cancer.net Artic.* Available at: <https://www.cancer.net/navigating-cancer-care/how-cancer-treated/immunotherapy-and-vaccines/understanding-immunotherapy> [Accessed July 13, 2018].
21. Kanwar SS, Poolla A MA (2012) Regulation of colon cancer recurrence and development of therapeutic strategies. *World J Gastrointest Pathophysiol* 3(1):1.
22. Markle B, May EJ, Majumdar APN (2010) Do nutraceuticals play a role in the prevention and treatment of colorectal cancer? *Cancer Metastasis Rev* 29(3):395–404.
23. Westphalen CB, Asfaha S, Hayakawa Y, Takemoto Y, Lukin DJ, Nuber AH, Brandtner A, Setlik W, Remotti H, Muley A, Chen X, May R, Houchen CW, Fox JG, Gershon MD, Quante M, Wang TC (2014) Long-lived intestinal tuft cells serve as colon cancer–initiating cells. *J Clin Invest* 124(3):1283–1295.
24. Schwitalla S, Fingerle AA, Cammareri P, Nebelsiek T, Göktuna SI, Ziegler PK, Canli O, Heijmans J, Huels DJ, Moreaux G, Rupec RA, Gerhard M, Schmid R, Barker N, Clevers H, Lang R, Neumann J, Kirchner T, Taketo MM, van den Brink GR, Sansom OJ, Arkan MC, Greten FR (2013) Intestinal Tumorigenesis Initiated by Dedifferentiation and Acquisition of Stem-Cell-like Properties. *Cell* 152(1–2):25–38.
25. Beyaz S, Mana MD, Roper J, Kedrin D, Saadatpour A, Hong SJ, Bauer-Rowe KE, Xifaras ME, Akkad A, Arias E, Pinello L, Katz Y, Shinagare S, Abu-Remaileh M, Mihaylova MM, Lamming DW, Dogum R, Guo G, Bell GW, Selig M, Nielsen GP, Gupta N, Ferrone CR, Deshpande V, Yuan GC, Orkin SH, Sabatini DM, Yilmaz ÖH (2016) High-fat diet enhances stemness and tumorigenicity of intestinal progenitors. *Nature* 531(7592):53–58.
26. Ricci-Vitiani L, Lombardi DG, Pilozzi E, Biffoni M, Todaro M, Peschle C, De Maria R (2007) Identification and expansion of human colon-cancer-initiating cells. *Nature* 445(7123):111–115.
27. Barker N, Ridgway RA, van Es JH, van de Wetering M, Begthel H, van den Born M, Danenberg E, Clarke AR, Sansom OJ, Clevers H (2009) Crypt stem cells as the cells-of-origin of intestinal cancer. *Nature* 457(7229):608–611.
28. Tomasetti C, Vogelstein B, Parmigiani G (2013) Half or more of the somatic mutations in cancers of self-renewing tissues originate prior to tumor initiation. *Proc Natl Acad Sci* 110(6):1999–2004.
29. Fearon EF, Vogelstein B (1990) A Genetic Model for Colorectal Tumorigenesis. *Cell* 61:759–767.
30. Pino MS, Chung DC (2010) The Chromosomal Instability Pathway in Colon Cancer. *Gastroenterology* 138(6):2059–2072.
31. Tomasetti C, Marchionni L, Nowak MA, Parmigiani G, Vogelstein B (2015) Only three driver gene mutations are required for the development of lung and colorectal cancers. *Proc Natl Acad Sci* 112(1):118–123.
32. Di Fiore P, Pierce J, Kraus M, Segatto O, King C, Aaronson S (1987) erbB-2 is a potent oncogene when overexpressed in NIH/3T3 cells. *Science (80-)* 237(4811):178–182.
33. Hunter T (1997) Oncoprotein Networks. *Cell* 88(3):333–346.
34. Giancotti FG (1999) Integrin Signaling. *Science (80-)* 285(5430):1028–1033.
35. Hanahan D, Weinberg R a (2011) Hallmarks of cancer: the next generation. *Cell* 144(5):646–74.
36. Fernald K, Kurokawa M (2013) Evading apoptosis in cancer. *Trends Cell Biol* 23(12):620–633.
37. Hanahan D, Folkman J (1996) Patterns and Emerging Mechanisms of the Angiogenic Switch during Tumorigenesis. *Cell* 86(3):353–364.
38. Toyota M, Ahuja N, Ohe-Toyota M, Herman JG, Baylin SB, Issa JP (1999) CpG island methylator phenotype in colorectal cancer. *Proc Natl Acad Sci U S A* 96(15):8681–6.
39. Weisenberger DJ, Siegmund KD, Campan M, Young J, Long TI, Faasse MA, Kang GH, Widschwendter M, Weener D, Buchanan D, Koh H, Simms L, Barker M, Leggett B, Levine J, Kim M, French AJ, Thibodeau SN, Jass J, Haile R, Laird PW (2006) CpG island methylator phenotype underlies sporadic

References

- microsatellite instability and is tightly associated with BRAF mutation in colorectal cancer. *Nat Genet* 38(7):787–793.
40. Nguyen H, Duong H-Q (2018) The molecular characteristics of colorectal cancer: Implications for diagnosis and therapy. *Oncol Lett* 16:9–18.
 41. Boland RC, Goel A (2010) Microsatellite Instability in Colorectal Cancer. *Gastroenterology* 138(6):2073–2087.
 42. Aquilina G, Hess P, Branch P, MacGeoch C, Casciano I, Karran P, Bignami M (1994) A mismatch recognition defect in colon carcinoma confers DNA microsatellite instability and a mutator phenotype. *Proc Natl Acad Sci* 91(19):8905–9.
 43. Tariq K, Ghias K (2016) Colorectal cancer carcinogenesis: a review of mechanisms. *Cancer Biol Med* 13(1):120–35.
 44. Wells A (1999) EGF receptor. *Int J Biochem Cell Biol* 31(6):637–643.
 45. Krasinskas AM (2011) EGFR Signaling in Colorectal Carcinoma. *Patholog Res Int* 2011:932932.
 46. Spano JP, Fagard R, Soria J-C, Rixe O, Khayat D, Milano G (2005) Epidermal growth factor receptor signaling in colorectal cancer: preclinical data and therapeutic perspectives. *Ann Oncol* 16(2):189–194.
 47. Citri A, Yarden Y (2006) EGF–ERBB signalling: towards the systems level. *Nat Rev Mol Cell Biol* 7(7):505–516.
 48. Frattini M, Saletti P, Molinari F, De Dosso S (2015) EGFR signaling in colorectal cancer: a clinical perspective. *Gastrointest Cancer Targets Ther* 5:21.
 49. Davies H, Bignell GR, Cox C, Stephens P, Edkins S, Clegg S, Teague J, Futreal PA, et al. (2002) Mutations of the BRAF gene in human cancer. *Nature* 417(6892):949–954.
 50. Rajagopalan H, Bardelli A, Lengauer C, Kinzler KW, Vogelstein B, Velculescu VE (2002) RAF/RAS oncogenes and mismatch-repair status. *Nature* 418(6901):934–934.
 51. FDA (2004) Erbitux Approval Letter. *Cent Drug Eval Res*.
 52. Giusti RM, Shastri KA, Cohen MH, Keegan P, Pazdur R (2007) FDA Drug Approval Summary: Panitumumab (Vectibix™). *Oncologist* 12(5):577–583.
 53. Sunada H, Magun BE, Mendelsohn J, MacLeod CL (1986) Monoclonal antibody against epidermal growth factor receptor is internalized without stimulating receptor phosphorylation. *Proc Natl Acad Sci U S A* 83(11):3825–9.
 54. Ciardiello F, Tortora G (2008) EGFR Antagonists in Cancer Treatment. *N Engl J Med* 358(11):1160–1174.
 55. Ciardiello F (2000) Epidermal Growth Factor Receptor Tyrosine Kinase Inhibitors as Anticancer Agents. *Drugs* 60(Supplement 1):25–32.
 56. Amado RG, Wolf M, Peeters M, Van Cutsem E, Siena S, Freeman DJ, Juan T, Sikorski R, Suggs S, Radinsky R, Patterson SD, Chang DD (2008) Wild-Type KRAS Is Required for Panitumumab Efficacy in Patients With Metastatic Colorectal Cancer. *J Clin Oncol* 26(10):1626–1634.
 57. Freeman DJ, Juan T, Reiner M, Hecht JR, Meropol NJ, Berlin J, Mitchell E, Sarosi I, Radinsky R, Amado RG (2008) Association of K-ras Mutational Status and Clinical Outcomes in Patients with Metastatic Colorectal Cancer Receiving Panitumumab Alone. *Clin Colorectal Cancer* 7(3):184–190.
 58. Warburg O, Wind F, Negelein E (1931) The Metabolism of Tumors. *Am J Med Sci* 182(1):123.
 59. Pavlova NN, Thompson CB (2016) The Emerging Hallmarks of Cancer Metabolism. *Cell Metab* 23(1):27–47.
 60. Zhang W, Zhang SL, Hu X, Tam KY (2015) Targeting tumor metabolism for cancer treatment: Is pyruvate dehydrogenase kinases (PDKs) a viable anticancer target? *Int J Biol Sci* 11(12):1390–1400.

References

61. Holm E, Staedt U, Schlickeiser G, Leweling H, Tokus M, Hagemüller E, Günther HJ, Kollmar HB (1995) Substrate Balances across Colonic Carcinomas in Humans. *Cancer Res* 55(6):1373–1378.
62. Yamamoto T, Seino Y, Fukumoto H, Koh G, Yano H, Inagaki N, Yamada Y, Inoue K, Manabe T, Imura H (1990) Over-expression of facilitative glucose transporter genes in human cancer. *Biochem Biophys Res Commun* 170(1):223–230.
63. Sengupta D, Pratz G (2016) Imaging metabolic heterogeneity in cancer. *Mol Cancer* 15(1):4.
64. Feron O (2009) Pyruvate into lactate and back: From the Warburg effect to symbiotic energy fuel exchange in cancer cells. *Radiother Oncol* 92(3):329–333.
65. Vander Heiden MG, Cantley LC, Thompson CB (2009) Understanding the Warburg Effect: The Metabolic Requirements of Cell Proliferation. *Science* (80-) 324(5930):1029–1033.
66. Dr. Jason Fung The Paradox of Cancer's Warburg Effect. Available at: <https://medium.com/@drjasonfung/the-paradox-of-cancers-warburg-effect-7fb572364b81> [Accessed August 1, 2018].
67. Hori A, Sasada R, Matsutani E, Naito K, Sakura Y, Fujita T, Kozai Y (1991) Suppression of solid tumor growth by immunoneutralizing monoclonal antibody against human basic fibroblast growth factor. *Cancer Res* 51:6180–6184.
68. Commisso C, Davidson SM, Soydaner-Azeloglu RG, Parker SJ, Kamphorst JJ, Hackett S, Grabocka E, Nofal M, Drebin JA, Thompson CB, Rabinowitz JD, Metallo CM, Vander Heiden MG, Bar-Sagi D (2013) Macropinocytosis of protein is an amino acid supply route in Ras-transformed cells. *Nature* 497(7451):633–637.
69. Sun Q, Luo T, Ren Y, Florey O, Shirasawa S, Sasazuki T, Robinson DN, Overholtzer M (2014) Competition between human cells by entosis. *Cell Res* 24(11):1299–1310.
70. Strohecker AM, Guo JY, Karsli-Uzunbas G, Price SM, Chen GJ, Mathew R, McMahan M, White E (2013) Autophagy Sustains Mitochondrial Glutamine Metabolism and Growth of BrafV600E-Driven Lung Tumors. *Cancer Discov* 3(11):1272–1285.
71. Azria D, Bibeau F, Barbier N, Zouhair A, Lemanski C, Rouanet P, Ychou M, Senesse P, Ozsahin M, Pèlerin A, Dubois J-B, Thèzenas S (2005) Prognostic impact of epidermal growth factor receptor (EGFR) expression on loco-regional recurrence after preoperative radiotherapy in rectal cancer. *BMC Cancer* 5(1):62.
72. Kemeny NE, Chou JF, Capanu M, Alexandra N, Cercek A, Kingham TP, Jarnagin WR, Dematteo RP, Allen PJ, Shia J, Ang C, Angelica MID, Sloan M, Cancer K, Sloan M, Cancer K, Sloan M, Cancer K, Sloan M, Cancer K (2014) KRAS Mutation Influences Recurrence Patterns in Patients Undergoing Hepatic Resection of Colorectal Metastases. *120(24):3965–3971*.
73. Longley D, Johnston P (2005) Molecular mechanisms of drug resistance. *J Pathol* 205(2):275–292.
74. Gottesman MM, Fojo T, Bates SE (2002) Multidrug resistance in cancer: role of ATP-dependent transporters. *Nat Rev Cancer* 2(1):48–58.
75. Misale S, Yaeger R, Hobor S, Scala E, Janakiraman M, Liska D, Valtorta E, Schiavo R, Buscarino M, Siravegna G, Bencardino K, Cercek A, Chen C, Veronese S, Zanon C, Sartore-Bianchi A, Gambacorta M, Galliechio M, Vakiani E, Boscaro V, Medico E, Weiser M, Siena S, Di Nicolantonio F, Solit D, Bardelli A (2012) Emergence of KRAS mutations and acquired resistance to anti-EGFR therapy in colorectal cancer. *Nature* 486(7404):532–536.
76. Diergaarde B, Tiemersma EW, Braam H, Van Muijen GNP, Nagengast FM, Kok FJ, Kampman E (2005) Dietary factors and truncating APC mutations in sporadic colorectal adenomas. *Int J Cancer* 113(1):126–132.
77. Renehan AG, Tyson M, Egger M, Heller RF ZM (2008) Body-mass index and incidence of cancer: a systematic review and meta-analysis of prospective observational studies. *Lancet* 371(November):569–578.

References

78. Ryan-Harshman M, Aldoori W (2007) Diet and colorectal cancer: Review of the evidence. *Can Fam physician Médecin Fam Can* 53(11):1913–20.
79. Orgel E, Mittelman SD (2013) The links between insulin resistance, diabetes, and cancer. *Curr Diab Rep* 13(2):213–222.
80. Poff AM, Ari C, Arnold P, Seyfried TN, D’Agostino DP (2014) Ketone supplementation decreases tumor cell viability and prolongs survival of mice with metastatic cancer. *Int J Cancer* 135(7):1711–1720.
81. Zhou W, Mukherjee P, Kiebish MA, Markis WT, Mantis JG, Seyfried TN (2007) The calorically restricted ketogenic diet, an effective alternative therapy for malignant brain cancer. *Nutr Metab (Lond)* 4(7):5.
82. Mavropoulos JC, Buschemeyer WC, Tewari AK, Rokhfeld D, Pollak M, Zhao Y, Febbo PG, Cohen P, Hwang D, Devi G, Demark-Wahnefried W, Westman EC, Peterson BL, Pizzo S V., Freedland SJ (2009) The Effects of Varying Dietary Carbohydrate and Fat Content on Survival in a Murine LNCaP Prostate Cancer Xenograft Model. *Cancer Prev Res* 2(6):557–565.
83. Otto C, Kaemmerer U, Illert B, Muehling B, Pfetzer N, Wittig R, Voelker HU, Thiede A, Coy JF (2008) Growth of human gastric cancer cells in nude mice is delayed by a ketogenic diet supplemented with omega-3 fatty acids and medium-chain triglycerides. *BMC Cancer* 8(1):122.
84. Guraya SY (2015) Association of type 2 diabetes mellitus and the risk of colorectal cancer: A meta-analysis and systematic review. *World J Gastroenterol* 21(19):6026–6031.
85. González N, Prieto I, del Puerto-Nevado L, Portal-Nuñez S, Ardura JA, Corton M, Fernández-Fernández B, Aguilera O, Gomez-Guerrero C, Mas S, Moreno JA, Ruiz-Ortega M, Sanz AB, Sanchez-Niño MD, Rojo F, Vivanco F, Esbrit P, Ayuso C, Alvarez-Llamas G, Egido J, García-Foncillas J, Ortiz A, Consortium DCC (2017) 2017 update on the relationship between diabetes and colorectal cancer: epidemiology, potential molecular mechanisms and therapeutic implications. *Oncotarget* 8(11):18456–18485.
86. Giovannucci E, Harlan DM, Archer MC, Bergenstal RM, Gapstur SM, Habel LA, Pollak M, Regensteiner JG, Yee D (2010) Diabetes and Cancer: A consensus report. *Diabetes Care* 33(7):1674–1685.
87. Karunanithi S, Levi L, DeVecchio J, Karagkounis G, Reizes O, Lathia JD, Kalady MF, Noy N (2017) RBP4-STRA6 Pathway Drives Cancer Stem Cell Maintenance and Mediates High-Fat Diet-Induced Colon Carcinogenesis. *Stem Cell Reports* 9(2):438–450.
88. Rous P (1914) The Influence of Diet on Transplanted and Spontaneous Mouse Tumors. *J Exp Med* 20(5):433–451.
89. Tannenbaum A (2006) Effects of Varying Caloric Intake Upon Tumor Incidence and Tumor Growth. *Ann N Y Acad Sci* 49(1).
90. Olivo-Marston SE, Hursting SD, Perkins SN, Schetter A, Khan M, Croce C, Harris CC, Lavigne J (2014) Effects of calorie restriction and diet-induced obesity on murine colon carcinogenesis, growth and inflammatory factors, and MicroRNA expression. *PLoS One* 9(4):1–11.
91. Colman RJ, Anderson RM, Johnson SC, Kastman EK, Kosmatka KJ, Beasley TM, Allison DB, Cruzen C, Simmons HA, Kemnitz JW, Weindruch R (2009) Caloric restriction delays disease onset and mortality in rhesus monkeys. *Science (80-)* 325(5937):201–204.
92. Ja WW, Carvalho GB, Zid BM, Mak EM, Brummel T, Benzer S (2009) Water- and nutrient-dependent effects of dietary restriction on *Drosophila* lifespan. *Proc Natl Acad Sci U S A* 106(44):18633–18637.
93. Mitchell SJ, Madrigal-Matute J, Scheibye-Knudsen M, Fang E, Aon M, González-Reyes JA, Cortassa S, Kaushik S, Gonzalez-Freire M, Patel B, Wahl D, Ali A, Calvo-Rubio M, Burón MI, Guitierrez V, Ward TM, Palacios HH, Cai H, Frederick DW, Hine C, Broeskamp F, Habering L, Dawson J, Beasley TM, Wan J, Ikeno Y, Hubbard G, Becker KG, Zhang Y, Bohr VA, Longo DL, Navas P, Ferrucci L, Sinclair DA, Cohen P, Egan JM, Mitchell JR, Baur JA, Allison DB, Anson RM, Villalba JM, Madeo F, Cuervo AM, Pearson KJ, Ingram DK, Bernier M, De Cabo R (2016) Effects of Sex, Strain, and Energy Intake on

References

- Hallmarks of Aging in Mice. *Cell Metab* 23(6):1093–1112.
94. Mair W, Piper MDW, Partridge L (2005) Calories do not explain extension of life span by dietary restriction in *Drosophila*. *PLoS Biol* 3(7):1305–1311.
95. Grandison RC, Piper MDW, Partridge L (2009) Amino-acid imbalance explains extension of lifespan by dietary restriction in *Drosophila*. *Nature* 462(7276):1061–1064.
96. Pamplona R, Barja G (2006) Mitochondrial oxidative stress, aging and caloric restriction: The protein and methionine connection. *Biochim Biophys Acta - Bioenerg* 1757(5–6):496–508.
97. Solon-Biet SM, McMahon AC, Ballard JWO, Ruohonen K, Wu LE, Cogger VC, Warren A, Huang X, Pichaud N, Melvin RG, Gokarn R, Khalil M, Turner N, Cooney GJ, Sinclair DA, Raubenheimer D, Le Couteur DG, Simpson SJ (2014) The Ratio of Macronutrients, Not Caloric Intake, Dictates Cardiometabolic Health, Aging, and Longevity in Ad Libitum-Fed Mice. *Cell Metab* 19(3):418–430.
98. Fontana L, Adelaye RM, Rastelli AL, Miles KM, Ciamporcerro E, Longo VD, Nguyen H, Vessella R, Pili R (2013) Dietary protein restriction inhibits tumor growth in human xenograft models of prostate and breast cancer. *Oncotarget* 4(12):2451–2461.
99. Levine ME, Suarez JA, Brandhorst S, Balasubramanian P, Cheng CW, Madia F, Fontana L, Mirisola MG, Guevara-Aguirre J, Wan J, Passarino G, Kennedy BK, Wei M, Cohen P, Crimmins EM, Longo VD (2014) Low protein intake is associated with a major reduction in IGF-1, cancer, and overall mortality in the 65 and younger but not older population. *Cell Metab* 19(3):407–417.
100. Lamming DW, Cummings NE, Rastelli AL, Gao F, Cava E, Bertozzi B, Spelta F, Pili R, Fontana L (2015) Restriction of dietary protein decreases mTORC1 in tumors and somatic tissues of a tumor-bearing mouse xenograft model. *Oncotarget* 6(31):31233–31240.
101. Sahu N, Dela Cruz D, Gao M, Sandoval W, Haverty PM, Liu J, Stephan JP, Haley B, Classon M, Hatzivassiliou G, Settleman J (2016) Proline Starvation Induces Unresolved ER Stress and Hinders mTORC1-Dependent Tumorigenesis. *Cell Metab* 24(5):753–761.
102. Tatar M, Post S, Yu K (2014) Nutrient control of *Drosophila* longevity. *Trends Endocrinol Metab* 25(10):509–517.
103. Tatar M (2006) Diet Restriction in *Drosophila melanogaster*. *Mechanisms of Dietary Restriction in Aging and Disease* (KARGER, Basel), pp 115–136.
104. Kapahi P, Zid BM, Harper T, Koslover D, Sapin V, Benzer S (2004) Regulation of Lifespan in *Drosophila* by Modulation of Genes in the TOR Signaling Pathway. *Curr Biol* 14(10):885–890.
105. Puig O (2005) Transcriptional feedback control of insulin receptor by dFOXO/FOXO1. *Genes Dev* 19(20):2435–2446.
106. Ma XM, Blenis J (2009) Molecular mechanisms of mTOR-mediated translational control. *Nat Rev Mol Cell Biol* 10(5):307–318.
107. De Virgilio C, Loewith R (2006) The TOR signalling network from yeast to man. *Int J Biochem Cell Biol* 38(9):1476–1481.
108. Johns N, Stephens NA, Fearon KCH (2013) Muscle wasting in cancer. *Int J Biochem Cell Biol* 45(10):2215–2229.
109. Evans WJ, Morley JE, Argilés J, Bales C, Baracos V, Guttridge D, Jatoi A, Kalantar-Zadeh K, Lochs H, Mantovani G, Marks D, Mitch WE, Muscaritoli M, Najand A, Ponikowski P, Rossi Fanelli F, Schambelan M, Schols A, Schuster M, Thomas D, Wolfe R, Anker SD (2008) Cachexia: A new definition. *Clin Nutr* 27(6):793–799.
110. Figueroa-Claevega A, Bilder D (2015) Malignant *Drosophila* Tumors Interrupt Insulin Signaling to Induce Cachexia-like Wasting. *Dev Cell* 33(1):47–55.
111. Kwon Y, Song W, Droujinine IA, Hu Y, Asara JM, Perrimon N (2015) Systemic Organ Wasting Induced by Localized Expression of the Secreted Insulin/IGF Antagonist ImpL2. *Dev Cell* 33(1):36–46.

References

112. Kemnitz JW, Roecker EB, Weindruch R, Elson DF, Baum ST, Bergman RN (1994) Dietary restriction increases insulin sensitivity and lowers blood glucose in rhesus monkeys. *Am J Physiol Metab* 266(4):E540–E547.
113. Kang W, Lee MS, Baik M (2011) Dietary Protein Restriction Alters Lipid Metabolism and Insulin Sensitivity in Rats. *Asian-Australasian J Anim Sci* 24(9):1274–1281.
114. Duan W, Guo Z, Jiang H, Ware M, Mattson MP (2003) Reversal of Behavioral and Metabolic Abnormalities, and Insulin Resistance Syndrome, by Dietary Restriction in Mice Deficient in Brain-Derived Neurotrophic Factor. *Endocrinology* 144(6):2446–2453.
115. Adams MD (2000) The Genome Sequence of *Drosophila melanogaster*. *Science* (80-) 287(5461):2185–2195.
116. Brand AH, Perrimon N (1993) Targeted gene expression as a means of altering cell fates and generating dominant phenotypes. *Development* 118:401–415.
117. McGuire SE, Mao Z, Davis RL (2004) Spatiotemporal Gene Expression Targeting with the TARGET and Gene-Switch Systems in *Drosophila*. *Sci Signal* 2004(220):pl6-pl6.
118. Fortini ME, Skupski MP, Boguski MS, Hariharan IK (2000) A Survey of Human Disease Gene Counterparts in the *Drosophila* Genome. *J Cell Biol* 150(2):F23–F30.
119. Salomon RN, Jackson FR (2008) Tumors of the testis and midgut in aging flies. *Fly (Austin)* 2(6):265–268.
120. Siudeja K, Nassari S, Gervais L, Skorski P, Lameiras S, Stolfa D, Zande M, Bernard V, Frio TR, Bardin AJ (2015) Frequent Somatic Mutation in Adult Intestinal Stem Cells Drives Neoplasia and Genetic Mosaicism during Aging. *Cell Stem Cell* 17(6):663–674.
121. Hanahan D, Weinberg R (2000) The Hallmarks of Cancer. *Cell* 100:57–70.
122. Christofi T, Apidianakis Y (2013) *Drosophila* and the Hallmarks of Cancer. *Advances in Biochemical Engineering/Biotechnology*, pp 79–110.
123. Read RD (2011) *Drosophila melanogaster* as a model system for human brain cancers. *Glia* 59(9):1364–1376.
124. Levine BD, Cagan RL (2016) *Drosophila* Lung Cancer Models Identify Trametinib plus Statin as Candidate Therapeutic. *Cell Rep* 14(6):1477–1487.
125. Martorell O, Merlos-Suarez A, Campbell K, Barriga FM, Christov CP, Miguel-Aliaga I, Batlle E, Casanova J, Casali A (2014) Conserved mechanisms of tumorigenesis in the *Drosophila* adult midgut. *PLoS One* 9(2).
126. Markstein M, Dettorre S, Cho J, Neumüller R, Craig-Müller S, Perrimon N (2014) Systematic screen of chemotherapeutics in *Drosophila* stem cell tumors. *Proc Natl Acad Sci U S A* 111(12):4530–4535.
127. Ong C, Yung LYL, Cai Y, Bay BH, Baeg GH (2015) *Drosophila melanogaster* as a model organism to study nanotoxicity. *Nanotoxicology* 9(3):396–403.
128. St Johnston D (2002) The art and design of genetic screens: *Drosophila melanogaster*. *Nat Rev Genet* 3(3):176–188.
129. Price J V., Clifford RJ, Schüpbach T (1989) The maternal ventralizing locus torpedo is allelic to faint little ball, an embryonic lethal, and encodes the *Drosophila* EGF receptor homolog. *Cell* 56(6):1085–1092.
130. Schejter ED, Shilo B-Z (1989) The *Drosophila* EGF receptor homolog (DER) gene is allelic to faint little ball, a locus essential for embryonic development. *Cell* 56(6):1093–1104.
131. Baker NE, Rubin GM (1992) Ellipse mutations in the *Drosophila* homologue of the EGF receptor affect pattern formation, cell division, and cell death in eye imaginal discs. *Dev Biol* 150(2):381–396.
132. Jiang H, Grenley MO, Bravo MJ, Blumhagen RZ, Edgar B a. (2011) EGFR/Ras/MAPK signaling

References

- mediates adult midgut epithelial homeostasis and regeneration in *Drosophila*. *Cell Stem Cell* 8(1):84–95.
133. Lusk J, Lam V, Tolwinski N (2017) Epidermal Growth Factor Pathway Signaling in *Drosophila* Embryogenesis: Tools for Understanding Cancer. *Cancers (Basel)* 9(12):16.
 134. Brown KE, Kerr M, Freeman M (2007) The EGFR ligands Spitz and Keren act cooperatively in the *Drosophila* eye. *Dev Biol* 307(1):105–113.
 135. Shilo B (2003) Signaling by the *Drosophila* epidermal growth factor receptor pathway during development. *Exp Cell Res* 284(1):140–149.
 136. Urban S, Lee JR, Freeman M (2002) A family of Rhomboid proteases activates all Drosod intramembrane phila membrane-tethered EGF ligands. *EMBO J* 21(16):4277–4286.
 137. Jiang H, Edgar BA (2009) EGFR signaling regulates the proliferation of *Drosophila* adult midgut progenitors. *Development* 136(3):483–493.
 138. Gabay L, Scholz H, Golembo M, Klaes a, Shilo BZ, Klämbt C (1996) EGF receptor signaling induces pointed P1 transcription and inactivates Yan protein in the *Drosophila* embryonic ventral ectoderm. *Development* 122(11):3355–3362.
 139. Jin MH, Sawamoto K, Ito M, Okano H (2000) The interaction between the *Drosophila* secreted protein argos and the epidermal growth factor receptor inhibits dimerization of the receptor and binding of secreted spitz to the receptor. *Mol Cell Biol* 20(6):2098–2107.
 140. Klein DE, Stayrook SE, Shi F, Narayan K, Lemmon MA (2008) Structural basis for EGFR ligand sequestration by Argos. *Nature* 453(7199):1271–1275.
 141. Ghigliione C, Carraway KL, Amundadottir LT, Boswell RE, Perrimon N, Duffy JB (1999) The Transmembrane Molecule Kekk1 Acts in a Feedback Loop to Negatively Regulate the Activity of the *Drosophila* EGF Receptor during Oogenesis. *Cell* 96(6):847–856.
 142. Reich A, Sapir A, Shilo B (1999) Sprouty is a general inhibitor of receptor tyrosine kinase signaling. *Development* 126(18):4139–47.
 143. Kuraishi T, Binggeli O, Opota O, Buchon N, Lemaitre B (2011) Genetic evidence for a protective role of the peritrophic matrix against intestinal bacterial infection in *Drosophila melanogaster*. *Proc Natl Acad Sci* 108(38):15966–15971.
 144. Liu X, Hodgson JJ, Buchon N (2017) *Drosophila* as a model for homeostatic, antibacterial, and antiviral mechanisms in the gut. *PLOS Pathog* 13(5):e1006277.
 145. Ohlstein B, Spradling A (2006) The adult *Drosophila* posterior midgut is maintained by pluripotent stem cells. *Nature* 439(7075):470–474.
 146. Micchelli CA, Perrimon N (2006) Evidence that stem cells reside in the adult *Drosophila* midgut epithelium. *Nature* 439(7075):475–479.
 147. Buchon N, Osman D, David FPA, Yu Fang H, Boquete JP, Deplancke B, Lemaitre B (2013) Morphological and Molecular Characterization of Adult Midgut Compartmentalization in *Drosophila*. *Cell Rep* 3(5):1725–1738.
 148. Lemaitre B, Miguel-Aliaga I (2013) The digestive tract of *Drosophila melanogaster*. *Annu Rev Genet* 47:377–404.
 149. Overend G, Luo Y, Henderson L, Douglas AE, Davies SA, Dow JAT (2016) Molecular mechanism and functional significance of acid generation in the *Drosophila* midgut. *Sci Rep* 6(March):1–11.
 150. Jung AC (2005) Renal Tubule Development in *Drosophila*: A Closer Look at the Cellular Level. *J Am Soc Nephrol* 16(2):322–328.
 151. Liang J, Balachandra S, Ngo S, O'Brien LE (2017) Feedback regulation of steady-state epithelial turnover and organ size. *Nature* 548(7669):588–591.
 152. Jiang H, Patel PH, Kohlmaier A, Grenley MO, McEwen DG, Edgar BA (2009) Cytokine/Jak/Stat

References

- Signaling Mediates Regeneration and Homeostasis in the *Drosophila* Midgut. *Cell* 137(7):1343–1355.
153. Antonello Z a, Reiff T, Ballesta-Illan E, Dominguez M (2015) Robust intestinal homeostasis relies on cellular plasticity in enteroblasts mediated by miR-8-Escargot switch. *EMBO J* 34(15):2025–2041.
154. De Navascués J, Perdigoto CN, Bian Y, Schneider MH, Bardin AJ, Martínez-Arias A, Simons BD (2012) *Drosophila* midgut homeostasis involves neutral competition between symmetrically dividing intestinal stem cells. *EMBO J* 31(11):2473–2485.
155. Jin Y, Patel PH, Kohlmaier A, Pavlovic B, Zhang C, Edgar BA (2017) Intestinal Stem Cell Pool Regulation in *Drosophila*. *Stem Cell Reports* 8(6):1479–1487.
156. Jiang H, Tian A, Jiang J (2016) Intestinal stem cell response to injury: lessons from *Drosophila*. *Cell Mol Life Sci* 73(17):3337–3349.
157. Huang J-H, Douglas AE (2015) Consumption of dietary sugar by gut bacteria determines *Drosophila* lipid content. *Biol Lett* 11(9):20150469.
158. Keebaugh ES, Yamada R, Obadia B, Ludington WB, Ja WW (2018) Microbial Quantity Impacts *Drosophila* Nutrition, Development, and Lifespan. *iScience* 4:247–259.
159. Wong AC-N, Dobson AJ, Douglas AE (2014) Gut microbiota dictates the metabolic response of *Drosophila* to diet. *J Exp Biol* 217(11):1894–1901.
160. Ramírez Camejo LA, Michael GA, Génesis MM, Paul B (2017) Probiotics may protect *Drosophila* from infection by *Aspergillus flavus*. *Int J Pharm Sci Res* 8(4):1624–1632.
161. Jones TA, Hernandez DZ, Wong ZC, Wandler AM, Guillemin K (2017) The bacterial virulence factor CagA induces microbial dysbiosis that contributes to excessive epithelial cell proliferation in the *Drosophila* gut. *PLOS Pathog* 13(10):e1006631.
162. Buchon N, Broderick NA, Poidevin M, Pradervand S, Lemaitre B (2009) *Drosophila* Intestinal Response to Bacterial Infection: Activation of Host Defense and Stem Cell Proliferation. *Cell Host Microbe* 5(2):200–211.
163. Guo L, Karpac J, Tran SL, Jasper H (2014) PGRP-SC2 promotes gut immune homeostasis to limit commensal dysbiosis and extend lifespan. *Cell* 156(1–2):109–122.
164. Badisco L, Van Wielendaele P, Vanden Broeck J (2013) Eat to reproduce: a key role for the insulin signaling pathway in adult insects. *Front Physiol* 4(August):1–16.
165. Géminard C, Rulifson EJ, Léopold P (2009) Remote Control of Insulin Secretion by Fat Cells in *Drosophila*. *Cell Metab* 10(3):199–207.
166. Rajan A, Perrimon N (2012) *Drosophila* Cytokine Unpaired 2 Regulates Physiological Homeostasis by Remotely Controlling Insulin Secretion. *Cell* 151(1):123–137.
167. Okamoto N, Yamanaka N, Yagi Y, Nishida Y, Kataoka H, O'Connor MB, Mizoguchi A (2009) A Fat Body-Derived IGF-like Peptide Regulates Postfeeding Growth in *Drosophila*. *Dev Cell* 17(6):885–891.
168. Owusu-Ansah E, Perrimon N (2014) Modeling metabolic homeostasis and nutrient sensing in *Drosophila*: implications for aging and metabolic diseases. *Dis Model Mech* 7(3):343–350.
169. Kannan K, Fridell Y-WC (2013) Functional implications of *Drosophila* insulin-like peptides in metabolism, aging, and dietary restriction. *Front Physiol* 4(October):288.
170. Nässel DR (2012) Insulin-producing cells and their regulation in physiology and behavior of *Drosophila* 1 This review is part of a virtual symposium on recent advances in understanding a variety of complex regulatory processes in insect physiology and endocrinology, includ. *Can J Zool* 90(4):476–488.
171. Nässel DR, Kubrak OI, Liu Y, Luo J, Lushchak O V. (2013) Factors that regulate insulin producing cells and their output in *Drosophila*. *Front Physiol* 4 SEP(September):1–13.
172. Veenstra JA, Agricola H-J, Sellami A (2008) Regulatory peptides in fruit fly midgut. *Cell Tissue Res* 334(3):499–516.

References

173. O'Brien LE, Soliman SS, Li X, Bilder D (2011) Altered Modes of Stem Cell Division Drive Adaptive Intestinal Growth. *Cell* 147(3):603–614.
174. Fernandez R, Tabarini D, Azpiazu N, Frasch M, Schlessinger J (1995) The *Drosophila* insulin receptor homolog: a gene essential for embryonic development encodes two receptor isoforms with different signaling potential. *EMBO J* 14(14):3373–84.
175. Shilo B-Z (2014) The regulation and functions of MAPK pathways in *Drosophila*. *Methods* 68(1):151–159.
176. Maehama T, Dixon JE (1998) The Tumor Suppressor, PTEN/MMAC1, Dephosphorylates the Lipid Second Messenger, Phosphatidylinositol 3,4,5-Trisphosphate. *J Biol Chem* 273(22):13375–13378.
177. Alessi DR, Cohen P (1998) Mechanism of activation and function of protein kinase B. *Oncogene Cell Prolif* 308:55–62.
178. Brunet A, Bonni A, Zigmond MJ, Lin MZ, Juo P, Hu LS, Anderson MJ, Arden KC, Blenis J, Greenberg ME (1999) Akt promotes cell survival by phosphorylating and inhibiting a forkhead transcription factor. *Cell* 96(6):857–868.
179. Webb AE, Kundaje A, Brunet A (2016) Characterization of the direct targets of FOXO transcription factors throughout evolution. *Aging Cell* 15(4):673–685.
180. Martins R, Lithgow GJ, Link W (2016) Long live FOXO: unraveling the role of FOXO proteins in aging and longevity. *Aging Cell* 15(2):196–207.
181. Grewal SS (2009) Insulin/TOR signaling in growth and homeostasis: A view from the fly world. *Int J Biochem Cell Biol* 41(5):1006–1010.
182. Teleman AA, Chen YW, Cohen SM (2005) 4E-BP functions as a metabolic brake used under stress conditions but not during normal growth. *Genes Dev* 19(16):1844–1848.
183. Manning BD, Tee AR, Logsdon MN, Blenis J, Cantley LC (2002) Identification of the Tuberous Sclerosis Complex-2 Tumor Suppressor Gene Product Tuberin as a Target of the Phosphoinositide 3-Kinase/Akt Pathway. *Mol Cell* 10(1):151–162.
184. Colombani J, Raisin S, Pantalacci S, Radimerski T, Montagne J, Léopold P (2003) A Nutrient Sensor Mechanism Controls *Drosophila* Growth. *Cell* 114(6):739–749.
185. Romey-Glüsing R, Li Y, Hoffmann J, von Frieling J, Knop M, Pfefferkorn R, Bruchhaus I, Fink C, Roeder T (2017) Nutritional regimens with periodically recurring phases of dietary restriction extend lifespan in *Drosophila*. *FASEB J* 32(4):1993–2003.
186. Schneider CA, Rasband WS, Eliceiri KW (2012) NIH Image to ImageJ: 25 years of image analysis. *Nat Methods* 9(7):671–675.
187. Markstein M, Pitsouli C, Villalta C, Celniker SE, Perrimon N (2008) Exploiting position effects and the gypsy retrovirus insulator to engineer precisely expressed transgenes. *Nat Genet* 40(4):476–83.
188. Wayland MT, Defaye A, Rocha J, Jayaram SA, Royet J, Miguel-Aliaga I, Leulier F, Cognigni P (2014) Spotting the differences: Probing host/microbiota interactions with a dedicated software tool for the analysis of faecal outputs in *Drosophila*. *J Insect Physiol* 69:126–135.
189. Rera M, Bahadorani S, Cho J, Koehler CL, Ulgherait M, Hur JH, Ansari WS, Lo T, Jones DL, Walker DW (2011) Modulation of longevity and tissue homeostasis by the *Drosophila* PGC-1 homolog. *Cell Metab* 14(5):623–634.
190. Clark RI, Salazar A, Yamada R, Fitz-Gibbon S, Morselli M, Alcaraz J, Rana A, Rera M, Pellegrini M, Ja WW, Walker DW (2015) Distinct Shifts in Microbiota Composition during *Drosophila* Aging Impair Intestinal Function and Drive Mortality. *Cell Rep* 12(10):1656–1667.
191. Rausch P, Basic M, Batra A, Bischoff SC, Blaut M, Clavel T, Gläsner J, Gopalakrishnan S, Grassl GA, Günther C, Haller D, Hirose M, Ibrahim S, Loh G, Mattner J, Nagel S, Pabst O, Schmidt F, Siegmund B, Strowig T, Volynets V, Wirtz S, Zeissig S, Zeissig Y, Bleich A, Baines JF (2016) Analysis of factors contributing to variation in the C57BL/6J fecal microbiota across German animal facilities. *Int J Med*

References

- Microbiol* 306(5):343–355.
192. Haas BJ, Gevers D, Earl AM, Feldgarden M, Ward D V., Giannoukos G, Ciulla D, Tabbaa D, Highlander SK, Sodergren E, Methé B, DeSantis TZ, Petrosino JF, Knight R, Birren BW (2011) Chimeric 16S rRNA sequence formation and detection in Sanger and 454-pyrosequenced PCR amplicons. *Genome Res* 21(3):494–504.
 193. Caporaso JG, Kuczynski J, Stombaugh J, Bittinger K, Bushman FD, Costello EK, Fierer N, Peña AG, Goodrich JK, Gordon JI, Huttley G a, Kelley ST, Knights D, Koenig JE, Ley RE, Lozupone C a, McDonald D, Muegge BD, Pirrung M, Reeder J, Sevinsky JR, Turnbaugh PJ, Walters W a, Widmann J, Yatsunenkov T, Zaneveld J, Knight R (2010) QIIME allows analysis of high-throughput community sequencing data. *Nat Methods* 7(5):335–336.
 194. Leitão-Gonçalves R, Carvalho-Santos Z, Francisco AP, Fioreze GT, Anjos M, Baltazar C, Elias AP, Itskov PM, Piper MDW, Ribeiro C (2017) Commensal bacteria and essential amino acids control food choice behavior and reproduction. *PLOS Biol* 15(4):e2000862.
 195. Hildebrandt A, Bickmeyer I, Kühnlein RP (2011) Reliable *Drosophila* body fat quantification by a coupled colorimetric assay. *PLoS One* 6(9).
 196. Yatsenko AS, Marrone AK, Kucherenko MM, Shcherbata HR (2014) Measurement of Metabolic Rate in *Drosophila* using Respirometry. *J Vis Exp* (88):1–5.
 197. Pfeiffenberger C, Lear BC, Keegan KP, Allada R (2010) Locomotor activity level monitoring using the *Drosophila* activity monitoring (DAM) system. *Cold Spring Harb Protoc* 5(11).
 198. Ro J, Harvanek ZM, Pletcher SD (2014) FLIC : High-Throughput , Continuous Analysis of Feeding Behaviors in *Drosophila*. 9(6).
 199. Kim D, Perteza G, Trapnell C, Pimentel H, Kelley R, Salzberg SL (2013) TopHat2: accurate alignment of transcriptomes in the presence of insertions, deletions and gene fusions. *Genome Biol* 14(4):R36.
 200. Anders S, Pyl PT, Huber W (2015) HTSeq-A Python framework to work with high-throughput sequencing data. *Bioinformatics* 31(2):166–169.
 201. Szklarczyk D, Morris JH, Cook H, Kuhn M, Wyder S, Simonovic M, Santos A, Doncheva NT, Roth A, Bork P, Jensen LJ, von Mering C (2017) The STRING database in 2017: quality-controlled protein–protein association networks, made broadly accessible. *Nucleic Acids Res* 45(D1):D362–D368.
 202. Micallef L, Rodgers P (2014) euler APE: Drawing area-proportional 3-Venn diagrams using ellipses. *PLoS One* 9(7).
 203. Reiff T, Jacobson J, Cognigni P, Antonello Z, Ballesta E, Tan KJ, Yew JY, Dominguez M, Miguel-Aliaga I (2015) Endocrine remodelling of the adult intestine sustains reproduction in *Drosophila*. *Elife* 4(JULY 2015):1–19.
 204. Bokulich NA, Chung J, Battaglia T, Henderson N, Jay M, Li H, D. Lieber A, Wu F, Perez-Perez GI, Chen Y, Schweizer W, Zheng X, Contreras M, Dominguez-Bello MG, Blaser MJ (2016) Antibiotics, birth mode, and diet shape microbiome maturation during early life. *Sci Transl Med* 8(343):343ra82–343ra82.
 205. David LA, Maurice CF, Carmody RN, Gootenberg DB, Button JE, Wolfe BE, Ling A V, Devlin AS, Varma Y, Fischbach MA, Biddinger SB, Dutton RJ, Turnbaugh PJ (2014) Diet rapidly and reproducibly alters the human gut microbiome. *Nature* 505(7484):559–563.
 206. Wang B, Yao M, Lv L, Ling Z, Li L (2017) The Human Microbiota in Health and Disease. *Engineering* 3(1):71–82.
 207. Raskov H, Burcharth J, Pommergaard H-C (2017) Linking Gut Microbiota to Colorectal Cancer. *J Cancer* 8(17):3378–3395.
 208. von Frieling J, Fink C, Hamm J, Klischies K, Forster M, Bosch TCG, Roeder T, Rosenstiel P, Sommer F (2018) Grow With the Challenge – Microbial Effects on Epithelial Proliferation, Carcinogenesis, and Cancer Therapy. *Front Microbiol* 9(September):1–9.

References

209. Kohsaka A, Laposky AD, Ramsey KM, Estrada C, Joshu C, Kobayashi Y, Turek FW, Bass J (2007) High-Fat Diet Disrupts Behavioral and Molecular Circadian Rhythms in Mice. *Cell Metab* 6(5):414–421.
210. Birse RT, Choi J, Reardon K, Rodriguez J, Graham S, Diop S, Ocorr K, Bodmer R, Oldham S (2010) High-Fat-Diet-Induced Obesity and Heart Dysfunction Are Regulated by the TOR Pathway in *Drosophila*. *Cell Metab* 12(5):533–544.
211. Branecky KL, Niswender KD, Pendergast JS (2015) Disruption of daily rhythms by high-fat diet is reversible. *PLoS One* 10(9):1–12.
212. Musselman LP, Kühnlein RP (2018) *Drosophila* as a model to study obesity and metabolic disease. *J Exp Biol* 221(Suppl 1):jeb163881.
213. Karpac J, Biteau B, Jasper H (2013) Misregulation of an Adaptive Metabolic Response Contributes to the Age-Related Disruption of Lipid Homeostasis in *Drosophila*. *Cell Rep* 4(6):1250–1261.
214. Bross TG, Rogina B, Helfand SL (2005) Behavioral, physical, and demographic changes in *Drosophila* populations through dietary restriction. *Aging Cell* 4(6):309–317.
215. Ghimire S, Kim MS (2015) Enhanced Locomotor Activity Is Required to Exert Dietary Restriction-Dependent Increase of Stress Resistance in *Drosophila*. *Oxid Med Cell Longev* 2015:1–8.
216. Slattery ML, Mullany LE, Sakoda LC, Wolff RK, Samowitz WS, Herrick JS (2018) The MAPK-signaling pathway in colorectal cancer: Dysregulated genes and their association with micrnas. *Cancer Inform* 17.
217. Slattery ML, Lundgreen A, Wolff RK (2013) Dietary Influence on MAPK-Signaling Pathways and Risk of Colon and Rectal Cancer. *Nutr Cancer* 65(5):729–738.
218. Teng J-A, Wu S-G, Chen J-X, Li Q, Peng F, Zhu Z, Qin J, He Z-Y (2016) The Activation of ERK1/2 and JNK MAPK Signaling by Insulin/IGF-1 Is Responsible for the Development of Colon Cancer with Type 2 Diabetes Mellitus. *PLoS One* 11(2):e0149822.
219. Majumdar SR, Fletcher RH, Evans AT (1999) How does colorectal cancer present? Symptoms, duration, and clues to location. *Am J Gastroenterol* 94(10):3039–3045.
220. Hoffman F (1937) Cancer and diet. With facts and observations on related subjects. *Am J Surg* 37(3):544.
221. Grosso G, Bella F, Godos J, Sciacca S, Del Rio D, Ray S, Galvano F, Giovannucci EL (2017) Possible role of diet in cancer: systematic review and multiple meta-analyses of dietary patterns, lifestyle factors, and cancer risk. *Nutr Rev* 75(6):405–419.
222. Warren S (1932) Immediate causes of death in cancer. *Am J Med Sci* 184(5):610–615.
223. Tuca A, Guell E, Martinez-Losada E, Codorniu N (2012) Malignant bowel obstruction in advanced cancer patients: epidemiology, management, and factors influencing spontaneous resolution. *Cancer Manag Res* 4(1):159.
224. Winner M, Mooney SJ, Hershman DL, Feingold DL, Allendorf JD, Wright JD, Neugut AI (2013) Management and Outcomes of Bowel Obstruction in Patients with Stage IV Colon Cancer. *Dis Colon Rectum* 56(7):834–843.
225. Chen W, Tan X, Ye J, Liu Q, Zeng Q, Wang L, Wang J (2014) Effect of bowel obstruction on stage IV colorectal cancer. *Mol Clin Oncol* 2(2):308–312.
226. Woodcock KJ, Kierdorf K, Pouchelon CA, Vivancos V, Dionne MS, Geissmann F (2015) Macrophage-Derived upd3 Cytokine Causes Impaired Glucose Homeostasis and Reduced Lifespan in *Drosophila* Fed a Lipid-Rich Diet. *Immunity* 42(1):133–144.
227. Calle E, Rodriguez C, Walker-Thurmond K, Thun M (2003) Overweight, Obesity, and Mortality from Cancer in a Prospectively Studied Cohort of U.S. Adults. *N Engl J Med* 348(17):1625–1638.
228. De Stefani E, Mendilaharsu M, Deneo-Pellegrini H, Ronco A (1997) Influence of dietary levels of fat,

References

- cholesterol, and calcium on colorectal cancer. *Nutr Cancer* 29(1):83–89.
229. Bartsch H, Nair J, Owen RW (1999) Dietary polyunsaturated fatty acids and cancers of the breast and colorectum: emerging evidence for their role as risk modifiers. *Carcinogenesis* 20(12):2209–2218.
230. Gerber M, Thiébaud A, Astorg P, Clavel-Chapelon F, Combe N (2005) Dietary fat, fatty acid composition and risk of cancer. *Eur J Lipid Sci Technol* 107(7–8):540–559.
231. Reddy BS, Maeura Y (1984) Tumor Promotion by Dietary Fat in Azoxymethane-Induced Colon Carcinogenesis in Female F344 Rats: Influence of Amount and Source of Dietary Fat. *JNCI J Natl Cancer Inst* 72(3):745–750.
232. Chang W-CL, Chapkin RS, Lupton JR (1998) Fish Oil Blocks Azoxymethane-Induced Rat Colon Tumorigenesis by Increasing Cell Differentiation and Apoptosis Rather Than Decreasing Cell Proliferation. *J Nutr* 128(3):491–497.
233. Bartram HP, Gostner A, Scheppach W, Reddy BS, Rao C V, Dusel G, Richter F, Richter A, Kasper H (1993) Effects of fish oil on rectal cell proliferation, mucosal fatty acids, and prostaglandin E2 release in healthy subjects. *Gastroenterology* 105(5):1317–1322.
234. Terry P, Bergkvist L, Holmberg L, Wolk A (2001) No association between fat and fatty acids intake and risk of colorectal cancer. *Cancer Epidemiol Biomarkers Prev* 10(8):913–914.
235. Carrillo C, Cavia MDM, Alonso-Torre SR (2003) Antitumor effect of oleic acid; mechanisms of action: a review. *Nutr Hosp* 27(6):1860–5.
236. Binker-Cosen MJ, Richards D, Oliver B, Gaisano HY, Binker MG, Cosen-Binker LI (2017) Palmitic acid increases invasiveness of pancreatic cancer cells AsPC-1 through TLR4/ROS/NF- κ B/MMP-9 signaling pathway. *Biochem Biophys Res Commun* 484(1):152–158.
237. Jevtić P, Edens LJ, Vuković LD, Levy DL (2014) Sizing and shaping the nucleus: mechanisms and significance. *Curr Opin Cell Biol* 28(1):16–27.
238. Kadota K, Nitadori J, Woo KM, Sima CS, Finley DJ, Rusch VW, Adusumilli PS, Travis WD (2014) Comprehensive Pathological Analyses in Lung Squamous Cell Carcinoma: Single Cell Invasion, Nuclear Diameter, and Tumor Budding Are Independent Prognostic Factors for Worse Outcomes. *J Thorac Oncol* 9(8):1126–1139.
239. Gullett NP, Mazurak VC, Hebbar G, Ziegler TR (2011) Nutritional Interventions for Cancer-Induced Cachexia. *Curr Probl Cancer* 35(2):58–90.
240. Fearon KCH, Glass DJ, Guttridge DC (2012) Cancer Cachexia: Mediators, Signaling, and Metabolic Pathways. *Cell Metab* 16(2):153–166.
241. Kwon Y, Song W, Droujinine IA, Hu Y, Asara JM, Perrimon N (2015) Systemic Organ Wasting Induced by Localized Expression of the Secreted Insulin/IGF Antagonist ImpL2. *Dev Cell* 33(1):36–46.
242. Ye J (2013) Mechanisms of insulin resistance in obesity. *Front Med* 7(1):14–24.
243. Morris SNS, Coogan C, Chamseddin K, Fernandez-Kim SO, Kolli S, Keller JN, Bauer JH (2012) Development of diet-induced insulin resistance in adult *Drosophila melanogaster*. *Biochim Biophys Acta - Mol Basis Dis* 1822(8):1230–1237.
244. Rubio-Patiño C, Bossowski JP, De Donatis GM, Mondragón L, Villa E, Aira LE, Chiche J, Mhaidly R, Lebeau-pin C, Marchetti S, Voutetakis K, Chatziioannou A, Castelli FA, Lamourette P, Chu-Van E, Fenaille F, Avril T, Passeron T, Patterson JB, Verhoeven E, Bailly-Maitre B, Chevet E, Ricci JE (2018) Low-Protein Diet Induces IRE1 α -Dependent Anticancer Immunosurveillance. *Cell Metab*:1–15.
245. Appleton BS, Campbell TC (1981) Inhibition of Aflatoxin-Initiated Preneoplastic Liver Lesions by Low Dietary Protein. *Nutr Cancer* 3(4):200–206.
246. Johnson SC, Rabinovitch PS, Kaeberlein M (2013) MTOR is a key modulator of ageing and age-related disease. *Nature* 493(7432):338–345.
247. Yuan R, Kay A, Berg WJ, Leibold D (2009) Targeting tumorigenesis: development and use of mTOR

References

- inhibitors in cancer therapy. *J Hematol Oncol* 2(1):45.
248. Xu K, Liu P, Wei W (2014) mTOR signaling in tumorigenesis. *Biochim Biophys Acta - Rev Cancer* 1846(2):638–654.
249. Guertin DA, Sabatini DM (2007) Defining the Role of mTOR in Cancer. *Cancer Cell* 12(1):9–22.
250. Panasyuk G, Nemazanyy I, Zhyvoloup A, Filonenko V, Davies D, Robson M, Pedley RB, Waterfield M, Gout I (2009) mTOR β Splicing Isoform Promotes Cell Proliferation and Tumorigenesis. *J Biol Chem* 284(45):30807–30814.
251. Fontana L, Adelaiye RM, Rastelli AL, Miles KM, Ciamporcero E, Longo VD, Nguyen H, Vessella R, Pili R (2013) Dietary protein restriction inhibits tumor growth in human xenograft models of prostate and breast cancer. *Oncotarget* 4(12):2451–2461.
252. Kalaany NY, Sabatini DM (2009) Tumours with PI3K activation are resistant to dietary restriction. *Nature* 458(7239):725–731.
253. Yin J, Ren W, Huang X, Li T, Yin Y (2018) Protein restriction and cancer. *Biochim Biophys Acta - Rev Cancer* 1869(2):256–262.
254. Fang JY, Richardson BC (2005) The MAPK signalling pathways and colorectal cancer. *Lancet Oncol* 6(5):322–327.
255. Guertin DA, Guntur KVP, Bell GW, Thoreen CC, Sabatini DM (2006) Functional Genomics Identifies TOR-Regulated Genes that Control Growth and Division. *Curr Biol* 16(10):958–970.
256. Sabatini DM (2017) Twenty-five years of mTOR: Uncovering the link from nutrients to growth. *Proc Natl Acad Sci* 114(45):11818–11825.
257. Sengupta S, Peterson TR, Sabatini DM (2010) Regulation of the mTOR Complex 1 Pathway by Nutrients, Growth Factors, and Stress. *Mol Cell* 40(2):310–322.
258. Jünger MA, Rintelen F, Stocker H, Wasserman JD, Végh M, Radimerski T, Greenberg ME, Wikstrom M, et al. (2003) The *Drosophila* Forkhead transcription factor FOXO mediates the reduction in cell number associated with reduced insulin signaling. *J Biol* 2(3):20.
259. Medema RH, Kops GJPL, Bos JL, Burgering BMT (2000) AFX-like Forkhead transcription factors mediate cell-cycle regulation by Ras and PKB through p27kip1. *Nature* 404(6779):782–787.
260. Dijkers PF, Medema RH, Pals C, Banerji L, Thomas NSB, Lam EW-F, Burgering BMT, Raaijmakers JAM, Lammers J-WJ, Koenderman L, Coffey PJ (2000) Forkhead Transcription Factor FKHR-L1 Modulates Cytokine-Dependent Transcriptional Regulation of p27KIP1. *Mol Cell Biol* 20(24):9138–9148.
261. Shim HS, Wei M, Brandhorst S, Longo VD (2015) Starvation Promotes REV1 SUMOylation and p53-Dependent Sensitization of Melanoma and Breast Cancer Cells. *Cancer Res* 75(6):1056–1067.
262. Raffaghello L, Lee C, Safdie FM, Wei M, Madia F, Bianchi G, Longo VD (2008) Starvation-dependent differential stress resistance protects normal but not cancer cells against high-dose chemotherapy. *Proc Natl Acad Sci* 105(24):8215–8220.
263. Shi Y, Felley-Bosco E, Marti TM, Orłowski K, Pruschy M, Stahel RA (2012) Starvation-induced activation of ATM/Chk2/p53 signaling sensitizes cancer cells to cisplatin. *BMC Cancer* 12(1):571.
264. Raffaghello L, Safdie F, Bianchi G, Dorff T, Fontana L, Longo VD (2010) Fasting and differential chemotherapy protection in patients. *Cell Cycle* 9(22):4474–4476.
265. Safdie FM, Dorff T, Quinn D, Fontana L, Wei M, Lee C, Cohen P, Longo VD (2009) Fasting and cancer treatment in humans: A case series report. *Aging (Albany NY)* 1(12):988–1007.
266. Porporato PE (2016) Understanding cachexia as a cancer metabolism syndrome. *Oncogenesis* 5(2):e200-10.
267. Zyllicz Z, Schwantje O, Wagener DJT, Folgering HT (1990) Metabolic response to enteral food in

References

- different phases of cancer cachexia in rats. *Oncology* 47(1):87–91.
268. Hulbert A., Clancy DJ, Mair W, Braeckman BP, Gems D, Partridge L (2004) Metabolic rate is not reduced by dietary-restriction or by lowered insulin/IGF-1 signalling and is not correlated with individual lifespan in *Drosophila melanogaster*. *Exp Gerontol* 39(8):1137–1143.
269. Simpson SJ, Raubenheimer D (2005) Obesity: The protein leverage hypothesis. *Obes Rev* 6(2):133–142.
270. Huang XY, Huang ZL, Yang JH, Xu YH, Sun JS, Zheng Q, Wei C, Song W, Yuan Z (2016) Pancreatic cancer cell-derived IGFBP-3 contributes to muscle wasting. *J Exp Clin Cancer Res* 35(1):1–13.
271. Evans JMM, Donnelly LA, Emslie-Smith AM, Alessi DR, Morris AD (2005) Metformin and reduced risk of cancer in diabetic patients. *BMJ* 330(7503):1304–1305.
272. Hosono K, Endo H, Takahashi H, Sugiyama M, Sakai E, Uchiyama T, Suzuki K, Iida H, Sakamoto Y, Yoneda K, Koide T, Tokoro C, Abe Y, Inamori M, Nakagama H, Nakajima A (2010) Metformin Suppresses Colorectal Aberrant Crypt Foci in a Short-term Clinical Trial. *Cancer Prev Res* 3(9):1077–1083.
273. Goodwin P, Pritchard K, Ennis M, Clemons M, Graham M, Fantus IG (2008) Insulin-lowering effects of metformin in women with early breast cancer. *Clin Breast Cancer* 8(6):501–505.
274. El-Mir M-Y, Nogueira V, Fontaine E, Avéret N, Rigoulet M, Leverve X (2000) Dimethylbiguanide Inhibits Cell Respiration via an Indirect Effect Targeted on the Respiratory Chain Complex I Dimethylbiguanide Inhibits Cell Respiration via an Indirect Effect Targeted on the Respiratory Chain Complex I *. *J Biol Chem* 275(1):223–228.
275. Slack C, Foley A, Partridge L (2012) Activation of AMPK by the Putative Dietary Restriction Mimetic Metformin Is Insufficient to Extend Lifespan in *Drosophila*. *PLoS One* 7(10):e47699.
276. Inoki K, Zhu T, Guan K-L (2003) TSC2 Mediates Cellular Energy Response to Control Cell Growth and Survival. *Cell* 115(5):577–590.
277. Gwinn DM, Shackelford DB, Egan DF, Mihaylova MM, Mery A, Vasquez DS, Turk BE, Shaw RJ (2008) AMPK Phosphorylation of Raptor Mediates a Metabolic Checkpoint. *Mol Cell* 30(2):214–226.
278. Hwang J-T, Kwak DW, Lin SK, Kim HM, Kim YM, Park OJ (2007) Resveratrol Induces Apoptosis in Chemoresistant Cancer Cells via Modulation of AMPK Signaling Pathway. *Ann N Y Acad Sci* 1095(1):441–448.
279. Wei M, Brandhorst S, Shelehchi M, Mirzaei H, Cheng CW, Budniak J, Groshen S, Mack WJ, Guen E, Di Biase S, Cohen P, Morgan TE, Dorff T, Hong K, Michalsen A, Laviano A, Longo VD (2017) Fasting-mimicking diet and markers/risk factors for aging, diabetes, cancer, and cardiovascular disease. *Sci Transl Med* 9(377):eaa18700.
280. Brandhorst S, Choi IY, Wei M, Cheng CW, Sedrakyan S, Navarrete G, Dubeau L, Yap LP, Park R, Vinciguerra M, Di Biase S, Mirzaei H, Mirisola MG, Childress P, Ji L, Groshen S, Penna F, Odetti P, Perin L, Conti PS, Ikeno Y, Kennedy BK, Cohen P, Morgan TE, Dorff TB, Longo VD (2015) A Periodic Diet that Mimics Fasting Promotes Multi-System Regeneration, Enhanced Cognitive Performance, and Healthspan. *Cell Metab* 22(1):86–99.
281. McLeod C, Wang L, Wong C, Jones D (2010) Stem cell dynamics in response to nutrient availability. *Curr Biol* 20(23):2100–2105.
282. Obata F, Tsuda-Sakurai K, Yamazaki T, Nishio R, Nishimura K, Kimura M, Funakoshi M, Miura M (2018) Nutritional Control of Stem Cell Division through S-Adenosylmethionine in *Drosophila* Intestine. *Dev Cell* 44(6):741–751.e3.
283. Lee C, Raffaghello L, Brandhorst S, Safdie FM, Bianchi G, Martin-Montalvo A, Pistoia V, Wei M, Hwang S, Merlino A, Emionite L, de Cabo R, Longo VD (2012) Fasting Cycles Retard Growth of Tumors and Sensitize a Range of Cancer Cell Types to Chemotherapy. *Sci Transl Med* 4(124):124ra27-124ra27.
284. Shi Y, Felley-Bosco E, Marti TM, Orłowski K, Pruschy M, Stahel RA (2012) Starvation-induced

References

- activation of ATM/Chk2/p53 signaling sensitizes cancer cells to cisplatin. *BMC Cancer* 12(1):571.
285. Lee C, Longo VD (2011) Fasting vs dietary restriction in cellular protection and cancer treatment: from model organisms to patients. *Oncogene* 30(30):3305–3316.
286. Vigne P, Tauc M, Frelin C (2009) Strong Dietary Restrictions Protect *Drosophila* against Anoxia/Reoxygenation Injuries. *PLoS One* 4(5):e5422.
287. Brandhorst S, Choi IY, Wei M, Cheng CW, Sedrakyan S, Navarrete G, Dubeau L, Yap LP, Park R, Vinciguerra M, Di Biase S, Mirzaei H, Mirisola MG, Childress P, Ji L, Groshen S, Penna F, Odetti P, Perin L, Conti PS, Ikeno Y, Kennedy BK, Cohen P, Morgan TE, Dorff TB, Longo VD (2015) A Periodic Diet that Mimics Fasting Promotes Multi-System Regeneration, Enhanced Cognitive Performance, and Healthspan. *Cell Metab* 22(1):86–99.
288. Mendelsohn AR, Larrick JW (2014) Prolonged Fasting/Refeeding Promotes Hematopoietic Stem Cell Regeneration and Rejuvenation. *Rejuvenation Res* 17(4):385–389.
289. Kouda K, Nakamura H, Kohno H, Ha-Kawa SK, Tokunaga R, Sawada S (2004) Dietary restriction: effects of short-term fasting on protein uptake and cell death/proliferation in the rat liver. *Mech Ageing Dev* 125(5):375–380.
290. Marden JH, Rogina B, Montooth KL, Helfand SL (2003) Conditional tradeoffs between aging and organismal performance of Indy long-lived mutant flies. *Proc Natl Acad Sci* 100(6):3369–3373.
291. Wang P-Y, Neretti N, Whitaker R, Hosier S, Chang C, Lu D, Rogina B, Helfand SL (2009) Long-lived Indy and calorie restriction interact to extend life span. *Proc Natl Acad Sci* 106(23):9262–9267.
292. Rogina B, Reenan RA, Nilsen SP, Helfand SL (2000) Extended Life-Span Conferred by Cotransporter Gene Mutations in *Drosophila*. *Science* (80-) 290(5499):2137–2140.
293. Magnuson B, Ekim B, Fingar DC (2012) Regulation and function of ribosomal protein S6 kinase (S6K) within mTOR signalling networks. *Biochem J* 441(1):1–21.
294. Marygold SJ, Leever SJ (2002) Growth Signaling: TSC Takes Its Place. *Curr Biol* 12(22):R785–R787.
295. Aversa Z, Pin F, Lucia S, Penna F, Verzaro R, Fazi M, Colasante G, Tirone A, Fanelli FR, Ramaccini C, Costelli P, Muscaritoli M (2016) Autophagy is induced in the skeletal muscle of cachectic cancer patients. *Sci Rep* 6(1):30340.
296. Penna F, Costamagna D, Pin F, Camperi A, Fanzani A, Chiarpotto EM, Cavallini G, Bonelli G, Baccino FM, Costelli P (2013) Autophagic degradation contributes to muscle wasting in cancer cachexia. *Am J Pathol* 182(4):1367–1378.
297. Pettersen K, Andersen S, Degen S, Tadini V, Grosjean J, Hatakeyama S, Tesfahun AN, Moestue S, Kim J, Nonstad U, Romundstad PR, Skorpen F, Sørhaug S, Amundsen T, Grønberg BH, Strasser F, Stephens N, Hoem D, Molven A, Kaasa S, Fearon K, Jacobi C, Bjørkøy G (2017) Cancer cachexia associates with a systemic autophagy-inducing activity mimicked by cancer cell-derived IL-6 trans-signaling. *Sci Rep* 7(1):2046.
298. Peller CR, Bacon EM, Bucheger JA, Blumenthal EM (2009) Defective gut function in drop-dead mutant *Drosophila*. *J Insect Physiol* 55(9):834–839.
299. Fraune S, Anton-Erxleben F, Augustin R, Franzenburg S, Knop M, Schröder K, Willoweit-Ohl D, Bosch TCG (2015) Bacteria–bacteria interactions within the microbiota of the ancestral metazoan *Hydra* contribute to fungal resistance. *ISME J* 9(7):1543–1556.
300. Chaucheyras-Durand F, Maseglier S, Fonty G, Forano E (2010) Influence of the Composition of the Cellulolytic Flora on the Development of Hydrogenotrophic Microorganisms, Hydrogen Utilization, and Methane Production in the Rumen of Gnotobiotically Reared Lambs. *Appl Environ Microbiol* 76(24):7931–7937.
301. Sommer F, Nookaew I, Sommer N, Fogelstrand P, Bäckhed F (2015) Site-specific programming of the host epithelial transcriptome by the gut microbiota. *Genome Biol* 16(1):1–15.
302. Buchon N, Broderick NA, Chakrabarti S, Lemaitre B (2009) Invasive and indigenous microbiota impact

References

- intestinal stem cell activity through multiple pathways in *Drosophila*. *Genes Dev* 23(19):2333–2344.
303. Broderick NA, Buchon N, Lemaitre B (2014) Microbiota-Induced Changes in *Drosophila melanogaster* Host Gene Expression and Gut Morphology. *MBio* 5(3):1–13.
304. Savage DC, Siegel JE, Snellen JE, Whitt DD (1981) Transit time of epithelial cells in the small intestines of germfree mice and ex-germfree mice associated with indigenous microorganisms. *Appl Environ Microbiol* 42(6):996–1001.
305. Rubinstein MR, Wang X, Liu W, Hao Y, Cai G, Han YW (2013) *Fusobacterium nucleatum* Promotes Colorectal Carcinogenesis by Modulating E-Cadherin/ β -Catenin Signaling via its FadA Adhesin. *Cell Host Microbe* 14(2):195–206.
306. Goodwin AC, Shields CED, Wu S, Huso DL, Wu X, Murray-Stewart TR, Hacker-Prietz A, Rabizadeh S, Woster PM, Sears CL, Casero RA (2011) Polyamine catabolism contributes to enterotoxigenic *Bacteroides fragilis*-induced colon tumorigenesis. *Proc Natl Acad Sci* 108(37):15354–15359.
307. Boleij A, Hechenbleikner EM, Goodwin AC, Badani R, Stein EM, Lazarev MG, Ellis B, Carroll KC, Albesiano E, Wick EC, Platz EA, Pardoll DM, Sears CL (2015) The *Bacteroides fragilis* Toxin Gene Is Prevalent in the Colon Mucosa of Colorectal Cancer Patients. *Clin Infect Dis* 60(2):208–215.
308. Macfarlane GT, Allison C, Gibson SAW, Cummings JH (1988) Contribution of the microflora to proteolysis in the human large intestine. *J Appl Bacteriol* 64(1):37–46.
309. Lin R, Liu W, Piao M, Zhu H (2017) A review of the relationship between the gut microbiota and amino acid metabolism. *Amino Acids* 49(12):2083–2090.
310. Yamada R, Deshpande SA, Bruce KD, Mak EM, Ja WW (2015) Microbes Promote Amino Acid Harvest to Rescue Undernutrition in *Drosophila*. *Cell Rep* 10(6):865–872.
311. Warnecke F, Luginbühl P, Ivanova N, Ghassemian M, Richardson TH, Stege JT, Cayouette M, McHardy AC, Djordjevic G, Aboushadi N, Sorek R, Tringe SG, Podar M, Martin HG, Kunin V, Dalevi D, Madejska J, Kirton E, Platt D, Szeto E, Salamov A, Barry K, Mikhailova N, Kyrpides NC, Matson EG, Ottesen EA, Zhang X, Hernández M, Murillo C, Acosta LG, Rigoutsos I, Tamayo G, Green BD, Chang C, Rubin EM, Mathur EJ, Robertson DE, Hugenholtz P, Leadbetter JR (2007) Metagenomic and functional analysis of hindgut microbiota of a wood-feeding higher termite. *Nature* 450(7169):560–565.
312. Ohkuma M (2003) Termite symbiotic systems: efficient bio-recycling of lignocellulose. *Appl Microbiol Biotechnol* 61(1):1–9.
313. Yatsunenkov T, Rey FE, Manary MJ, Trehan I, Dominguez-Bello MG, Contreras M, Magris M, Hidalgo G, Baldassano RN, Anokhin AP, Heath AC, Warner B, Reeder J, Kuczynski J, Caporaso JG, Lozupone CA, Lauber C, Clemente JC, Knights D, Knight R, Gordon JI (2012) Human gut microbiome viewed across age and geography. *Nature* 486(7402):222–227.
314. LeBlanc JG, Milani C, de Giori GS, Sesma F, van Sinderen D, Ventura M (2013) Bacteria as vitamin suppliers to their host: A gut microbiota perspective. *Curr Opin Biotechnol* 24(2):160–168.
315. Xu X, Zhang X (2015) Effects of cyclophosphamide on immune system and gut microbiota in mice. *Microbiol Res* 171:97–106.
316. Imhann F, Bonder MJ, Vich Vila A, Fu J, Mujagic Z, Vork L, Tigchelaar EF, Jankipersadsing SA, Cenit MC, Harmsen HJM, Dijkstra G, Franke L, Xavier RJ, Jonkers D, Wijmenga C, Weersma RK, Zhernakova A (2016) Proton pump inhibitors affect the gut microbiome. *Gut* 65(5):740–748.
317. Modi SR, Collins JJ, Relman DA (2014) Antibiotics and the gut microbiota. *J Clin Invest* 124(10):4212–4218.
318. Forslund K, Hildebrand F, Nielsen T, Falony G, Le Chatelier E, Sunagawa S, Prifti E, Vieira-Silva S, Gudmundsdottir V, Krogh Pedersen H, Arumugam M, Kristiansen K, Yvonne Voigt A, Vestergaard H, Herczeg R, Igor Costea P, Roat Kultima J, Li J, Jørgensen T, Levenez F, Dore J, Bjørn Nielsen H, Brunak S, Raes J, Hansen T, Wang J, Dusko Ehrlich S, Bork P, Pedersen O (2015) Disentangling type 2 diabetes and metformin treatment signatures in the human gut microbiota. *Nature* 528(7581):262–266.

References

319. De Filippo C, Cavalieri D, Di Paola M, Ramazzotti M, Poullet JB, Massart S, Collini S, Pieraccini G, Lionetti P (2010) Impact of diet in shaping gut microbiota revealed by a comparative study in children from Europe and rural Africa. *Proc Natl Acad Sci* 107(33):14691–14696.
320. Veiga P, Pons N, Agrawal A, Oozeer R, Guyonnet D, Brazeilles R, Faurie J-M, van Hylckama Vlieg JET, Houghton LA, Whorwell PJ, Ehrlich SD, Kennedy SP (2015) Changes of the human gut microbiome induced by a fermented milk product. *Sci Rep* 4(1):6328.
321. Graf D, Di Cagno R, Fåk F, Flint HJ, Nyman M, Saarela M, Watzl B (2015) Contribution of diet to the composition of the human gut microbiota. *Microb Ecol Heal Dis* 26(0):1–11.
322. Murphy EA, Velazquez KT, Herbert KM (2015) Influence of High-Fat-Diet on Gut Microbiota: A Driving Force for Chronic Disease Risk. *Curr Opin Clin Nutr Metab Care* 18(5):515–520.
323. Ridaura VK, Faith JJ, Rey FE, Cheng J, Duncan AE, Kau AL, Griffin NW, Lombard V, Henrissat B, Bain JR, Muehlbauer MJ, Ilkayeva O, Semenkovich CF, Funai K, Hayashi DK, Lyle BJ, Martini MC, Ursell LK, Clemente JC, Van Treuren W, Walters WA, Knight R, Newgard CB, Heath AC, Gordon JI (2013) Gut Microbiota from Twins Discordant for Obesity Modulate Metabolism in Mice. *Science (80-)* 341(6150):1241214–1241214.
324. Clarke SF, Murphy EF, O’Sullivan O, Lucey AJ, Humphreys M, Hogan A, Hayes P, O’Reilly M, Jeffery IB, Wood-Martin R, Kerins DM, Quigley E, Ross RP, O’Toole PW, Molloy MG, Falvey E, Shanahan F, Cotter PD (2014) Exercise and associated dietary extremes impact on gut microbial diversity. *Gut* 63(12):1913–1920.
325. Cotillard A, Kennedy SP, Kong LC, Prifti E, Pons N, Le Chatelier E, Almeida M, Quinquis B, Levenez F, Galleron N, Gougis S, Rizkalla S, Batto J-M, Renault P, Doré J, Zucker J-D, Clément K, Ehrlich SD (2013) Dietary intervention impact on gut microbial gene richness. *Nature* 500(7464):585–588.
326. van Beek AA, Hugenholtz F, Meijer B, Sovran B, Perdijk O, Vermeij WP, Brandt RMC, Barnhoorn S, Hoeijmakers JHJ, de Vos P, Leenen PJM, Hendriks RW, Savelkoul HFJ (2017) Frontline Science: Tryptophan restriction arrests B cell development and enhances microbial diversity in WT and prematurely aging *Erc1* $^{-\Delta 7}$ mice. *J Leukoc Biol* 101(4):811–821.
327. Zapata RC, Singh A, Ajdari NM, Chelikani PK (2018) Dietary Tryptophan Restriction Dose-Dependently Modulates Energy Balance, Gut Hormones, and Microbiota in Obesity-Prone Rats. *Obesity* 26(4):730–739.
328. Chen X, Song P, Fan P, He T, Jacobs D, Levesque CL, Johnston LJ, Ji L, Ma N, Chen Y, Zhang J, Zhao J, Ma X (2018) Moderate Dietary Protein Restriction Optimized Gut Microbiota and Mucosal Barrier in Growing Pig Model. *Front Cell Infect Microbiol* 8(July).
329. Fan P, Liu P, Song P, Chen X, Ma X (2017) Moderate dietary protein restriction alters the composition of gut microbiota and improves ileal barrier function in adult pig model. *Sci Rep* 7(1):43412.
330. Li G, Xie C, Lu S, Nichols RG, Tian Y, Li L, Patel D, Ma Y, Brocker CN, Yan T, Krausz KW, Xiang R, Gavrilova O, Patterson AD, Gonzalez FJ (2017) Intermittent Fasting Promotes White Adipose Browning and Decreases Obesity by Shaping the Gut Microbiota. *Cell Metab* 26(5):801.
331. Beli E, Yan Y, Moldovan L, Vieira CP, Gao R, Duan Y, Prasad R, Bhatwadekar A, White FA, Townsend SD, Chan L, Ryan CN, Morton D, Moldovan EG, Chu F-I, Oudit GY, Derendorf H, Adorini L, Wang XX, Evans-Molina C, Mirmira RG, Boulton ME, Yoder MC, Li Q, Levi M, Busik J V., Grant MB (2018) Restructuring of the Gut Microbiome by Intermittent Fasting Prevents Retinopathy and Prolongs Survival in db/db Mice. *Diabetes* 67(9):1867–1879.
332. Mortzfeld BM, Taubenheim J, Fraune S, Klimovich A V., Bosch TCG (2018) Stem Cell Transcription Factor FoxO Controls Microbiome Resilience in *Hydra*. *Front Microbiol* 9(APR):1–10.
333. Andoh A, Sakata S, Koizumi Y, Mitsuyama K, Fujiyama Y, Benno Y (2007) Terminal restriction fragment length polymorphism analysis of the diversity of fecal microbiota in patients with ulcerative colitis. *Inflamm Bowel Dis* 13(8):955–962.
334. Takahashi K, Nishida A, Fujimoto T, Fujii M, Shioya M, Imaeda H, Inatomi O, Bamba S, Andoh A, Sugimoto M (2016) Reduced Abundance of Butyrate-Producing Bacteria Species in the Fecal Microbial

References

- Community in Crohn's Disease. *Digestion* 93(1):59–65.
335. Nishino K, Nishida A, Inoue R, Kawada Y, Ohno M, Sakai S, Inatomi O, Bamba S, Sugimoto M, Kawahara M, Naito Y, Andoh A (2018) Analysis of endoscopic brush samples identified mucosa-associated dysbiosis in inflammatory bowel disease. *J Gastroenterol* 53(1):95–106.
336. Huang YJ, Nelson CE, Brodie EL, DeSantis TZ, Baek MS, Liu J, Woyke T, Allgaier M, Bristow J, Wiener-Kronish JP (2011) Airway microbiota and bronchial hyperresponsiveness in patients with suboptimally controlled asthma. *J Allergy Clin Immunol* 127(2):372–381.e3.
337. Hilty M, Burke C, Pedro H, Cardenas P, Bush A, Bossley C, Davies J, Ervine A, Poulter L, Pachter L, Moffatt MF, Cookson WOC (2010) Disordered Microbial Communities in Asthmatic Airways. *PLoS One* 5(1):e8578.
338. Turnbaugh PJ, Hamady M, Yatsunenko T, Cantarel BL, Duncan A, Ley RE, Sogin ML, Jones WJ, Roe BA, Affourtit JP, Egholm M, Henrissat B, Heath AC, Knight R, Gordon JI (2009) A core gut microbiome in obese and lean twins. *Nature* 457(7228):480–484.
339. Qin J, Li Y, Cai Z, Li S, Zhu J, Zhang F, Liang S, Wang J, et al. (2012) A metagenome-wide association study of gut microbiota in type 2 diabetes. *Nature* 490(7418):55–60.
340. Tomova A, Husarova V, Lakatosova S, Bakos J, Vlkova B, Babinska K, Ostatnikova D (2015) Gastrointestinal microbiota in children with autism in Slovakia. *Physiol Behav* 138:179–187.
341. Wang L, Christophersen CT, Soric MJ, Gerber JP, Angley MT, Conlon MA (2011) Low Relative Abundances of the Mucolytic Bacterium *Akkermansia muciniphila* and *Bifidobacterium spp.* in Feces of Children with Autism. *Appl Environ Microbiol* 77(18):6718–6721.
342. Peters BA, Dominianni C, Shapiro JA, Church TR, Wu J, Miller G, Yuen E, Freiman H, Lustbader I, Salik J, Friedlander C, Hayes RB, Ahn J (2016) The gut microbiota in conventional and serrated precursors of colorectal cancer. *Microbiome* 4(1):69.
343. Feng Q, Liang S, Jia H, Stadlmayr A, Tang L, Lan Z, Zhang D, Xia H, Xu X, Jie Z, Su L, Li X, Li X, Li J, Xiao L, Huber-Schönauer U, Niederseer D, Xu X, Al-Aama JY, Yang H, Wang J, Kristiansen K, Arumugam M, Tilg H, Datz C, Wang J (2015) Gut microbiome development along the colorectal adenoma–carcinoma sequence. *Nat Commun* 6(1):6528.
344. Dejea CM, Wick EC, Hechenbleikner EM, White JR, Mark Welch JL, Rossetti BJ, Peterson SN, Snesrud EC, Borisy GG, Lazarev M, Stein E, Vadivelu J, Roslani AC, Malik AA, Wanyiri JW, Goh KL, Thevambiga I, Fu K, Wan F, Llosa N, Housseau F, Romans K, Wu X, McAllister FM, Wu S, Vogelstein B, Kinzler KW, Pardoll DM, Sears CL (2014) Microbiota organization is a distinct feature of proximal colorectal cancers. *Proc Natl Acad Sci* 111(51):18321–18326.
345. Driver CJI, Cosopodiotis G (1979) The effect of dietary fat on longevity of *Drosophila melanogaster*. *Exp Gerontol* 14(3):95–100.
346. Schultzhause JN, Bennett CJ, Iftikhar H, Yew JY, Mallett J, Carney GE (2018) High fat diet alters *Drosophila melanogaster* sexual behavior and traits: decreased attractiveness and changes in pheromone profiles. *Sci Rep* 8(1):5387.
347. Lee C, Raffaghello L, Brandhorst S, Safdie FM, Bianchi G, Martin-Montalvo A, Pistoia V, Wei M, Hwang S, Merlino A, Emionite L, de Cabo R, Longo VD (2012) Fasting Cycles Retard Growth of Tumors and Sensitize a Range of Cancer Cell Types to Chemotherapy. *Sci Transl Med* 4(124):124ra27–124ra27.
348. López-lázaro M (2015) Selective amino acid restriction therapy (SAART): a non- pharmacological strategy against all types of cancer cells. *Oncoscience* 2(10):857.
349. Meadows GG, Fu Y-M (2005) Dietary Restriction of Specific Amino Acids Modulates Tumor and Host Interactions. *Integration/Interaction of Oncologic Growth* (Springer-Verlag, Berlin/Heidelberg), pp 271–283.
350. Ryu J-H, Kim S-H, Lee H-Y, Bai JY, Nam Y-D, Bae J-W, Lee DG, Shin SC, Ha E-M, Lee W-J (2008) Innate Immune Homeostasis by the Homeobox Gene Caudal and Commensal-Gut Mutualism in

References

- Drosophila*. *Science* (80-) 319(5864):777–782.
351. Cox CR, Gilmore MS (2007) Native Microbial Colonization of *Drosophila melanogaster* and Its Use as a Model of *Enterococcus faecalis* Pathogenesis. *Infect Immun* 75(4):1565–1576.

7. Acknowledgements

Ich möchte mich ganz besonders bei meinem Doktorvater Prof. Dr. Thomas Roeder für seine wissenschaftliche Betreuung bedanken. Dank Thomas war es mir möglich, mein Projekt nach meinen eigenen Vorstellungen zu formen, inklusive aller experimenteller Exkursionen und Spinnereien. Ich bin sehr dankbar, dass er mich nicht nur in seine Arbeitsgruppe aufgenommen hat, sondern immer Zeit, Geld und motivierende Worte gefunden hat, um mich bei meiner Arbeit zu unterstützen.

Ich danke Daniela Esser, Benedikt Mortzfeld und Jan Taubenheim für die Hilfe beim Auswerten meiner Daten und für Diskussionen, die dazu beigetragen haben, aus dem Wust von Daten, sinnvolle Interpretationen und Schlüsse zu ziehen.

Ich bedanke mich bei der AG Roeder für die schöne Zeit und die Zusammenarbeit, für witzige Gespräche und neue Denkanstöße, für persönliche und professionelle Hilfestellungen und besonders für die tollen Freundschaften. Insbesondere bin ich froh, dass ich mit euch, Judith und Jakob, die allermeisten Tage der letzten vier Jahre verbringen konnte!

Mein besonderer Dank gilt der Arbeitsgruppe Bosch, die mir nicht nur ein zweites Zuhause im Bioturm gegeben hat, sondern jeden meiner Arbeitstage beim Mittagessen mit aufbrausenden Diskussionen, Charme und Kreativität bereichert hat. Ich werde euch, Jan, Jörg und Kai, ganz besonders vermissen und bin froh, euch als Freunde in meinem Leben zu wissen.

Ich bedanke mich bei meiner Familie für die unendliche Unterstützung, für ihre Liebe und die vielen motivierenden Worte. Ohne euch wäre mir das Studium nicht möglich gewesen und mir diese Doktorarbeit so unendlich schwer gefallen! Es ist schön zu wissen, dass ich in Hellingst und in Hamburg immer ein Zuhause habe.

Zum Schluss bedanke ich mich noch bei dir, Bene, für dein Herz und deinen Rückhalt und deinen klugen Kopf. Du unterstützt mich und machst mir Mut. Egal ob wandernd im Himalaya oder schläfrig auf dem Sofa - jeder Tag ist besser, wenn ich ihn mit dir verbringe.

8. Declaration

I declare that the dissertation titled “The impact of nutritional interventions on the progression of intestinal tumors in *Drosophila melanogaster*”, apart from my supervisor’s guidance and the listed references, is my own literary property and represents my own work. This dissertation has not been submitted elsewhere in order to obtain an academic degree and was prepared according to the *Rules of Good Scientific Practice* of the German research Foundation.

Hiermit erkläre ich, dass die vorliegende Dissertation mit dem Titel “The impact of nutritional interventions on the progression of intestinal tumors in *Drosophila melanogaster*”, die ich unter der Betreuung durch meinen Supervisor Prof. Dr. Thomas Roeder und unter Zuhilfenahme der angegebenen Referenzen angefertigt habe, mein eigenes geistiges Eigentum ist und meine eigene Arbeit widerspiegelt. Die Arbeit wurde unter Berücksichtigung der *Regeln guter wissenschaftlicher Praxis* der Deutschen Forschungsgesellschaft angefertigt und an keiner weiteren Stelle im Rahmen eines Promotionsvorhabens eingereicht.

Kiel, den 27. September 2018

Roxana Pfefferkorn

9. Curriculum Vitae

Name: Roxana Pfefferkorn
DOB: 19.12.1987 in Henstedt-Ulzburg
Nationality: German

EDUCATION

2014 - 2018 **PhD candidate** in the group of Prof. Thomas Roeder, Christian-Albrechts-University Kiel, Germany

Dissertation Title

‘The impact of nutritional interventions on the progression of intestinal tumors in *Drosophila melanogaster*’

2011 - 2013 **Master of Science:** Department of Biology, Christian-Albrechts-University Kiel, Germany

Master’s Thesis (Supervisor: Dr. Hinrich Schulenburg)

‘Functional characterization of candidate genes identified from genetic analyses of experimentally evolved *Pseudomonas aeruginosa*’

2010 **Internship** at the Bernhard Nocht Institute for Tropical Medicine, Department of Molecular Biology and Immunology, Research Group Leishmaniasis (Supervisor: PD Dr. Joachim Clos)

2008 - 2011 **Bachelor of Science:** Department of Biology, Christian-Albrechts-University Kiel, Germany

Bachelor’s Thesis (Supervisor: Prof. Thomas Roeder)

‘Etablierung eines Zellkultursystems für Neuronen des dopaminergen Systems der Fruchtfliege *Drosophila melanogaster*’

1998 - 2007 Secondary School: Städtisches Gymnasium, Bad Segeberg

1994 - 1998 Primary School: Dr.-Gerlich-Schule, Trappenkamp

10. Appendix

Tab. S1: Product Information on ingredients of standard cornmeal diet.

Product	Company	Head Office
brewer's yeast	Leiber GmbH	Hafenstraße 24, 49565 Bramsche, Germany
cornmeal	Mühle Schlingemann e.K.	Hochstraße 2-4, 45731 Waltrop, Germany
molasses	Biohof Heidelicht Handelsunternehmen	Am Berge 7, 29581 Groß Süstedt, Germany
sugar beet syrup	Kanne Brottrunk GmbH & Co. Betriebsgesellschaft KG	Bahnhofstraße 68, 59379 Selm-Bork, Germany

Phosphate buffered saline (PBS)

136 mM	NaCl
7 mM	Na ₂ HPO ₄
2.7 mM	KCl
1.5 mM	KH ₂ PO ₄

Dissolve in appropriate amount ddH₂O, adjust pH to 7.3 using HCl and autoclave.

Tab. S2: Bacteria used for recolonization experiments. All strains were a gift from Carlos Ribeiro (194).

Bacteria	Culturing Medium	Original Reference
<i>Acetobacter pomorum</i>	mannitol medium (194)	Ryu <i>et al.</i> 2008 (350)
<i>Commensalibacter intestini</i> ^{A911T}	mannitol medium (194)	Ryu <i>et al.</i> 2008 (350)
<i>Enterococcus faecalis</i>	LB (Sigma-Aldrich, #L3022)	Cox and Gilmore 2007 (351)
<i>Lactobacillus brevis</i> ^{EW}	MRS (Sigma-Aldrich, #69966)	Ryu <i>et al.</i> 2008 (350)
<i>Lactobacillus plantarum</i> ^{WJL}	MRS (Sigma-Aldrich, #69966)	Ryu <i>et al.</i> 2008 (350)

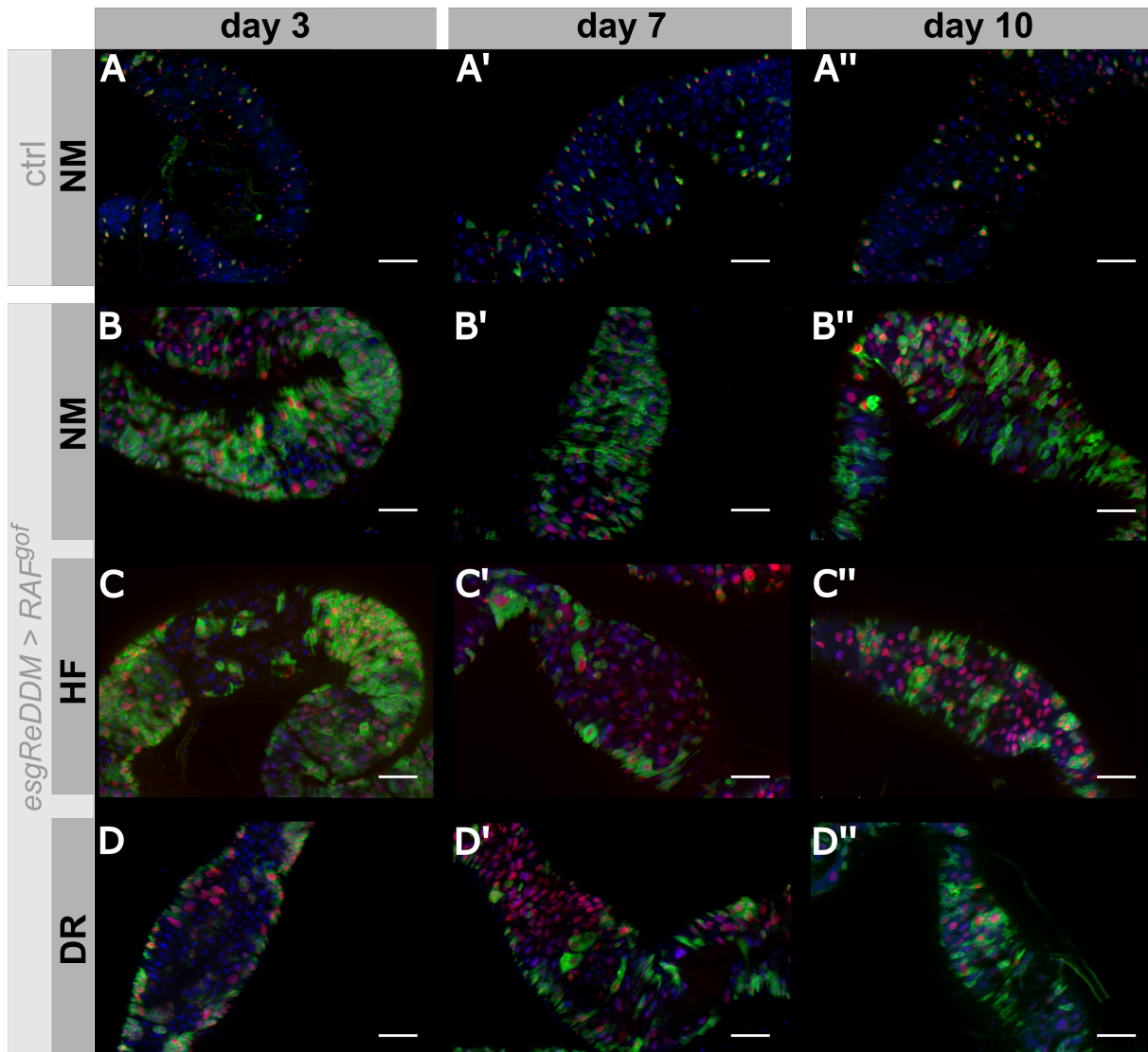


Fig. S1: Lineage tracing in the R3 midgut region of control flies and flies expressing RAF^{gof} in ISCs and EBs. Flies of the genotype $esgReDDM > RAF^{gof}$ were shifted to 29 °C to induce overproliferation and dissected on days three, seven and ten (scale bar 50 μm). The ReDDM system (153) identifies ISCs and EBs with nuclear RFP as well as cytoplasmic GFP. During differentiation the short lived GFP fades, therefore, differentiated cells retain only RFP. GFP: green fluorescent protein, green; RFP: red fluorescent protein, red; DAPI: nuclei, blue.

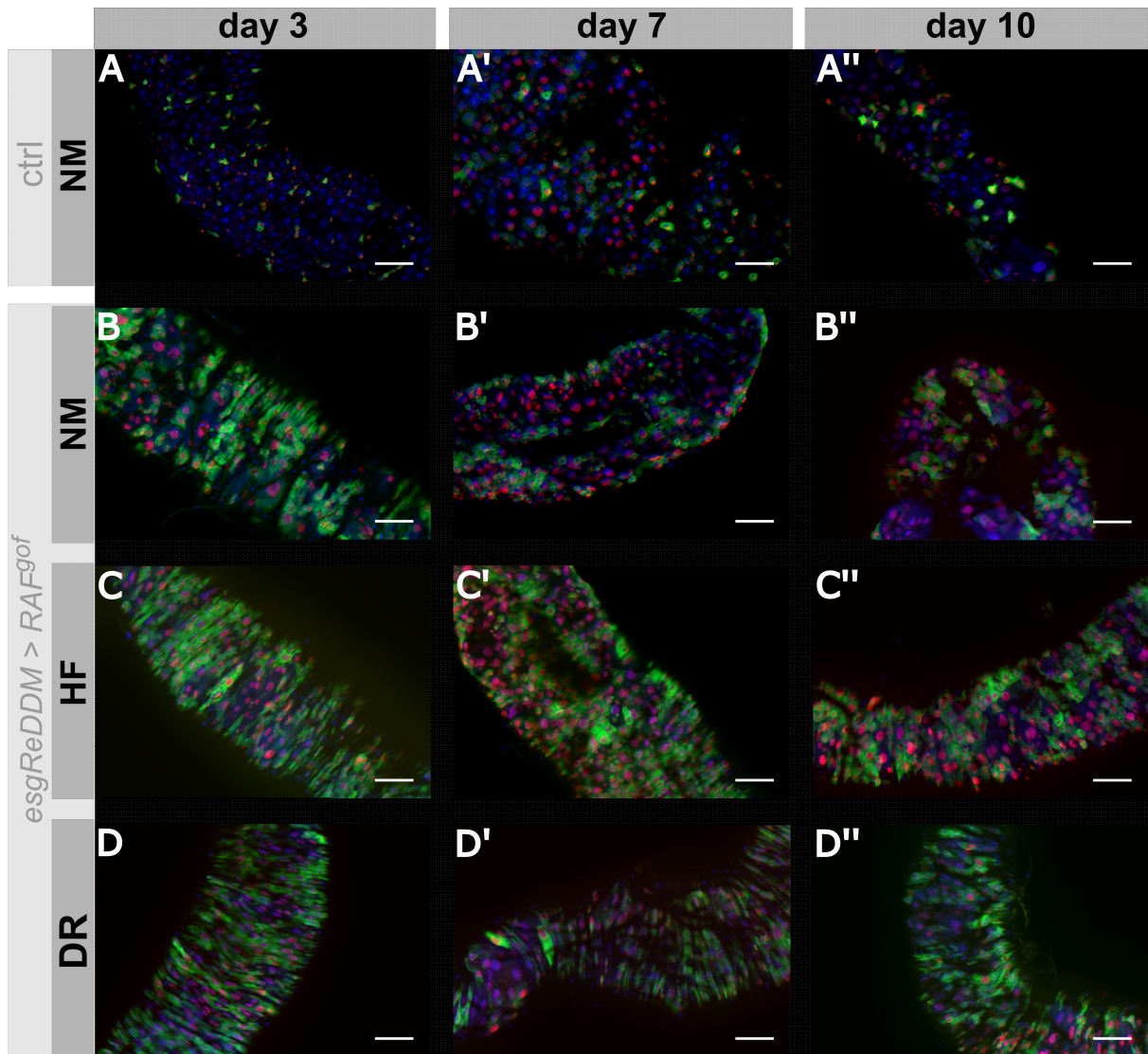


Fig. S2: Lineage tracing in the R4 midgut region of control flies and flies expressing RAF^{gof} in ISCs and EBs. Flies of the genotype $esgReDDM > RAF^{gof}$ were shifted to 29 °C to induce overproliferation and dissected on days three, seven and ten (scale bar 50 μ m). The ReDDM system (153) identifies ISCs and EBs with nuclear RFP as well as cytoplasmic GFP. During differentiation the short lived GFP fades, therefore, differentiated cells retain only RFP. GFP: green fluorescent protein, green; RFP: red fluorescent protein, red; DAPI: nuclei, blue.

Appendix

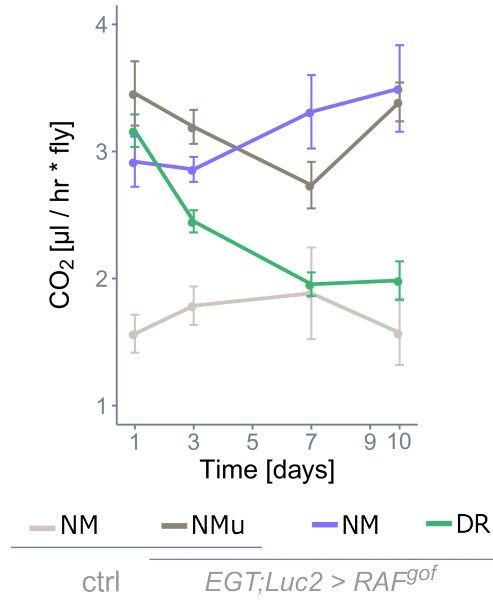


Fig. S3: Measurement of the basic metabolic rate of tumor bearing and control flies after subjection to the indicated food regime. ctrl = control ($w^{1118} > EGT;Luc2$), NM = normal medium, NMu = NM uninduced (at 20 °C), HF = high fat medium, DR = dietary restriction medium.

Tab. S3: Statistical analysis of the principal component analysis of microbial diversity.

Samples	Metric	Anosim		Adonis	
		R	P value	R ²	P value
genotype	Binary Pearson	0.11	0.001 ***	0.03	0.001 ***
	Pearson	0.16	0.001 ***	0.11	0.001 ***
	Unweighted Unifrac	0.04	0.012 *	0.02	0.011 *
	Weighted Unifrac	0.05	0.010 **	0.05	0.031 *
media	Binary Pearson	0.00	0.52	0.03	0.513
	Pearson	-0.01	0.69	0.01	0.84
	Unweighted Unifrac	0.03	0.113	0.03	0.144
	Weighted Unifrac	-0.02	0.907	0.01	0.961
days	Binary Pearson	0.05	0.017 *	0.03	0.004 **
	Pearson	0.06	0.013 *	0.15	0.001 ***
	Unweighted Unifrac	0.09	0.001 ***	0.04	0.001 ***
	Weighted Unifrac	0.10	0.004 **	0.16	0.001 ***

* $p \leq 0.05$, ** $p \leq 0.01$, *** $p \leq 0.001$.